LITHIC INCLUSIONS IN THE TAUPO PUMICE FORMATION

by

Tadiwos Chernet

A thesis submitted for the degree of

Master of Science in Geology at the

Research School of Earth Sciences

Victoria University of Wellington

January, 1987

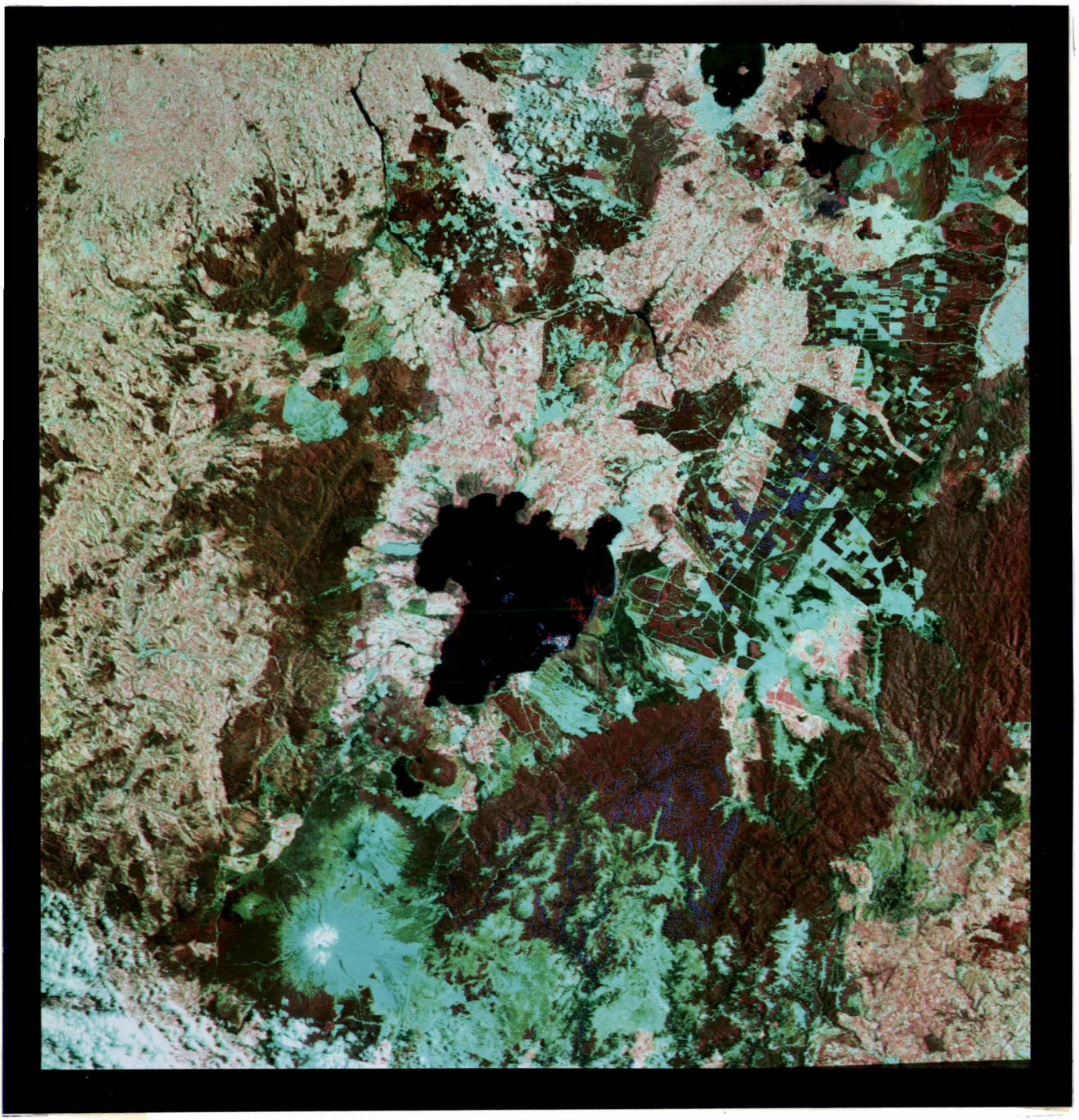

FRONTISPIECE

Subscene of Pel 18821 colour mosaic (courtesy of Physics and Engineering Labratory, D.S.I.R.) consists of photos taken by Landsat 1 on 22 Dec 1975 and 15 Feb 1976. The picture shows most part of the TVZ, with Lake Taupo Volcanic Centre in the middle. The greywacke ranges and ignimbrite plateau to the east and west of the TVZ are distinct from the active volcanic region which runs in the north-east direction. Products of the 1800a Taupo eruption have covered most part of the area shown.

ABSTRACT

The Taupo Pumice Formation is a product of the Taupo eruption of about 1800a, and consists of three phreatomagmatic ash deposits, two plinian pumice deposits and a major low-aspect ratio and low grade (unwelded) ignimbrite which covered most part of the central North Island of New Zealand. The vent area for the eruption is located at Horomatangi Reefs in Lake Taupo.

Lithics in the phreatoplinian ash deposits are negligible in quantity, but the plinian pumice deposits contain 5-10% lithics by volume in most near-vent sections. Lithics in the plinian pumice deposits are dominantly banded and spherulitic rhyolite with minor welded tuff, dacite and andesite. The ground layer which forms the base of the ignimbrite unit consists of dominantly lithics and crystals and is formed by the gravitational sedimentation of the 'heavies' from the strongly fluidized head of the pyroclastic flow. Lithic blocks in the ground layer are dominantly banded and spherulitic phenocryst-poor rhyolite, welded tuff with minor dacite and andesite. Near-vent exposures of the ground layer contain boulders upto 2 m in diameter. Friable blocks of hydrothermally altered rhyolite, welded tuff and lake sediments are found fractured but are preserved intact after transportation. This shows that the fluid/pyroclastic particle mixture provided enough support to carry such blocks upto a distance of 10 km from the vent.

The rhyolite blocks are subdivided into hypersthene rhyolite, hypersthene-hornblende rhyolite and biotite-bearing rhyolite on the basis of the dominant ferromagnesian phenocryst assamblage. Hypersthene is the dominant ferromagnesian phenocryst in most of the rhyolite blocks in the ground layer and forms the major ferromagnesian crystal of the Taupo Sub-group tephra. The rhyolite blocks have similar whole rock chemistry to the Taupo Sub-group tephra and are probably derived from lava extrusions associated with the tephra eruptions from the Taupo Volcanic Centre in the last 10 ka. Older rhyolite domes and flows in the area are probably represented by the intensely hydrothermally altered rhyolite blocks in the ground layer.

The dacite blocks contain hypersthene and augite as a major ferromagnesian phenocryst. Whole rock major and trace element analyses shows that the dacite blocks are distinct from the Tauhara dacites and from the dacites of Tongariro Volcanic Centre. The occurrence of dacite inclusions in significant quantity in the Taupo Pumice Formation indicates the presence of other dacite flows near the vent area.

Four types of andesite blocks; hornblende andesite, plagioclase-pyroxene andesite, pyroxene andesite and olivine andesite occur as lithic blocks in the ground layer. The andesites are petrographically distinct from those encountered in deep drillholes at Wairakei (Waiora Valley Andesites), and are different from the Rolles Peak andesite in having lower Sr content. The andesite blocks show similar major and trace element content to those from the Tongariro Volcanic Centre. The roundness of the andesite blocks indicates that the blocks were transported as alluvium or lahars in to the lake basin before being incorporated into the pyroclastic flow.

Two types of welded ignimbrite blocks are described. The lithic-crystal rich ignimbrite is correlated with a post-Whakamaru Group Ignimbrite (ca. 100 ka ignimbrite erupted from Taupo Volcanic Centre) which crops out to the north of Lake Taupo. The crystal rich ignimbrite is tentatively correlated with the Whakamaru Group Ignimbrites. The lake sediment boulders, pumiceous mudstone and siltstone in the ground layer probably correlate to the Huka Group sediments or younger Holocene sediments in the lake basin.

A comparative mineral chemistry study of the lithic blocks was done. A change in chemistry of individual mineral species was found to accompany the variation in wholerock major element constituents in the different types of lithics.

The large quantity of lithic blocks in the ground layer suggests extensive vent widening at the begining of the ignimbrite eruption. A simple model of flaring and collapse of the vent area caused by the down ward movement of the fragmentation surface is presented to explain the origin of the lithic blocks in the ground layer. The lithics in the Taupo Pumice Formation are therfore produced by the disruption of the country rock around the vent during the explosion and primary xenoliths from depths of magma generation were not found.

Stratigraphic relations suggest that the most important depth of incorporation of lithics is within the post-Whakamaru Group Ignimbrite volcanics and volcaniclastic sedimentary units.

ACKNOWLEDGEMENTS

Many people have contributed directly or indirectly to this work and I can not hope to mention them all. I thank all the academic and non-academic staff and graduate students of the Research School of Earth Sciences (Victoria University of Wellington). First and foremost I am very grateful to my supervisor Dr Jim Cole without whose instruction and constant encouragement this work could have not been possible.

I am very grateful to Dr John Gamble, Dr Rodney Grapes and Dr Russele Howorth for their help in many problems related to this project. I am also very grateful to Mr Ken Palmer for instructions and assistance given in using the analytical facilities at the Research School of Earth Sciences and for providing his computer programmes used for most of the calculations in this work. I am very grateful for Dr Paul Froggatt (Center of Continuing Education, Victoria University of Wellington) for his interest in the work, important comments and help in reviewing the text.

Special thanks are due to Dr Bruce F. Houghton of the New Zealand Geological Survey and Dr Colin J. N. Wilson (University of Auckland) for the invaluable advice and discussions concerning the field work for this study. I thank all the staff of Geological Survey of New Zealand (Rotorua branch) for the material support (maps, sample bags etc.) and moral encouragment in the course of this work.

I am very grateful to Mr Philip White for help in many ways during my labratory work and writing of this thesis and Mr John Keale for many important discussions about some of the topics in this thesis and for proof reading most of the text. I am very grateful to Mr John Carter for the preparation of thin sections and polished sections and Mr Steven Eagar for his help in getting maps, slides and photos in the department.

Most of the thesis is typed by the author and I am responsible for most of the typing mistakes however I am very grateful for Mrs. Val Herbert and Ms. Betty Finlayson for help with typing and preparation of the this thesis.

CONTENTS

WHOLEROCK CHEMISTRY OF LITHIC BLOCKS

CORRELATION

APPENDICES

LIST OF FIGURES

(captions are abbreviated)

LIST OF TABLES

(captions are abbreviated)

Chapter 1

INTRODUCTION

Taupo Volcano is located near the centre of the North Island of New Zealand and is the southern most of the dominantly rhyolitic volcanic centres in the Taupo Volcanic Zone (Frontispiece). Taupo Volcano consists of a large basin roughly 50 km across and 300-500 m deep, the central 600 km^2 of which is covered by Lake Taupo. Even the earliest observations suggest that the lake was a result of a unique type of volcanic activity. Grange (1937) stated that previous explanations of the origin of the lake were centred around the idea that the lake was formed as a result of subsidence through withdrawal of support at depth due to volcanic activity and/or craters formed by volcanic explosions. He suggested that both phenomena had contributed to the formation of the lake basin and later studies have consistently supported this view. Cole (1979) suggested that the volcanic centre represents multiple calderas with each major pyroclastic eruption having been followed by a collapse of the vent area. Walker (1981) describes it as an "inverse volcano" formed by eruptions which have been so powerfully explosive that the near vent accumulation of ejecta was insufficient to counterbalance subsidence caused by magma withdrawal.

There have been several pyroclastic and lava eruptions from the Taupo Volcanic Centre in the last 350 ka. A study of the voluminous material erupted from this volcano has led to an intimate knowlege of its eruptive history. A thick pile of volcanic ejecta is well preserved about Lake Taupo, and road cuttings and other construction works have provided exposures that have allowed a detailed stratigraphy and distribution of these tephras to be established.

The purpose of this work is to study the lithic inclusions in pyroclastic deposits from Taupo Volcano, especially in the youngest series of eruptions which produced the

Taupo Pumice Formation. This eruption has been of particular interest for several reasons:

1. It was one of the largest explosive eruptions in the world within the last 7000 years, and according to Walker (1980) includes the most powerful plinian and violent ignimbrite-forming events yet documented. Walker (1980) considered various factors in establishing the size of a volcanic eruption.

   (a). Magnitude determined from the total volume.

   (b). Intensity- determined from the discharge rate.

   (c). Dispersive power- the extent of dispersal.

   (d). Violence- the importance of momentum and

   (e). Destructive potential- the extent of real or potential destruction of life or property.

   The Taupo eruption has a modest volume but had a high intensity, dispersive power, violence and destructive potential as documented by its deposits.

2. It generated a great variety of pyroclastic deposits; three phreatoplinian deposits, two plinian pumice falls, and three ignimbrite flow units (including some intra-plinian units) which have a great variety of facies and structures.

3. The vent was located within a large lake and magma/water interaction determined the style of parts of the eruption. Furthermore the phreatomagmatic deposits are of particular interest on their own.

4. The eruption occurred at an inverse volcano covered by a lake and represents a style of activity which may be typical of such volcanoes.

The term lithics in pyroclastic deposits is generally used to describe the dense components in the deposit irrespective of their origin. Lithic fragments rarely exceed 5 percent of the total volume in intermediate to large volume pyroclastic flow and fall deposits. Many small volume pyroclastic flow deposits can be composed almost entirely of juvenile lithic fragments and broken crystals with adhering matrix derived from the explosive disruption of the neck and dome of a volcano.

In most pyroclastic flow or fall deposits there are three major sources of lithic fragments :

1. Slowly cooled and crystallized magma "rinds" from chamber margins or non-vesiculated juvenile rock fragments.
2. Rock fragments from the conduit walls or country rock which has been explosively ejected during the eruption.
3. In the case of pyroclastic flows and surges, rock fragments picked up along the path of the pyroclastic flow.

The three genetic types of lithics in pyroclastic deposits are termed "cognate lithics", "accessory lithics" and "accidental lithics" respectively by Wright et al. (1980). Cognate and accessory lithics can give information on the depth to the magma chamber if the regional stratigraphy is well known.

The ground layer of the Taupo Ignimbrite in particular offers good exposures of lithic rich zones on which most of this study is based. In order to correlate the various types of lithics in the pyroclastics from Taupo Volcano with the major stratigraphic units in area, it is essential to establish the stratigraphy in the vent area. The Taupo Volcanic Centre covers a considerable area but most of the centre is covered by Lake Taupo. This presents a problem in the direct study of the stratigraphy. The stratigraphy of the vent area has therefore been inferred from regional geologic mapping of the area. Variations in intra-caldera lava flow and dome stratigraphy are to be expected, but most of the pyroclastic deposits erupted from the centre can be assumed to occur throughout the volcanic centre.

The correlation of the different type of lithics to known stratigraphic units in the area is based on petrographic study and major and trace element wholerock analyses of the lithic blocks from the ground layer. A comparative mineral chemistry study of the various types of lithic blocks in the ground layer was done to demonstrate the difference in mineral chemistry which accompany the wholerock chemical variations.

Chapter 11

REGIONAL GEOLOGY

2.1 TECTONIC SETTING

The North Island of New Zealand is on the boundary between the Pacific and Indian plates. In the vicinity of the North Island, oceanic crust of the Pacific Plate is obliquely subducted beneath continental crust of the Indian Plate to form the Taupo-Hikurangi arc trench system. The main tectonic elements of this arc trench system are shown on Fig 2.1.

The volcanic component of this system is the Taupo Volcanic Zone (TVZ) which comprises a Quaternary andesite-dacite arc, to the west of which is the Taupo-Rotorua Depression, a basin filled with approximately 2 km of low density volcanics. Most of these volcanics are rhyolitic and have been erupted in the last 1My from the volcanic centres in the depression (Murphy and Seward, 1981).

A genetic model for the TVZ has been discussed by Cole (1979) and a model of migrating volcanic arc systems is suggested to have preceded the present tectonic setting in the TVZ. During the period 18-6 Ma the Northland arc had a north-westerly trend and extended from North Auckland to the southern end of the Coromandel Peninsula. Later volcanism extended south-eastwards still with a north-westerly trend, until andesite volcanism commenced from the Tongariro Volcanic Centre, probably in the early Pleistocene. The present NNE trending Taupo arc is very recent and has influenced volcanism in the TVZ for the past 1-2 MY.

Normal faults are common in the Taupo-Rotorua Depression and some have been active in historic times. Where open fissures are formed, no strike slip movements have been recorded. Based on this evidence together with the presence of basaltic dikes in the depression, Cole (1985) suggested that the area is an extensional ensialic marginal basin.

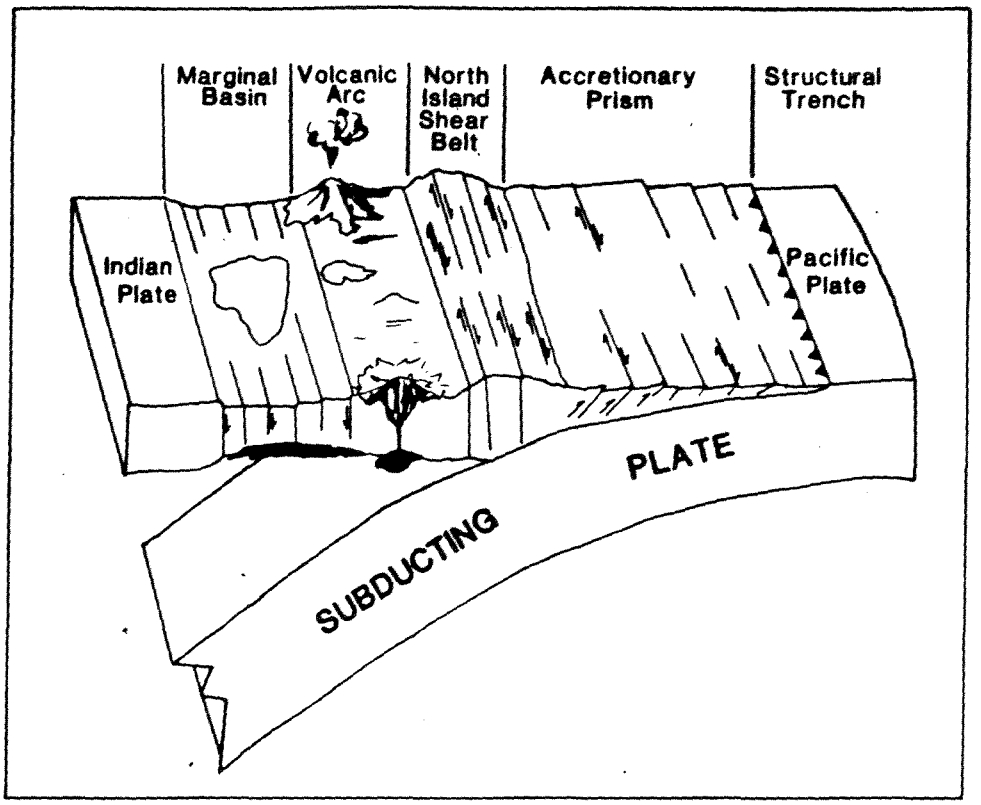

Figure 2.1 : Tectonic elements of the Taupo-Hikurangi arc-trench system. (From Cole 1985, Fig. 9)

2.2 *THE TAUPO VOLCANIC ZONE*

The TVZ extends for approximately 300 km from Ohakune to White Island (Fig 2.2). The name Taupo Volcanic Zone was first coined by Healy (1961) for a 15-25 km wide belt of Quaternary volcanism in the region. Earlier observations were made by Hochstetter (1864) but it was not until Grange (1937) that additional general information on the structure and petrology became available.

Various criteria have been used to define the boundaries of the TVZ. In current usage (eg. Cole (1979)) the TVZ consists of a northern segment of the andesite volcanoes of Whale and White Island, a central segment of overwhelmingly rhyolitic volcanism extending from Okataina to Taupo (Taupo-Rotorua Depression; the ensialic marginal basin) and a southern segment containing andesite volcanoes of the Tongariro Volcanic Centre. The andesite volcanoes at the northern and southern end of the TVZ are part of the andesite-dacite arc to the east of the Taupo-Rotorua Depression.

Grindley (1961) broadly divided the structural development of the central part of the TVZ into two epochs. In the early Pleistocene, a rapidly subsiding basin or series of basins formed which extended from Western Bay, Lake Taupo to Rotorua (Taupo-Rotorua Basin) and filled with pumiceous pyroclastic and alluvium of the Ohakuri Group, followed by block faulting and tilting. The eastern margin of this depression was most probably the Kaingaroa Fault. Following subsidence there was probably a long period when the sediments of the basin were block faulted and tilted.

The second stage commenced with the eruption of thick ignimbrite units [cf. Whakamaru Group Ignimbrites of Wilson et. al. (1986)] and a major fault belt (Taupo Fault Belt) extending from Ruapehu through Tongariro, Lake Taupo to the Paeroa Range, Tarawera and Whakatane became the dominant feature in late Pleistocene. North of Lake Taupo the Taupo Fault Belt cuts an older fault (Hauraki Fault) that continues north to the Hauraki Graben. Following this a rapidly subsiding basin the Taupo-Reporoa Basin was formed on the south eastern side of the Taupo Fault Belt. The structural development of the Taupo-Reporoa Basin was accompanied by the accumulation of a considerable thickness of Huka Group pyroclastics and sediments.

ure 2.2 : Location map of the Taupo Volcanic Centre, North Island, New Zealand. Taupo Volcanic Zone is enclosed by the heavier dashed line. The main andesite-dacite arc to the east is shown as a dotted area. Major volcanic Centres in the zone are numbered 1-6
1.Rotorua 2.Okataina
3.Maroa 4.Tongariro
Boundaries not shown (5.Mangakino 6.Kapenga)
Older NW-trending eruptive vents are shown by open circles while younger NNE-trending eruptive vents are shown by filled circles (modified from Cole 1985)

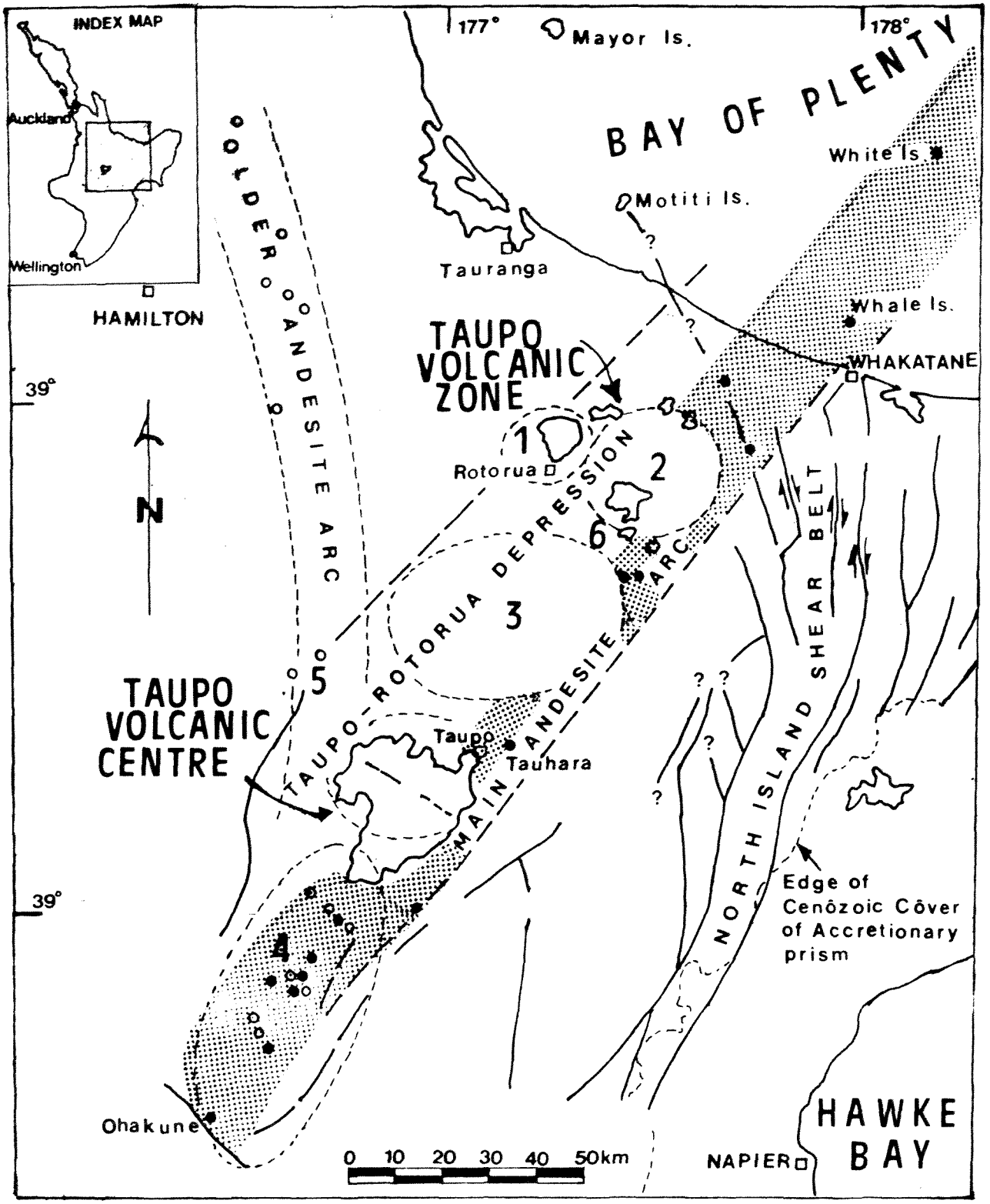

The rhyolites mostly were erupted from large multi-vent caldera volcanoes. Four rhyolitic volcanic centres (Rotorua, Okataina, Maroa and Taupo) were defined by Healy (1962) (Fig 2.2). Two other rhyolitic centres Mangakino and Kapenga were defined by Wilson et al. (1984) mainly on geophysical grounds. The rhyolites although mainly coeval with Huka Falls Formation deposition are associated with later development of subsidiary block faulted structures such as the parallel horst and graben structures on the north side of Lake Taupo. South of Wairakei the rhyolites form domes and sill like intrusions in the Huka group and have depressed older rocks thus obliteraing part of the earlier structural relief. Similar rhyolite intrusions to the north of Wairakei are shown by large magnetic anomalies as well as some surface exposures (Grindley, 1965).

The total amount of downfaulting in the Taupo-Rotorua Depression is considerable. Modriniak and Studt (1959) consider basement throughout most of the area to be more than 2000m below sea-level. Recent gravity modelling in the central TVZ (Rogan, 1982) shows a broad basement depression reaching 500-1000 m below sea-level with further 1-4km deep depressions marking the caldera structures and three other basins.

Fault movements are still continuing (Nairn, 1971). Nairn and Hull (1986) recorded numerous recent faults with visible surface expressions in the Waiotapu-Rotorua region and movements on many of the faults has been dated by the relative displacement of the tephras. Gregg (1960) has also recorded NNE-trending faults on either side of Tongariro massif some of which show recent displacement of up to 15 m; downthrown towards the volcanoes.

The TVZ is flanked by a plateau of flat lying sheets of ignimbrites erupted from vents within the zone which together with the TVZ was named the Central Volcanic Region by Thompson (1964).

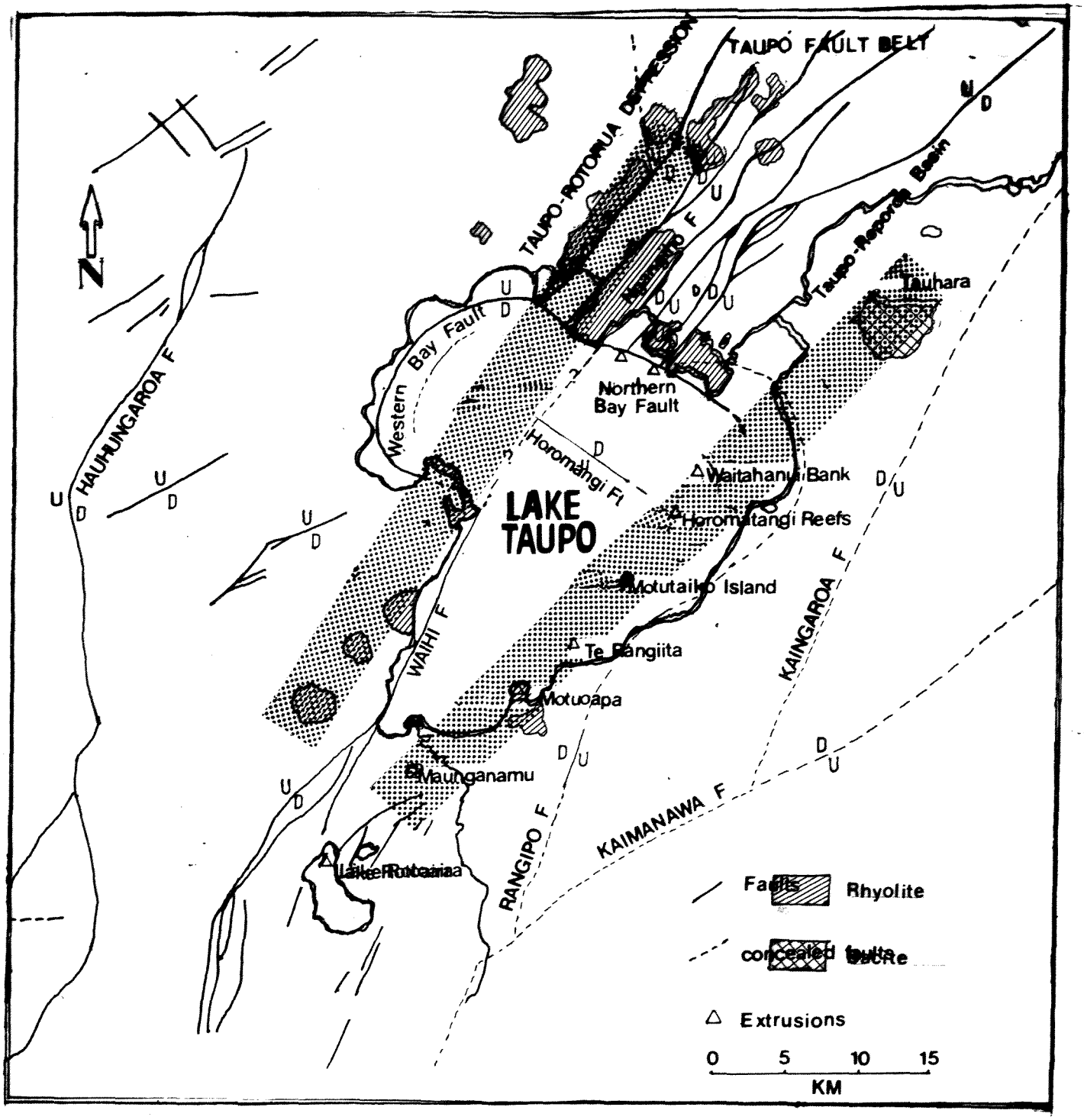

gure 2.3 : Structure of the Taupo Volcanic Centre, rhyolite dome extrusions in the centre are shown by triangles, some of these domes represent vents for some of the major pyroclastics erupted from the centre. Major faults associated with the centre are after Grindley (1960) and Northey (1982) U indicates upthrown side and D indicates downthrown side. The two shaded areas represent inferred deep-seated fractures controlling vent positions, the dashed line east of Tauhara represents a deep seated fracture.

2.3 THE TAUPO VOLCANIC CENTRE

2.3.1 Structures

As most of the other rhyolitic volcanic centres in the TVZ the boundaries of the Taupo Volcanic Centre are not well defined, Briggs (1976) notes a change in the slope of the Whakamaru Ignimbrites to the north-west of the Western Bay Lake Taupo, which probably reflects the outer limit of a major caldera collapse. According to Cole (1979) both the northern and the southern boundaries have almost certainly been displaced by the NNE-trending faults (Fig 2.3) to such an extent that no surface expressions are now visible. The north-eastern boundary has also been totally obscured by Holocene tephras.

Geophysical data over most of the lake are scarce, depth to basement is modelled from onshore gravity data. Two modest negative gravity anomalies at the north and south ends of the lake are considered to reflect the extremities of a large area of down faulted basement over most of the lake. Rogan (1982) notes that the down faulted basement over most of the lake area appears to lie greater than 2 km below sea-level and the total basement relief into the basin to be about 4 km below sea-level.

Major faults associated with the centre are mapped from onshore geology (Grindley, 1960, 1961) and seismic surveys (Northey, 1982). Faulting in the northern half of the lake is complex and reflects localized areas of collapse and tilting associated with young volcanism. In contrast, the southern half of the lake is underlain by a nearly continuous sub-horizontal 330-230 ka welded ignimbrite reflector and appears to represent a simple graben structure. Several large displacements (locally > 400 m) associated with NE-SW trending normal faults north of the lake are truncated by a fault with an offset exceeding 500 m which curves around and has determined the shape of the Western Bay (Fig 2.3; Western Bay Fault and Northern Bays Fault). The Western Bay Fault is presumably an old caldera fault. It has been generally accepted that this caldera structure which includes most of the northern part of the the lake is related to the Whakamaru Ignimbrite eruption ca. 300 ka (Briggs, 1973; Northey, 1983 and others), but Wilson et al. (1984) consider that the Western Bay area including the northern part of the lake was a

remenant caldera structure infilled by the 20 ka Kawakawa eruption. Another caldera structure on the NE part of Lake Taupo is interpreted to be a result of the 1800 years B.P. Taupo eruption. Central Lake Taupo is bounded by Northern Bay Fault, Waihi-Ngangiho(?), Horomatangi Fault and possibly the northward extension of Rangipo Fault. All these faults together with Western Bay Fault, have vertical offsets in excess of 500 m.

The southern portion of Lake Taupo is a graben between the Waihi and Rangipo Faults. These faults are related to those that control the structures in Northern Bay. Both belong to the Taupo Fault Belt and Northey (1983) suggested that they occur in an en echelon fashion with a left lateral displacement at Horomatangi Fault. Some seismic evidence of faulting in the southern part of the lake has been reported by Northey (1983).

The NE-SW trend is seen on several scales. On a large scale it extends beyond the area and reflects the overall structure of the TVZ. On a smaller scale it is seen in both vent lineations and fault orientations. Alignment of vents can be seen in the linear array of young vents down the east side of Lake Taupo (Froggatt, 1982; Wilson et al., 1984). Based on this evidence it was suggested that there are two deep seated fractures which determine the vent positions (Fig 2.3). Other large NE-SW trending faults are postulated to occur east of the lake but are concealed beneath young pyroclastics. North and south of the lake, displacement on the NE-SW trending faults decreases markedly. The southern extension of the Waihi Fault can however be traced for 25 km into the Tongariro Volcanic Centre.

Lake Taupo can be divided into an 'active' volcanic area in the region of the Horomatangi Reefs, and an older volcanic vent beneath the Western Bay. These two inferred vent areas have also been defined by magnetic anomalies which occur on both the Western Bay and Horomatangi Reefs area. Heatflow measurements beneath Lake Taupo show higher than average heatflow in the area of Horomatangi Reefs and Kawakawa Bay which is an evidence for the comparatively recent activity in those areas (Northey, 1983).

To the north of the Taupo Volcanic Centre is the Maroa Volcanic Centre. Lying between Maroa and the Taupo Volcanic Centre is the sediment filled Wairakei Basin, with a basement depression of 2 km below sea level. Wilson et al. (1986) postulated a major caldera which lies between Maroa and Taupo Volcanic Centre (Whakamaru Group Ignimbrite Caldera, the largest caldera yet postulated in the TVZ) The Whakamaru Group Ignimbrites which includes most of the 330-230 Ka ignimbrite in the Taupo-Maroa area this unit is described in more detail in the next chapter.

2.3.2 *Eruptive History*

The eruptive history of the pyroclastic and lava flows and domes from Taupo Volcanic Centre since activity started is summarized by Froggatt (1982), Wilson et al. (1984) and others. Older lava flows and domes from the volcanic centre include a rhyolite dome at Karangahape which has a different phenocryst content from the ignimbrites erupted from the centre (Ewart, 1968), and is surmounted by a small basic andesite scoria cone K-Ar dated as 290 ka (Stipp, 1968).

Pyroclastic eruptions from the general area of the Taupo Volcanic Centre may have started with the Whakamaru Group Ignimbrites. Since then the only significant ignimbrite unit from the the Taupo Volcanic Centre until the recent volcanism which commenced about 50 ka is a distinctive, poorly welded, brown ignimbrite which occurs on the north eastern end of lake Taupo and also occurs as lithic clasts in the 1800 years B.P. Taupo Ignimbrite which erupted from the Horomatangi Reefs area. From the presence of big boulders of this unit as lithics in the Taupo Ignimbrite, Wilson et al. (1984) suggested that the 1800 years vent was underlain by an in situ brown ignimbrite. At least two other ignimbrites are seen as vent derived lithics in the 20 ka and 1800a ignimbrites but their age and nature are unknown.

Post-Whakamaru Group, pre-20 ka volcanic domes in the Taupo Volcanic Centre lie mostly to the north of the lake. There is no separation of the northern Taupo domes from the southern Maroa domes. The northern Taupo domes are given a K/Ar date of ca. 110 ka (Stipp, 1968). This is supported by other field evidence (such as their degrees of

dissection). Obsidian bearing airfall, flow and surge deposits are associated with some of the domes and represent subordinate explosive activity probably preceding or associated with dome growth (Wilson et al., 1986).

Several small basaltic deposits occur in the vicinity of Lake Taupo. Four scoria cones (K-Trig basalts), one of which is K/Ar dated at ca 140 ka (Stipp, 1968), crop out along a linear trend west of Taupo township (Grindley, 1961). Tauhara, just east of Taupo, consists of several dacite flows and forms a prominent landform in the area. The dacite contains an unusual phenocryst assemblage of plagioclase, quartz, orthopyroxene, hornblende, magnesian olivine, and Fe-Ti oxide and is interpreted as a hybrid magma (Lewis, 1960).

From 50-20 ka five explosive eruptions occurred (Vucetich and Howorth, 1976) possibly from vents within the lake, and were substantial enough to generate widespread airfall deposits. At 20ka, a major eruption from within the lake generated extremely widespread airfall deposits and a volumino.us ignimbrite. Following the 20 ka eruption there is no record of any rhyolitic explosive activity until the current cycle of activity commenced at ca 10 ka. Since then nine explosive eruptions have occurred. The latest at ca 1800 a was the largest since the 20 ka event, and is the topic of this study.

Chapter III

PRE-TAUPO PUMICE FORMATION STRATIGRAPHY

3.1 INTRODUCTION

The stratigraphy in the vicinity of the Taupo Volcanic Centre has been established from surface geological mapping (Grindley, 1960, 1961), volcanological studies on the various tephra formations erupted from the Taupo Volcanic Centre and interbedded tephra from other volcanic centres in the TVZ (Healy et al, 1964 Vucetich and Pullar, 1973; Vucetich and Howorth, 1976; Froggatt, 1981 and others), and from geologic logs of geothermal boreholes in Wairakei area (Grindley, 1965; Steiner, 1970). Except for Holocene pumice which mantles the whole Wairakei area, and minor Holocene mudstones, drilling in the area has shown that the sub-surface rocks are late Tertiary to Pleistocene in age and consist of predominantly silicic volcanics and sedimentary rocks derived from them. Basic rocks are very rare and are present as xenoliths and basaltic ash. Andesites are locally present in subordinate quantities (Grindley, 1965).

The exact time when rhyolitic volcanism commenced in the central North Island is not known. Grindley (1965) considered that volcanism commenced at least as early as late Miocene and that it was well under way in the Pliocene reaching a climax in the early Pleistocene. Murphy and Seward (1981) have however presented fission-track dates and an assesment of available paleomagnetic dates which indicate that most of the ignimbrite formations of the Central Volcanic Region are Quaternary in age. The earlier rhyolitic volcanics may be buried deeply in the Taupo-Rotorua Depression and include most of the volcanics which are intercalated with the sediments of the Ohakuri Group. The oldest known ignimbrite formation from a source in the Taupo Volcanic Centre are members of the Whakamaru Group Ignimbrite.

The stratigraphy in the vicinity of the Taupo Volcanic Centre has to be considered in relation to the volcanic history of the area. To the north of Taupo is Maroa, and at least four distinct Maroa-derived ignimbrites mapped as Atiamuri, Haparangi, Huka and Orakonui ignimbrites and pumice breccias are known. Wilson et al. (1984) stated that these ignimbrites are not mapped beyond 40 km from the centre and are more localized than most of the other ignimbrites mapped in the TVZ. Field evidence suggests that they post-date the youngest of the 330-230 ka (Whakamaru Group) ignimbrites.

Rhyolitic pyroclastics, domes and flows are dominant in the Taupo Volcanic Centre, basalts, andesites and dacites form a minor constituent of the volcanic rocks of in the vicinity of Lake Taupo.

Fig 3.1 shows schematically the stratigraphic relationships of pyroclastic deposits, lava extrusions and intrusions and associated volcaniclastic sediments in the vicinity of the Taupo Volcanic Centre. Distribution and characteristics of each of the units are described in the text. The most important units from oldest to youngest are:

1.Ohakuri Group

2.Whakamaru Group Ignimbrites

3.Waiora Formation

4.Waiora Valley Andesites

5.Haparangi Rhyolite

6.Huka Falls Formation

7.Tauhara Dacite

8.Lake Taupo Group

a.Okaia Sub-group

b.Kawakawa Tephra Formation

c.Lake Taupo Sub-group

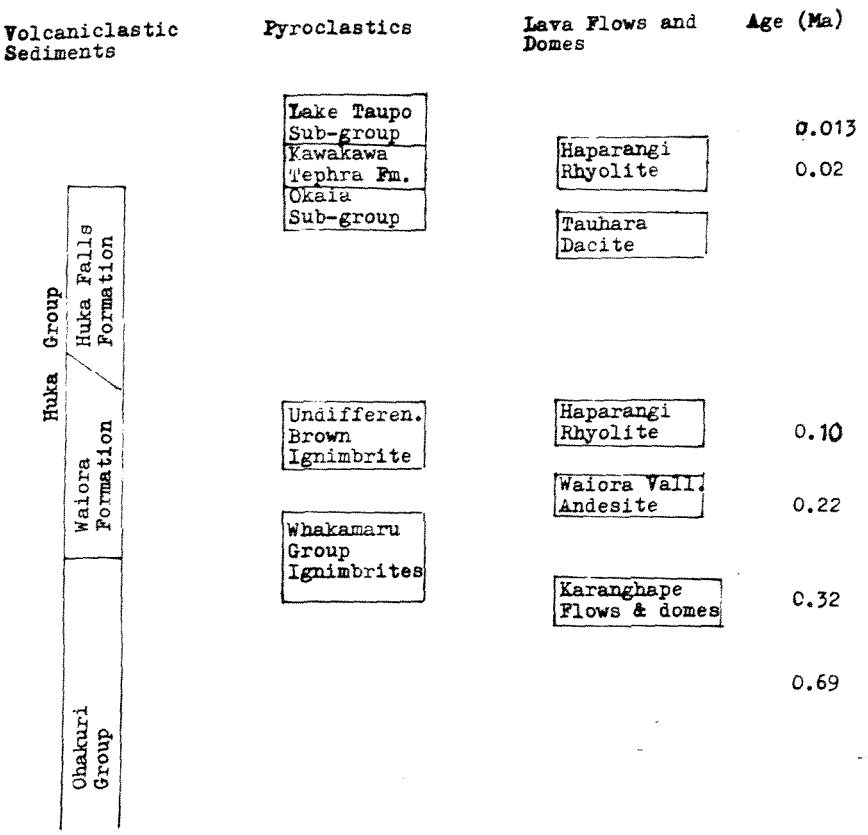

ure 3.1 : Generalized stratigraphic relationships of pyroclastic deposits, lava extrusions and associated volcaniclastic sediments in the vicinity of Taupo Volcanic Centre. Sources include Briggs (1973), Grindley (1965, 1960, 1961), Martin (1961), Steiner (1975) and Wilson *et al.* (*1985*).

3.2 *PRE-WHAKAMARU GROUP VOLCANICLASTIC SEDIMENTS (Ohakuri Group)*

3.2.1 *Name:*

The pre-Whakamaru group volcanics and volcaniclastic sediments were originally named the Ohakuri Group, for the exposures found in the Waiotapu area. A similar unit encountered by drilling at Wairakei underlying the Whakamaru Group ignimbrites (Wairakei Ignimbrites) was correlated to the Ohakuri Group (Grindley, 1965).

3.2.2 *Type Locality:*

Healy (1964) and othes designated Ohakuri dam as the type locality for Ohakuri Group. But recent studies have shown that the ignimbrite at Ohakuri Dam is younger than most of the ignimbrites of the Whakamaru Group, hence a type section at one of the Wairakei drillholes would be preferable.

3.2.3 *Age:*

From the relationship of these deposits to Paeroa and Marshall Ignimbrites, Briggs (1973) suggests that it is in part younger than 0.69 Ma and also younger than the Nukumaruan (Early Pleistocene) age assigned to it by most previous writers, The lower age limit is not exactly known.

3.2.4 *Source:*

The pre-Whakamaru Group volcaniclastic deposits accumulated in the rapidly subsiding volcano tectonic basins between Lake Taupo and Rotorua (Taupo-Rotorua Basin). Most of the pyroclastics have not yet been traced to their eruptive vents.

3.2.5 *Distribution and Stratigraphic Relationships:*

The Ohakuri Group crops out extensively in the Taupo-Rotorua Depression north of the Waikato River and has been encountered in deep drillholes in the Taupo-Reporoa Basin (Wairakei, Ohaaki, and Waiotapu). In the type area in the Taupo-Rotorua Depression, the Ohakuri Group is underlain by Marshall Ignimbrites and interbedded and overlain by

ignimbrites of the Paeroa Range Group, which in turn are overlain by the younger sediments and pyroclastics of the Huka Group (Briggs, 1973). At Wairakei this unit was drilled in only two wells and is overlain by the Wairakei ignimbrite (member of the Whakamaru Group Ignimbrites of Wilson et al. 1986) Although the holes continued for about 320 m below the Wairakei Ignimbrite it did not penetrate the full thickness of the deposits (Grindley, 1965).

3.2.6 Description:

The deposits comprise light brown to grey, weathered, often hydrothermally altered, massive to very thinly bedded pyroclastic flow deposits and interbedded fine-grained pumiceous sediments; which generally resemble the younger Waiora Formation. The pyroclastics are mainly lightly to non-welded, moderately compacted, pale grey to yellow brown, deeply weathered pumice breccia and tuff, and generally contain xenoliths of lithoidal rhyolite up to 25 mm in size. All the original glass at least in surface deposits is devitrified. The groundmass consists mainly of ash with a few pumice shards. Pumice fragments contain extremely flattened vesicles but are not appreciably distorted. Where hydrothermally altered (silicified), as at Ohakuri dam site, the pumice breccia form hard resistant outcrops. Deposition of the pyroclastics is closely related to accumulation of the lake sediments and some were probably deposited sub-aqueously (Briggs, 1973).

Steiner (1977) describes the unit penetrated by drilling at Wairakei as consisting of breccia with interbedded sandy waterlain tuff both essentially made up of varying amounts of pumice and rhyolite fragments. Detrital andesine and relatively rare quartz together with fine grained cryptocrystalline matrix fill the interstices. Pseudomorphs of ferromagnesian minerals are usually present, microscopic calcite veinlets are also common and rounded greywacke fragments are also reported. The rarity of quartz distinguishes the Ohakuri Group from the overlying Wairakei Ignimbrite.

3.3 WHAKAMARU GROUP IGNIMBRITES

3.3.1 Name:

The name Whakamaru Group Ignimbrite was informally given for the voluminous 330-230 ka welded ignimbrites cropping out in the central part of the TVZ by Wilson et al. (1986). The Whakamaru Group Ignimbrites include those ignimbrites mapped as Manunui and Whakamaru Ignimbrites to the west of the Taupo Volcanic Centre and Te Whaiti and Rangitaiki Ignimbrites to the east (Grindley, 1960; Martin, 1961; 1965; Briggs, 1973; 1976; and others). Members of the Whakamaru Group Ignimbrites have been encountered in geothermal drillholes in central TVZ. At Wairakei these ignimbrites were named Wairakei Ignimbrites (Grindley, 1965).

3.3.2 Type Locality:

Type localities for all the members of the Whakamaru Group Ignimbrites have been assigned by several previous workers (cf. Grindley, 1960; 1961; 1965; Martin, 1961; Briggs, 1973).

3.3.3 Age:

An age of 330-230 ka has been given for all members of the Whakamaru Group Ignimbrites based on fission track dates on several members of the group (Wilson et al. 1986).

3.3.4 Source:

It was generally accepted that the Whakamaru Group Ignimbrites were erupted from the northern Lake Taupo area and specifically the Western Bay has been considered a source caldera for ignimbrites exposed to the west of the lake. A new source represented by a major caldera in the northern Taupo-Maroa area is postulated on the basis of the distribution, volume and thicknesses of the members on surface outcrops and drillholes (Wilson et al., 1986).

3.3.5 *Distribution and Stratigraphic Relationships:*

The Whakamaru Group Ignimbrites are widespread in the central part of the TVZ. On the western side of the presumed source two distinct units, the Manunui and Whakamaru Ignimbrites of Martin (1961) were mapped west of the Hauhungaroa Range. The former is less crystal rich, having smaller and less numerous quartz phenocrysts, a lower content of hornblende and biotite and different lithologies of included lithic clasts. Some workers have regarded these two units as proximal (Whakamaru) and distal (Manunui) equivalents (Blank, 1965; Briggs, 1973), but Wilson et al. (1986) have suggested that the two units are separate. The Manunui Ignimbrite crops out mainly west of the Hauhangaroa Range. Between Hauhangaroa Range and Lake Taupo, thick exposures of the Whakamaru Ignimbrite, commonly containing Whakamaru-type lithics, forms all the surface outcrops.

In the Waikato River valley the outcrop has been intensively investigated and has been divided on various physical and mineralogical criteria into several sheets. Briggs (1976) reviews these divisions and broadly groups the ignimbrites into three sub-units. The Whakamaru Group Ignimbrites occur at the surface or at shallow depth over an area of several hundered kilometers east and north of the Waikato valley.

In the central TVZ, rocks correlated with the Whakamaru Group Ignimbrites have been recorded at several geothermal fields. The correlation with surface outcrops is on the basis of a very high phenocryst content, especially the presence of large, often corroded quartz crystals. From drillhole data Wilson et al. (1986) inferred that the ignimbrites are displaced downwards into the central axis of the TVZ and are also appreciably overthickened. At Wairakei only two drillholes penetrated the Whakamaru Group Ignimbrites (Wairakei Ignimbrites of Grindley, 1965) and then went in to a sequence of pumiceous pyroclastics (Ohakuri Group) and andesite lava. At Rotokawa two holes have passed through this group into a thick andesite lava which appears to be a pre-Whakamaru cone, at least 800 m high, resting on the basement greywacke.

In the central axis of the TVZ, Wilson et al. (1986) suggested that the Paeroa Ignimbrites (Martin, 1961; Healy et al., 1964), which occur to the north east of Maroa,

are probable correlatives, or lateral equivalents of one or more members of the Whakamaru Group Ignimbrites.

On the eastern side of the Taupo Volcanic Centre are the Te Whaiti and Rangitaiki Ignimbrites. Grindley (1960) mapped them as two separate units, but other workers (eg. Martin, 1961) have regarded the Rangitaiki as proximal and Te Whaiti as distal facies of the Whakamaru Group Ignimbrites. Wilson et al. (1986) have however presented several lines of evidence which suggest that they are entirely separate ignimbrite units.

3.3.6 Description:

The thickness of the Whakamaru Group Ignimbrites varies from the order of 50-150 m in surface exposures, and some drillholes (eg. Waiotapu and Broadlands) to greater than 300 m thick. From several sections, Wilson et al. (1986) suggest that at least four eruptions occurred during the period 330-230 Ka, which have contributed to the formation of the Whakamaru Group Ignimbrites.

Detailed petrographic and modal analysis data (Martin, 1961; Briggs,1973) show that these ignimbrites share a generally high crystal content (in order of decreasing abundance are plagioclase, quartz, hypersthene, sanidine, Fe-Ti oxides and rare biotite and hornblende). This assemblage, with abundant large quartz crystals, is very distinctive. As a result there has been a tendency to treat all these ignimbrites as the product of a single eruptive episode believed to have been centred in the Lake Taupo area. Considerable support for this view has been described by Froggatt et al. (1986) who present detailed glass major and rare earth element data which demonstrate that there is only one correlative distal airfall ash with the high crystal content, mineral assemblage and distinctive large quartz crysals typical of the Whakamaru Group Ignimbrites.

3.4 WAIORA FORMATION

3.4.1 Name:

The name Waiora Formation was given to pyroclastics and interbedded sediments between the Huka Formation and the top of the Wairakei Ignimbrites by Grindley (1965).

3.4.2 Type Locality:

The type locality for Waiora Formation is drillhole No 213 at Wairakei where Waiora Formation occurs between 255.4-154.9 m a.s.l. and between 81.4 m a.s.l.-445 m b.s.l. Waiora Formation excludes rhyolite which occur between 154.9-81.4 m a.s.l. at the type section (Grindley, 1965).

3.4.3 Age:

Waiora Formation is considered to be Castlecliffian by Grindley (1960; 1965)

3.4.4 Source:

The sediments of the Waiora Formation accumulated in fresh water lakes occupying the subsiding volcano-tectonic Taupo-Rotorua Basin. They are intimately associated and partly derived from the interbedded pyroclastic units.

3.4.5 Distribution and Stratigraphic Relationships:

Waiora Formation forms a thick sequence of pyroclastics and interbedded sediments that partially fill the Taupo-Reporoa Basin from Lake Taupo to the northern Paeroa scarp area. Outcrops of the Waiora Formation are scarce, apart from Rotokawa thermal area and a possible outcrop at the foot of the Kaiapo Fault scarp. Waiora Formation does not crop out in the southern part of the basin (Grindley, 1960; 1965). It is well represented in drillholes in the Wairakei geothermal field where it forms the main aquifer. At Wairakei it rests conformably on the Wairakei Ignimbrite, is capped by Huka Formation and is intruded by the Haparangi Rhyolite from the Taupo and Maroa volcanic centres. In the western part of the Wairakei geothermal field it is intruded by Waiora Valley andesites (Grindley, 1965).

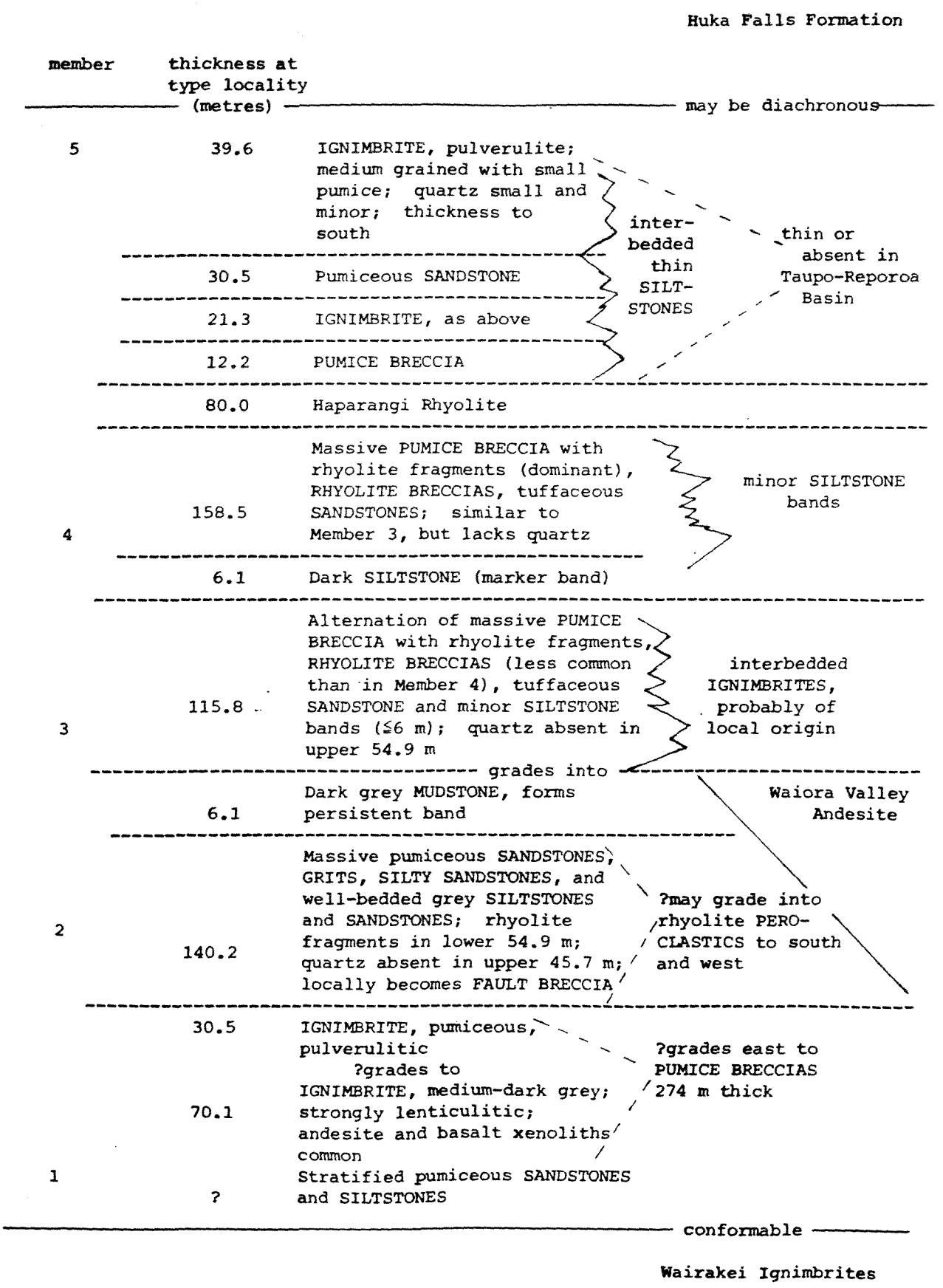

le 3.1 : Lithology and composition of the Waiora Formation in the Wairakei area, based on Grindley (1965), Healy (1965), Ewart (1968); after Briggs (1973).

Waiora Formation ranges from about 400 m over the Wairakei block to more than 760 m in the Taupo-Reporoa Basin to the east and small basins to the west. The pyroclastics of the Waiora Formation are apparently the product of numerous small pyroclastic eruptions. Grindley (1965) has suggested that much of this pyroclastic material possibly represent early rhyolitic eruptions from Taupo Volcanic Centre. The repeated occurrence of Atiamuri Ignimbrites within the upper Waiora Formation suggests that pyroclastics from the Maroa Volcanic Centre may be present.

3.4.6 Description:

Waiora Formation comprises buff coloured massive, non-sorted, non-welded pumice breccias commonly 3-5 m thick; tuff and ignimbrites alternating with lacustrine pumiceous sandstones and minor thin siltstones. Briggs (1973) further describes the Waiora Formation as more dominated by pyroclastics when compared to the Huka Formation, and generally similar to the older Ohakuri Group in appearance. The general sequence in the type area where Grindley (1965) has defined five members is shown on Table 3.1.

3.5 WAIORA VALLEY ANDESITE

3.5.1 Name:

The name Waiora Valley andesite was given by Grindley (1965) to andesite flows drilled in several of the deep steam wells in Wairakei geothermal field.

3.5.2 Type Locality:

The type locality for Waiora valley andesite is drillhole 48 at Wairakei where the andesite flows are thickest.

3.5.3 Age:

The Waiora Valley andesite is of the same age as member 2 of the Waiora Formation (Castlecliffian) according to Grindley (1965)

3.5.4 Source:

Grindley (1965) suggested that the andesite was probably extruded as separate plugs or pipes at intersection of three NW-trending faults with NE-trending faults in the Wairakei area.

3.5.5 Description:

In the Wairakei area the andesite is invariably altered and contains numerous large partly or completely altered andesine phenocrysts with comparatively small pseudomorphs of ferromagnesian minerals in a cryptocrystalline or hyalopilitic altered groundmass (Steiner, 1977).

Another andesite flow in the vicinity of Taupo Volcanic Centre occurrs at Rolles Peak (Grindley, 1961) north east of Mount Tauhara. It lies on or close to the Kaingaroa Fault and may have been erupted along it. Petrographically the rock is holocrystalline, containing sparse phenocrysts of zoned andesine and subordinate hypersthene set in a base composed of augite, hypersthene and labradorite with accessory magnetite and tridymite. From the degree of erosion, Grindley (1965) suggested an early to middle Hawera age for the Rolles Peak Andesite.

3.6 HUKA FALLS FORMATION

3.6.1 Name:

The unit occurring between the top of the Waiora Formation and the base of the Oruanui Formation (Kawakawa Formation or Wairakei Breccia) at Wairakei was named Huka Falls Formation.

3.6.2 Type Locality:

The type section of Huka Falls Formation established by Grindley (1965), is Wairakei drillhole 213.

3.6.3 Age:

The age of the Huka Falls Formation is from late Castlecliffian to early Hawera (ie. from about 300-20 ka) (Grindley, 1965).

3.6.4 Source:

Huka Falls Formation consists of fresh water sediments accumulated in lake(s) occupying the volcano-tectonic Taupo-Reporoa Basin (Fig 2.3) and smaller subsidence basins to the north; the location of source vents for the minor interbedded pyroclastics is uncertain.

3.6.5 Distribution and Stratigraphic Relationships:

Huka Falls Formation is a series of widespread, well-bedded, lake sediments and interbedded pyroclastics that occur between Lake Taupo and Bay of Plenty. The sediments accumulated in fresh water lake(s) formed in the subsiding Taupo-Reporoa basin and some areas to the north. Both commencement and termination of the deposits were probably diachronous; combined with the cyclic and local nature of the deposits and long period of accumulation, this makes correlation between sections and interbedded units generally unreliable. Grindley (1965) extended the deposition of the Huka Falls Formation from late Castlecliffian to early Haweran, based on dating and correlation of pollen sequences. If the correlation between Oruanui Formation and Wairakei Breccia is accepted, the uppermost Huka Falls Formation would be considerably younger than Grindley (1965) supposed (younger than 20 ka). According to Briggs (1973) deposition of Huka Falls Formation started earlier in the Bay of Plenty region than the Taupo-Reporoa Basin and elsewhere stratigraphic relationships suggest that deposition ceased somewhat earlier, probably due in part to local filling of depositional basins by major volcanic eruptions such as those producing the Kaingaroa Ignimbrite.

At the type locality at Wairakei, Huka Falls Formation is overlain by "Wairakei Breccia". Grindley (1965) has noted that the contact is conformable with no apparent break in depositon between the sandstone of the upper member of the Huka Falls Fomation and the basal tuff of the "Wairakei Breccia".

member	thickness at type section (metres)		
			Oruanui Formation ("Wairakei Breccia")
		conformable	
4	12.2	Tuffaceous SANDSTONE with pumice and rhyolite lapilli and abundant quartz	interbedded AIR-FALL-BEDS, probably include Mangaoni Lapilli and Rotoehu Ash
	18.3	Grey-green tuffaceous SANDSTONE, thin MUDSTONE bands	
3	24.4	Light grey MUDSTONE, thin SANDSTONE bands; commonly diatomaceous; locally (Taupo-Reporoa Basin) pure DIATOMITE; cold climate pollen	
2	9.1	Coarse tuffaceous SANDSTONE; interbedded vitric TUFF with pumice lapilli and scattered andesite-basalt fragments; includes (Taupo-Reporoa Basin) PUMICE BRECCIAS (Te Mihi Basin) thin MUDSTONE bands	
1	15.2	Medium to dark grey MUDSTONE, well bedded with SILTSTONE and SANDSTONE bands; similar to member 3 but diatoms absent to scarce; pollen generally indicates warmer climate than above; locally (Te Mihi Basin) apparently becomes CONGLOMERATE (hydrothermal mudflow?) with fine-grained pumiceous groundmass and interbedded pumiceous SANDSTONES	
	3	Dark grey MUDSTONE	
		may be diachronous	
			Waiora Formation

ble 3.2 : Lithology of Huka Falls Formation in the Wairakei area, based on Healy (1965) and Grindley (1965); after Briggs, 1973.

In the Taupo-Rotorua Basin it generally rests on either Waiora Formation or Rangitaiki Ignimbrites and is grouped with the Whakamaru Group Ignimbrites. Neither of these formations are dated, but Rangitaiki Ignimbrites are similar in age to Whakamaru Ignimbrites (ie. ca 330-230 Ka). From the above relationships, Briggs(1973) sugested that deposition of the Huka Falls Formation began in the uppermost Castlecliffian and continued through most of the Haweran up to ca 20 Ka. In the Bay of Plenty region and locally in the Taupo-Reporoa Basin, deposition ceased at an earlier age.

3.6.6 Description:

Huka Falls Formation consists dominantly of thinly bedded, buff-grey to cream, locally diatomaceous and carbonaceous lake sediments with interbedded pyroclastics. The general fine grain size of the sediments and their dominance over the pyroclastics serve to distinguish it from the Waiora Formation. The Huka Falls Formation ranges from less than 61m thick on the Wairakei Block to more than 305m in the Taupo-Reporoa Basin to the east. Four members have been distingished at the type area at Wairakei (Grindley, 1965 Table 3.2). These members extend from the Wairakei Block into the Taupo-Reporoa Basin to the east. Correlation of these four members outside the Wairakei area has not been possible (Briggs, 1973).

3.7 TAUHARA DACITE

Tauhara is a prominent dacite volcano located NE of the Taupo Volcanic Centre. Lewis (1968) describes Tauhara as a multiple volcano, consisting of five youthfully disected cumulo-domes with some talus banks surrounding the lower slopes of the two domes. He also describes Maunganamu (a rhyolite dome) located 5 km SW of Tauhara. Worthington (1985) recognized previously overlooked domes, and considers Tauhara to consist of at least seven (and probably eight) domes, several lava flows and two pyroclastic flows. He divided the domes and flows into five groups from structural, petrographic and chemical evidence.

3.7.1 Age:

A minimum age of 10 ka (Late Pleistocene) was given to Tauhara Volcano based on relation with Waitahanui Breccia which buries the disected base of the volcano (Grindley, 1961). Stipp (1968) obtained a K/Ar age of 31±3 ka for the Hipaua Dome of the Tauhara dome complex. Worthington (1985), taking into consideration the inherent sources of inaccuracy in the K/Ar dating method, suggested tephrostratigraphy is the best method in determining the age of Tauhara. Using the complete record of tephrochronology from the Taupo Volcanic Centre in the last 50,000 years, Worthington (1985) concluded that five of the seven Tauhara domes were extruded between 15 and 20 ka (probably 19-20 ka). The remaining Tauhara domes (western and central domes) are older but it is not known by how much.

3.7.2 Description:

The Tauhara dacites contain phenocrysts of plagioclase, orthopyroxene, clinopyroxene, amphibole (hornblende), and quartz with accessory olivine, biotite, magnetite, and apatite. These are set in a groundmass composed of plagioclase microlites, small crystals of magnetite, cristobalite, hornblende, orthopyroxene and rarely clinopyroxene. The texture ranges from hyalopilitic through pilotaxitic to felted. Using the phenocryst proportion scheme proposed by Clark (1960) for the andesites of the Tongariro Volcanic Centre, Worthington (1985) classifies dacites of the Tauhara Dome Complex into seven major types based on the proportion of plagioclase, pyroxene, and hornblende phenocrysts.

3.8 HAPARANGI RHYOLITE

3.8.1 Name:

The name Haparangi Rhyolite was first given by Grange (1937) to steep-sided, craterless rhyolite volcanic domes, common throughout the central volcanic region. Grindley (1960) classified the Haparangi Rhyolite into the younger and older dome building phases and gave the name Haparangi Rhyolite to the volcanic domes and Haparangi Rhyolite Pumice

to the associated pyroclastics. At Wairakei, Grindley (1965) applied the name to the subsurface rhyolites encoutered by drilling to the south-west and north of the production area.

3.8.2 Age:

The Haparangi Rhyolites cover a wide range of time in the Central Volcanic Region. Grindley (1960) mapped them as middle Pleistocene to late Pleistocene in age. The rhyolites mostly post date the sediments and pyroclastics of the Huka Group. Several large, faulted, compound and simple rhyolite domes just north of the lake appear to have an earlier age and one lava has been dated at 120 ka (Stipp, 1968).

3.8.3 Description:

The domes generally consist of a core of lithoidal rhyolite, commonly with steep dipping flow banding, chilled zones of banded obsidian and a perlitic rhyolite margin. Petrographically the rhyolites contain as essential minerals; oligoclase, quartz, and hornblende and as accessory minerals; hypersthene, augite, biotite, and magnetite. Texturally they may be pumiceous, perlitic, spherulitic, lithoidal or glassy obsidian.

Following the classification of rhyolitic lavas of TVZ by Ewart (1968), Daorerk (1972) classified members of the Haparangi Rhyolite domes in the Taupo Volcanic Centre into three types on the basis of their ferromagnesian phenocryst assemblages. Steiner (1977) classified the rhyolites encountered by drilling at Wairakei into quartz-free and quartz-bearing varieties.

3.9 LAKE TAUPO GROUP

The post-50 ka period was dominated by tephra erupted from Taupo Volcanic Centre. Numerous exposures in road cuttings etc. have enabled a particularly complete tephra stratigraphy record for this period to be compiled, as well as isopach maps from which tephra volumes have been estimated. Radiocarbon dating has enabled a detailed chronology to be constructed, particularly for the post-20 ka record.

		TEPHRA FORMATION		YEARS B.P. (TL OLD)	C14 No.	SAMPLE TYPE
LAKE TAUPO GROUP (LTG)	TAUPO SUBGROUP (TSG)	TAUPO PUMICE FORMATION	(TPF)			
		Taupo Ignimbrite	(TIg)			
		Taupo Lapilli	(TL)			
		Rotongaio Ash	(Rt)	1820 ± 20 (Mean)		
		Hatepe Tephra (ash / lapilli)	(Ht)			
				2010± 60	1068	P
		MAPARA TEPHRA Fm.	(Mp)	2150 ± 48	1069	P
				2670 ± 50	1070	P
		WHAKAIPO TEPHRA Fm.	(Wo)	2730 ± 60	1071	P
				3130 ± 65	1062	P
				3170 ± 80	504	P
				3280 ± 110	3947	P
		WAIMIHIA TEPHRA Fm.	(Wm)	3150 ± 90	180	C
		Waimihia Ignimbrite		3440 ± 80	2	C
		Waimihia Lapilli		3270 ± 65	1061	P
				3440 ± 80	505	P
		HINEMAIAIA TEPHRA Fm.	(Hm)	4650 ± 80	4574	C
				5680 ± 130	3950	P
		MOTUTERE TEPHRA Fm.	(Mt)	5370 ± 90	3951	P
				5370 ± 90	4846	C
		OPEPE TEPHRA Fm.	(Op)	8850 ± 1000	185	C
		PORONUI TEPHRA Fm.	(Po)	9740*		
		KARAPITI TEPHRA Fm.	(Kp)	9780 ± 170	1372	W
				9910 ± 130	4847	C
		KAWAKAWA TEPHRA Fm.	(Kk)			
		Oruanui Breccia				
		Scinde Island Ash		c.20,000#		
		Aokautere Ash				
	OKAIA SUBGROUP (OSG)	POIHIPI TEPHRA Fm.	(P)	20 500$		
		OKAIA TEPHRA Fm.	(O)	21 000$		
		TIHOI TEPHRA Fm.	(Ti)	38 000$		
		WAIHORA TEPHRA Fm.	(W)	39 000$		
		OTAKE TEPHRA Fm.	(Oe)	40 000$		

P = PEAT
C = CHARCOAL
W = WOOD

* Date extrapolated by Topping (1973).
\# Date from Vucetich & Howorth (1976a).
$ Ages estimated by Howorth (1976).

Table 3.3 : Stratigraphy of the Taupo Tephras, together with relevant radiocarbon dates and ages estimated for the older tephras (From Froggatt, 1982).

Howorth et al. (1981) grouped all the tephra erupted from the Taupo Volcanic Centre in this period into the Lake Taupo Group which consists of :

1.Okaia Sub-group

2.Kawakawa Tephra Formation

3.Taupo Sub-group

Table 3.3 shows the stratigraphy of all the post 50 ka tephra erupted from vents within the Taupo Volcanic Centre together with relevant radiocarbon dates.

3.9.1 Okaia Subgroup

From 50-20 ka five widespread rhyolitic airfall deposits were erupted from vents within the Taupo Volcanic Centre (Vucetich and Howorth, 1976), two of which were phreatomagmatic in nature. Froggatt (1982) regards the Okaia subgroup tephras as mineralogically distinct from the overlying Taupo Subgroup tephras on the basis of the mafic mineralogy (Fig 3.2). Other interbedded tephra from Okataina Volcanic Centre of this age in the Taupo district are described by Vucetich and Howorth (1976) and include Tahuna Tephra Formation and Rotoehu Ash member of the Rotoiti Breccia Formation.

3.9.2 Kawakawa Tephra Formation

3.9.2.1 Name:

The Kawakawa Tephra Formation was first defined by Vucetich and Howorth (1976). Their type section for this formation is on the Whangamata Road (N93/373458) and comprises three members; the Aokautere Ash, the Scinde Ash and the Oruanui Breccia. Self (1983) informally named this formation as the Wairakei Formation and introduced new members to the formation and gave volcanological interpretations to the eruption.

3.9.2.2 Source:

Froggatt (1982) considered all tephra in the Kawakawa Formation to be from a source from the Taupo Volcanic Centre.

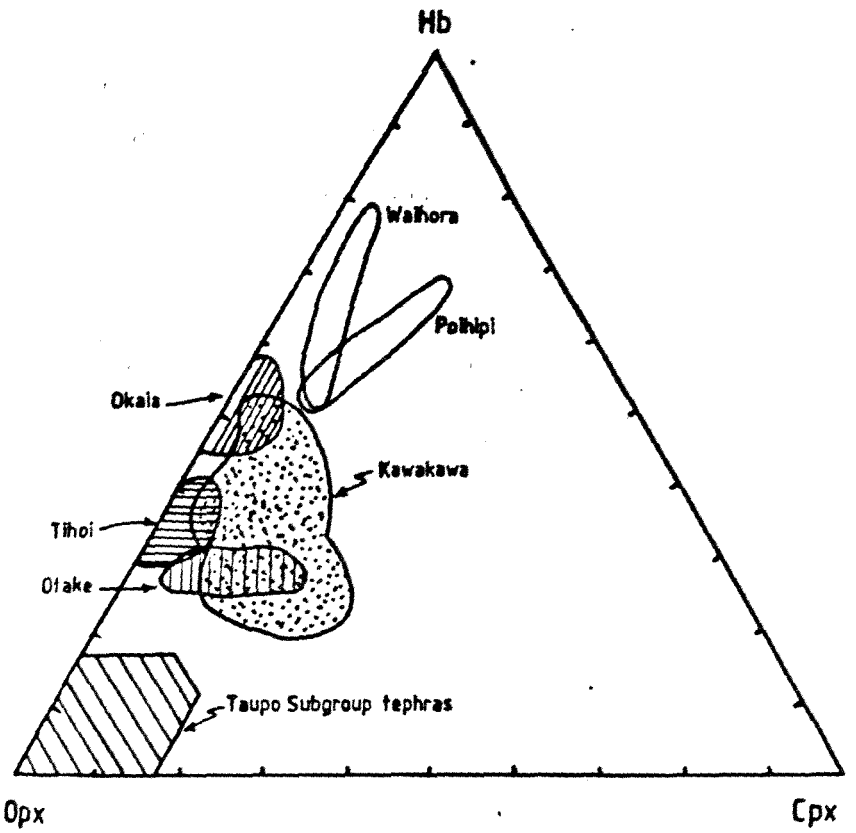

Figure 3.2 : Ternary plot showing the mafic mineralogy of the Lake Taupo Group tephras, data for Kawakawa Tephra from from Howorth et al. (1981) and for Okai Subgroup from Roxburg (1976); (From Froggatt, 1982)

Self (1983) has also shown from several isopach and isopleth maps of members of the Kawakawa Tephra Formation that the source is in the same general area. Wilson et al. (1984) postulated that the northern part of Lake Taupo including the Western Bay area is a result of caldera subsidence following this eruption.

3.9.2.3 Age:

The age of the Kawakawa Tephra Formation, as determined by several C-14 dates, is 20 ka (Vucetich and Howorth, 1976).

3.9.2.4 Distribution and Stratigraphic Relationships:

The Kawakawa Tephra Formation because of its unusually large volume (approximately 100 km^3 is widespread in the Central Volcanic Region. The eruptive episode which produced it was of very short duration and is recorded over a wide area. The deposits are widely used as marker horizons even in some marine sediments. The unwelded pyroclastic flow member (Oruanui Breccia member) has a similar distribution to that of the Taupo Ignimbrite in that it covers most of the central North Island, whereas the airfall members of the Kawakawa Tephra Formation are widespread to the south and southeast of the vent.

The Kawakawa Tephra Formation includes members of the Oruanui Formation of Vucetich and Pullar (1969) and was considered to be the direct equivalent of the "Wairakei Breccia" or "Wairakei Lapilli Tuff" of Steiner (1953) which overlies the Huka Falls Formation in many boreholes at Wairakei geothermal field.

To the south of Wairakei, members of the Kawakawa Tephra Formation correlate with or are equivalent to most or all of the pumice breccia mapped as Waitahanui Breccia (Grindley, 1960; 1961). Briggs (1973) has also suggested that the Oruanui Breccia may correlate with the Maroa derived Haparangi Rhyolite Pumice of Grindley (1960).

In the Taupo district the lower contact of the Oruanui Breccia Member is seldom exposed, and the top of the formation is almost invariably eroded and overlain by the aeolian Mokai Sands and the fluvial Hinuera Formation.

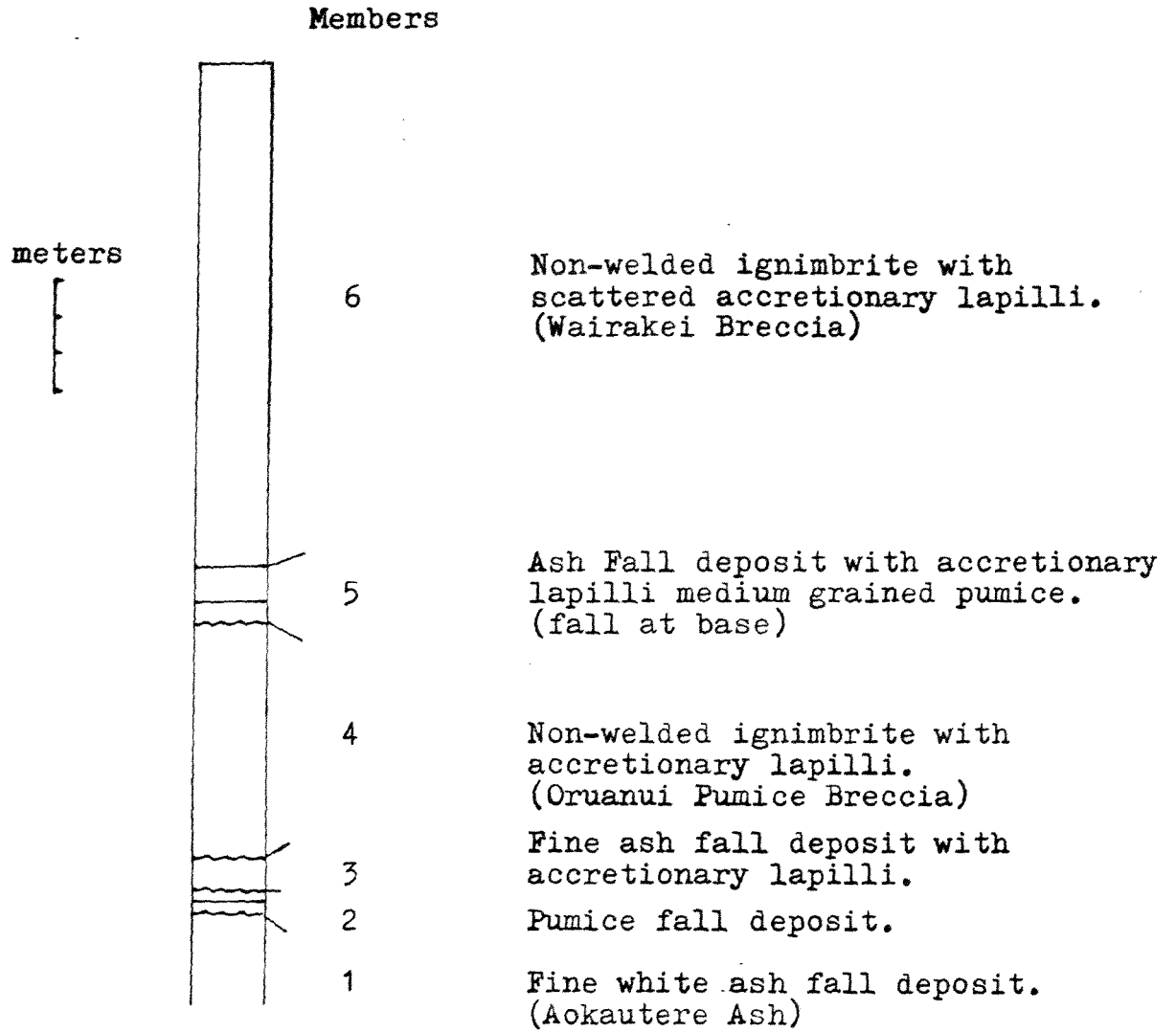

Figure 3.3 : Composite section through the Kawakawa Tephra Formation (Wairakei Formation) based on locations within 20 km from source; previous names of Vucetich and Howorth (1976) are given in parantheses. (From Self, 1983).

The eruption of the Kawakawa Tephra Formation was followed by a period of somewhat less than 10,000 years of rapid and extensive erosion and deposition, before the next rhyolitic tephra from Taupo was erupted.

3.9.2.5 Description:

Vucetich and Howorth (1976) have given a detailed description of the three members of the Kawakawa Tephra Formation at their type section on the Whangamata Road. Following this work a more comprehensive description supported by grain size analysis on several members of the formation was given by Self (1983). In the latter study six members were defined in the informally named Wairakei Formation, consisting of interbedded fine-grained, pyroclastic fall and flow deposits in the proximal regions. In many silicic eruptions ignimbrites are preceded by a plinian deposit (plinian activity). Both phreatoplinian units in the Kawakawa Tephra Formation (Wairakei) eruption were followed by an ignimbrite-forming phase. This eruption is interpreted to have been phreatomagmatic throughout. Each phase of the eruption sequence generated its own characteristic deposit. Changes in the eruption style were probably due to fluctuations in the mixing ratio of lake water with vesiculating magma, reflecting a complex interplay between water access, mixing processes and morphology of the vent area.

The sequence of events during this eruption is described by Self (1983). The air fall members are all of phreatoplinian type. The accretionary lapilli-rich layers represent some of the most completely fragmented, finest, ash beds yet documented. Violent rain flushing caused particle aggregation and formation of accretionary lapilli. The pyroclastic flows generated by the collapse of phreatoplinian eruption columns were steam laden, cool, thick and highly mobile. Froggatt (1982) has shown that the Kawakawa Tephra Formation is rich in hornblende when compared to other tephra formations erupted from vents in the Taupo Volcanic Centre.

3.9.3 Taupo Sub-group

The post 10 ka tephra erupted from vents within the Taupo Volcanic centre are collectively classified as the Taupo Sub-group by Howorth et al. (1981). The tephra formations are shown on Table3.3 with their radiocarbon ages. Source vents for each of the tephra formations have been located from isopach maps (Vucetich and Pullar, 1973).

Most of the members of the Taupo Sub-group consist of ash, pumice lapilli and rare lithics and are of air-fall origin. Two ignimbrite units, namely Waimihia Ignimbrite and Taupo Ignimbrite, were erupted during this period (Froggatt, 1982). The latter is among the major ignimbrite units erupted from a vent in Lake Taupo and covers a considerable area around the volcanic centre. Taupo Ignimbrite is described in detail in the following section. Five rhyolitic tephras from Okataina Volcanic Centre, one from Maroa and two prominent andesite tephras from Tongariro Volcanic Centre are interbedded with the Taupo Sub-group tephras in the Taupo district (Vucetich and Pullar, 1973). Froggatt (1982) has shown that the Taupo Sub-group tephras are distinct from other tephra formations in the Lake Taupo Group in that they contain orthopyroxene as a dominant mafic mineral.

Chapter IV

THE TAUPO PUMICE FORMATION

4.1 INTRODUCTION

The Taupo Pumice Formation is a widely dispersed pyroclastic deposit which reached most parts of the central North Island east and north-east of Lake Taupo. It is the product of the most recent series of eruptions from Lake Taupo. The C-14 age is about 1800Y.B.P. (Healy, 1964) but in a recent work by Wilson et al. (1980) historical evidence has been presented to show that the calendar date of the eruption may be 186 A.D. Arguments against the authenticity of the historical evidence have been presented by Froggatt (1981).

From isopach maps of the various members of the Taupo Pumice Formation, Healy (1964) deduced that the source vent was to the east of the present Lake Taupo. More recently, Froggatt (1979, 1981) and Walker et al. (1981b) have established the source to be within Lake Taupo, most probably at Horomatangi Reefs. Other evidence for the source of the Taupo Pumice Formation includes orientation of charred logs which are the prominent features of the Taupo Ignimbrite (Froggatt et al., 1981), grainsize distribution of pumice and lithic material, absence of ballistic lithics (which in plinian type eruptions usually occur in near vent areas) and bathymetry of Lake Taupo (Irwin, 1976).

The stratigraphy of the Taupo Pumice Formation has been the subject of several refinements from the early days of geological work in the area. Grange (1937) first defined the formation as the "Taupo Showers" and considered it to be airfall and much of the pumice to be water lain. Healy (1964) gave the Taupo eruption products formation status and introduced members to the Formation. Froggatt (1981) revised all previous works on the stratigraphy of the Taupo Pumice Formation, redefined some of the members and introduced new members to the formation.

Table 4.1 Summary of the stratigraphy of the Taupo Pumice Formation. Volume estimates are from Wilson (1985).

Healy (1964)	Froggatt (1981)	Wilson and Walker (1985)	Volume situ/km	Volume magma/km	Volume Lithics/km
Taupo Pumice	--	Secondary Deposits	-	-	-
Alluvium	--	Floated Giant Pumice	-	-	-
	Upper unit	Secondary Deposits	-	-	-
Upper Taupo Pumice and Rhyolite Block Bed members 1 & 2	Taupo Ignimbrite Middle unit Lithic lag Layer	Taupo Ignimbrite Layer 3 Layer 2 Layer 1	31	10	2.1
	Lower unit	Early Ignimbrite Flow units	1.5	0.5	0.05
Taupo Lapilli (member 3)	Taupo Lapilli	Taupo Plinian Pumice	23	5.1	0.73
Rotongaio Ash (member 4)	Rotongaio Ash	Rotongaio Phreatoplinian Ash	1.3	0.7	0.09
Putty-coloured Ash (member 5)	Hatepe Tephra	Hatepe Phreatoplinian Ash	2.5	1.0	0.12
Hatepe Lapilli (members 6-8)		Hatepe Plinian Pumice	6	1.4	0.18
		Initial Phreatomagmatic Ash	0.015	0.005	negl.
PALEOSOL DEVELOPED ON OLDER DEPOSITS			-	-	-
		Sub total Layer 3 deposits of Ignimbrite Phases	65 upto ca.20	18.7 upto ca.7	3.27 negl.
		Primary material now under Lake Taupo	20-60	8-20	?
		Total volumes	>105	>35	>3.27

Wilson and Walker (1985) gave new volcanological names and interpretations to some of the members. Table 4.1 summarizes the stratigraphy and volume estimates on the Taupo Pumice Formation. Volume estimates are from Wilson and Walker (1985).

Products of the Taupo eruption are found over a wide area in the central North Island and have been used as an important stratigraphic marker units for the Holocene tephra in the region.

4.2 ERUPTION HISTORY

The stratigraphic sequence of the erupted tephra shows that the Taupo eruption began with minor phreatomagmatic activity which generated the initial ash (Wilson and Walker, 1985). From the pumiceous nature of this unit it is thought that vesiculated magma reached the surface to mix with the pre-eruption Lake Taupo resulting in phreatomagmatic activity.

The initial ash was followed by eruption of the much coarser and more widely dispersed Hatepe Plinian Pumice which suggests that the mass eruption rate increased rapidly to clear the vent area of water and begin plinian activity. The eruption of the Hatepe Plinian Pumice was followed by the Hatepe Phreatoplinian Ash which implies a sudden increase in the lake water flux into the vent. However the pumiceous nature of the Hatepe Ash and the minor intercalated layers of plinian style material suggests that the vesiculation and fragmentation levels were at some depth and that the phreatomagmatic activity was caused by a normal plinian eruption column interacting with large quantities of surface water. After the eruption of the Hatepe Phreatoplinian Ash there was a time break, during which the phreatoplinian ash was eroded by water derived from the vent area (an explosive ejection of water due to the interaction of magma with the lake water).

The discharge of material then resumed, generating the phreatoplinian Rotongaio Ash, most of which is poorly or non vesiculated obsidian. The wide-spread nature of the Hatepe and Rotongaio phreatoplinian deposits suggests that the eruptions were fairly

powerful events, sustained by eruption rates comparable to that during the earlier plinian event. However, even if there were similar eruption rates, the eruption columun heights during the phreatoplinian activity would have been lower than during the plinian event owing to the loss of thermal energy in the magma-water interaction (Wilson et al. 1978).

At the close of the Rotongaio phreatoplinian phase, the nature of the eruption changed abruptly and the "wet" vent reverted to a "dry" vent again. The erupted material changed from obsidian or dense pumice to very low density pumice, implying that the vent was cleared of water and that both the vesiculation and the fragmentation surfaces moved downwards very rapidly. The Taupo plinian event was exceptionally energetic with an eruption column probably as high as 50 km and was classified into a new class of ultra-plinian eruption by Walker (1980).

The sequence to the end of the Rotongaio phreatoplinian phase could be interpreted as representing a single magma batch, initially volatile rich (initial ash and Hatepe Plinian) and later volatile poor (Rotongaio Ash). The abrupt renewal of plinian activity suggests the arrival of a new, more volatile rich magma batch, which had a similar phenocryst content (Froggatt, 1982).

The early ignimbrite flow units are undoubtedly intraplinian (formed during the eruption of Taupo Plinian Pumice) as described by Froggatt (1981) and the question as to whether they were generated synchronously with the plinian deposit or in discrete column collapse episodes is discussed by Wilson and Walker (1985). The Taupo Ignimbrite was then formed by a column collapse of the erupted material, because of the discharge rate was much greater than that capable of forming a stable plinian column. The high lithic content of pre-Taupo ignimbrite air-fall deposits plus early flow units (ca. 1.2 km^3) implies that vent widening by erosion was important and possibly led to column collapse during the course of the eruption.

The following sections give a breif description of the most important members of the Taupo Pumice Formation. Description of selected sections of the Taupo Pumice Formation is given in Appendix 1.1. Fig 4.1 shows the location of all described and sampled sections for the study of the lithics in the Taupo Pumice Formation.

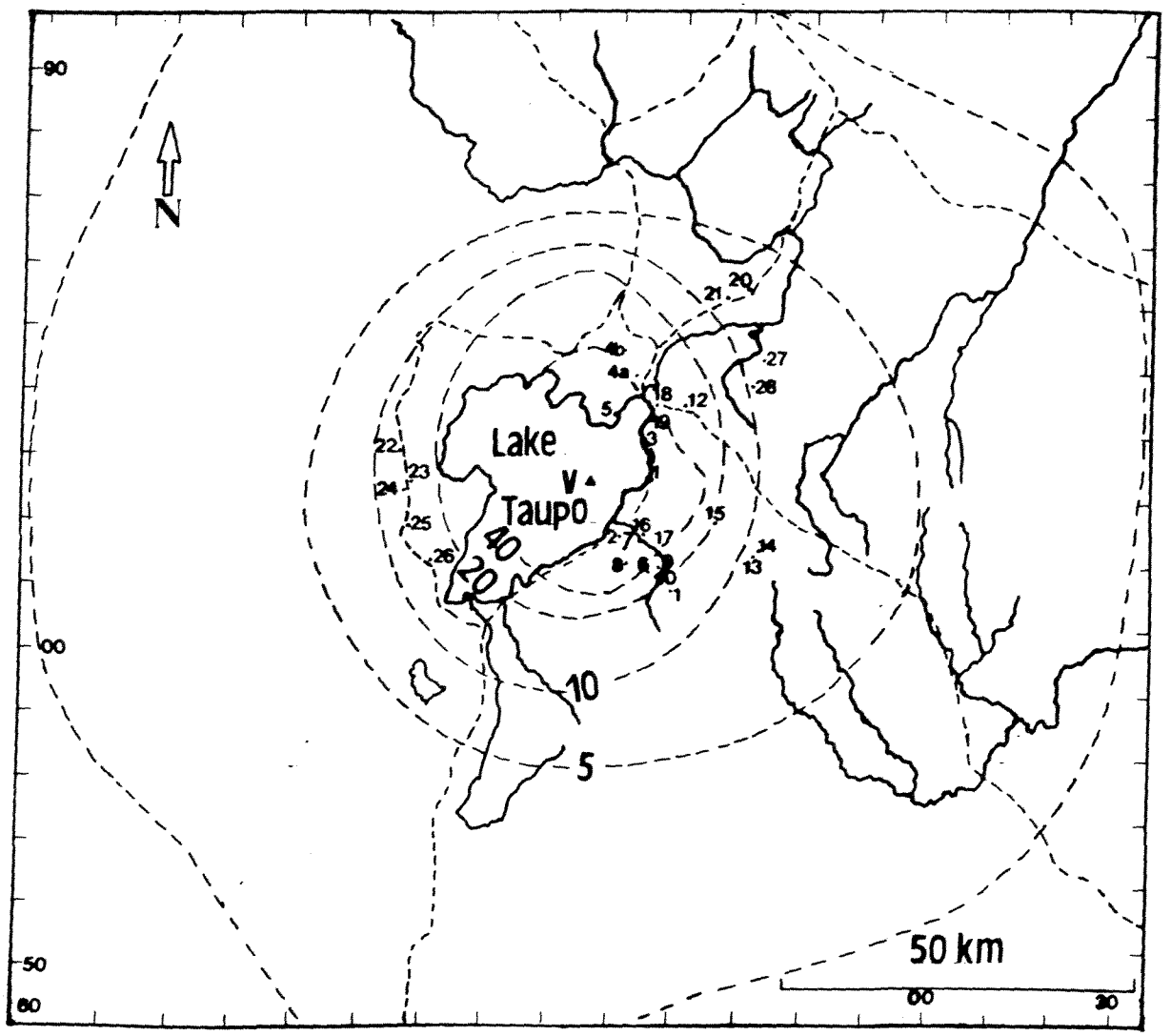

ure 4.1 : Map showing the localities where lithic inclusions from the Taupo Pumice Formation were collected. Grid references of the sections are given in Appendix 1. All sampling localities are within the 5 mm isopleth of the three largest lithics in the ground layer. The maximum isopleth of 40 cm is also shown, and the outer dotted line shows the approximate extent of the Taupo Ignimbrite.

4.3 HATEPE TEPHRA

The Hatepe Tephra (Froggatt, 1981) is the oldest member of the Taupo Pumice sequence, being the ash and lapilli beds paraconfomably overlying the paleosol on the Mapara Tephra and includes the initial phreatoplinian ash (Wilson and Walker, 1985). It is overlain by the Rotongaio Ash. Hatepe Tephra comprises a coarse lower pumice lapilli bed (Hatepe Plinian Pumice) conformably overlain by a uniform fine white ash with scattered pumice lapilli (Hatepe Phreatoplinian Ash).

The Hatepe Plinian Pumice is finer-grained than the Taupo Plinian Pumice, and shows no grading, only minor or rudimentary shower bedding. Pumice in this bed is white to pale yellow, well sorted, angular and moderately vesicular. Lithic clast content is moderate (<10%) with clasts being predominantly banded and spherulitic rhyolite with minor obsidian. Thicknesses exceeding 2 m near Lake Taupo are observed (Fig 4.2).

Conformably overlying the Hatepe Plinan Pumice is a generally equal thickness of fine, cream to white ash with scattered white pumice lapilli throughout. This fine grained nature typifies the Hatepe Phreatoplinian Ash. Bedding commonly occurs as layers of pumice lapilli conformable with the underlying topography and is characteristic of an air fall origin. The top surface of the Hatepe Ash is eroded by rain water and/or water explosively ejected from the vent to form an undulating top surface (Fig 4.2). The lithic content is low with lithic clasts generally inconspicuous. The widespread distribution and fine grained nature of this bed indicates a phreatoplinian origin (Fig 4.2).

4.4 ROTONGAIO PHREATOPLINIAN ASH

Rotongaio Ash is a charcteristic dark steel-grey fine to coarse ash unconformably overlying Hatepe Tephra and comformably overlain by Taupo Plinian Pumice. The type area is east of Lake Taupo (as defined by Froggatt, 1981). Rotonagaio Ash is finely bedded with all the ash material composed of fresh, glassy, non hydrated obsidian. Rotongaio ash is remarkably widespread for such a fine grainsize, and is recognizable even when very thin due to its dark grey colour

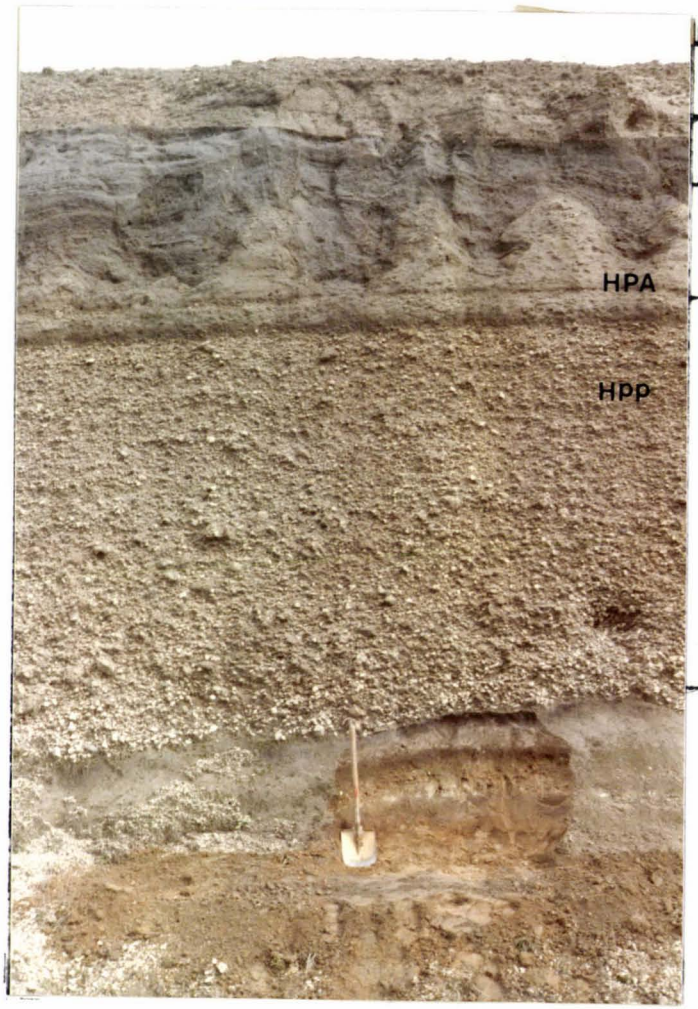

Figure 4.2 : A thick section of Hatepe Tephra is exposed at station 16. Hatepe Plinian Pumice (HPP; about 2 m thick) is overlain by the Hatepe Phreatoplinian Ash (HPA). The initial phreatomagmatic ash (dark grey) merges with the paleosol underlying the Taupo Pumice Formation (Grid ref. NZMS N103-551154).

ıre 4.3 : Rotongaio Ash (dark steel grey) forms an undulating layer over the erosion surface over the Hatepe Ash, its colour and land-scape mantling characterstics make it diagnostic for the Taupo Pumice Formation (Grid ref. NZMS N103-579103). (note a lense of Taupo Plinian Pumice overlain by a poorly developed ground layer in the gullies over the Rotongaio Ash in the middle of the photo

which contrasts with the surrounding white ash. It is thus diagnostic of the Taupo Pumice Formation over a large area. Its undulating structure in many outcrops is due to the ash mantling erosion gullies on the top surface of the Hatepe Ash, and is very characteristic of the unit (Fig 4.3). Lithic inclusions in the phreatoplinian Rotongaio ash are absent or rare.

4.5 TAUPO PLINIAN PUMICE

The Taupo Plinian Pumice deposit is a coarse and widely dispersed unit and according to Walker (1981) represents the most powerful plinian outburst yet documented. The Taupo Plinian Pumice occurs as a uniform, well sorted, pumice lapilli and block bed up to 2 m thick. Pumice clasts are moderately vesicular (60-70% porosity), yellowish white and extremly angular. In the area east of Lake Taupo varying amounts of Taupo Plinian Pumice deposit have been eroded by the succeeding pyroclastic, flows which formed the Taupo Ignimbrite, so that the true thickness of Taupo Plinian Pumice deposit is never seen. Lithic content of the Taupo Plinian Pumice is up to 10% by volume, and consists of banded, spherulitc rhyolite with minor ignimbrite, dacite and andesite.

4.6 THE TAUPO IGNIMBRITE

The Taupo Ignimbrite was first named as the Upper Taupo Pumice member and Rhyolite Block members of the Taupo Pumice Formation by Healy (1964). The name Taupo Ignimbrite was first formally introduced by Froggatt (1981) and comprises all the primary products of the pyroclastic flow(s) that followed the eruption of the Taupo Lapilli (Taupo Plinian Pumice) or those deposits occupying an eqivalent stratigraphic position where the Taupo Lapilli is absent.

Previous work on the Taupo Ignimbrite has covered a variety of aspects, as the ignimbrite has been of interest for several reasons.

1. The Taupo Ignimbrite is young, fresh, entirely non-welded (low-grade ignimbrite, Walker, 1983) and is exceptionally well preserved, with its full thickness exposed over a large area.

2. The great range of facies and varieties it displays enables the study of the processes of formation.

3. The distribution of the ignimbrite shows that the eruption was very violent which makes it possible to study the effects of violence on emplacement mechanisms of large pyroclastic flows (eg. turbulence, degree of expansion of flow).

4. Structures in the ignimbrite show that fluidization processes were important. They allow a check on predictions of fluidization behavior of pyroclastic flows inferred from experimental studies.

Wilson (1985) suggested that the ignimbrite was generated in a single short-lived episode which formed the eruption climax (about 400 sec) and that the overall distribution of the ignimbrite shows that the parent flow was little influenced by the often rugged topography apart from in a limited area south and south-east of Ruapehu. The outer limit of the ignimbrite is at 80+/- 10 km from the vent regardless of the intervening relief. The ignimbrite covers about 20,000 km^2 a figure which makes it among the most widely spread despite its modest volume. The ratio of the average thickness of an ignimbrite unit to its lateral spread (the latter is conveniently taken as the diameter of a circle which covers the same area as the ignimbrite) was defined as the aspect ratio by Walker et al. (1980), and an aspect ratio of 1:70,000 was calculated for the Taupo Ignimbrite which is very low compared to many well studied ignimbrites.

Even around its margins the ignimbrite crops out over a local height range of several hundred meters showing that the flow must have travelled at high speed right up to its outer limits, and the outer limit was controlled by the flow running out of material rather than merely slowing to a halt. The height of the obstacles climbed by the flow are used to estimate its velocity at various points. Wilson and Walker (1985) suggested that it is likely that the flow exceded 250-300 m/s near vent and sustained velocities in excess of 150 m/s to within a few kilometers of its outer limits. The high flow velocity is a result of the high magma dischage rate.

A model for depositional regimes in pyroclastic flows was presented by Wilson and Walker (1982). This considers a pyroclastic flow to consist of a head, a body and a tail. The resulting ignimbrite is described in terms of the layering scheme introduced by Sparks et al. (1973) as modified in Wilson and Walker (1982) into layers 1, 2 and 3 below:

Layer #1: consists of deposits which have been generated by processes operating in advance of the pyroclastic flow head and consists of two main facies named as layers 1(P) and 1(H). Layer 1(P) is a pumiceous, mildly to strongly fines depleted unit and is generated by the expulsion of material from the flow head by explosive expansion of air ingested by the flow and is named the "jetted deposit". The overlying unit is layer 1(H) which is a thinner, crystal and lithic rich fines depleted unit, generated by the sedimentation of the coarse/dense constituents segregated out by strong fluidization within the flow head and is named the "ground layer" (sec.4.3).

Layer #2: is deposited from the bulk of the flow and the tail, which is the trailing part slowed by ground friction. Layer 2 consists of two main facies with similar composition but contrasting morphologies. The valley ponded ignimbrite (VPI) is material left behind by the flow partially drained into depressions during emplacement, and its associated ignimbrite veneer deposit (IVD) which represents the basal and trailing part of the flow which were slowed by the ground friction and left behind as the flow travelled accross the landscape. Localized depositional modes within the body and tail generated distinctive coarse pumice concentration zones and lee-side lenses behind obstacles. At its outer limits the flow produced a distant facies which combines the features of both layer 1 and 2.

Layer #3: overlies Layer 2 and is deposited from the winnowing ash cloud elutriated from the pyroclastic flow and is very poorly preserved in the Taupo Ignimbrite.

The Taupo Ignimbrite shows great lateral variations which are documented by granulometric and component analyses and studies of maximum clast size and density

(Walker and Wilson, 1983). Each facies, and the variety of structures displayed exhibit systematic degrees of development with varying distance from vent. Wilson (1985) states that near vent, the flow consisted of batches of material which at about 25 km from the vent had coalesced into a single wavy flow and by about 40 km into a single wave. Three flow units which make up a single cooling unit have been described in near vent exposures (Froggatt, 1982). Out to about 13 km, the flow was rather dilute and highly turbulent as it deflated from the eruption column. Beyond this distance it was fairly concentrated, being about 100% expanded over its original non-fluidized compacted state, and had acquired a fluidization induced stable density stratification which strongly suppressed turbulence in the flow body. Deflation from the eruption column was largely completed by about 13 km but influenced the flow as far as 20-25 km from the vent.

The main body of the ignimbrite varies in thickness from less than 1 m to about 70 m and shows considerable colour variations, but mostly it is pale grey to white or stained pale brown. The variety of facies and fluidization structures displayed by the ignimbrite were discussed in detail by Wilson (1985). Without taking into consideration the various segregation structures (the ground layer, pumice concentration zone etc.) the main body of the ignimbrite contains variable amounts of lithics and a general decrease in lithic content away from the vent was observed.

4.7 THE GROUND LAYER

4.7.1 General

The ground layer of the Taupo Ignimbrite (Walker and Wilson, 1982) was first reported by Grange (1937) on the eastern shore of Lake Taupo and was given the name "Rhyolite Block Layer" by Healy (1964). Baumgart and Healy (1956) suggested that the "Rhyolite Block Member" was an unusual type of shower which when well developed consisted almost entirely of lapilli and blocks of banded and spherulitic rhyolite, obsidian with minor andesite, mudstone, welded ignimbrite and occasional pumice.

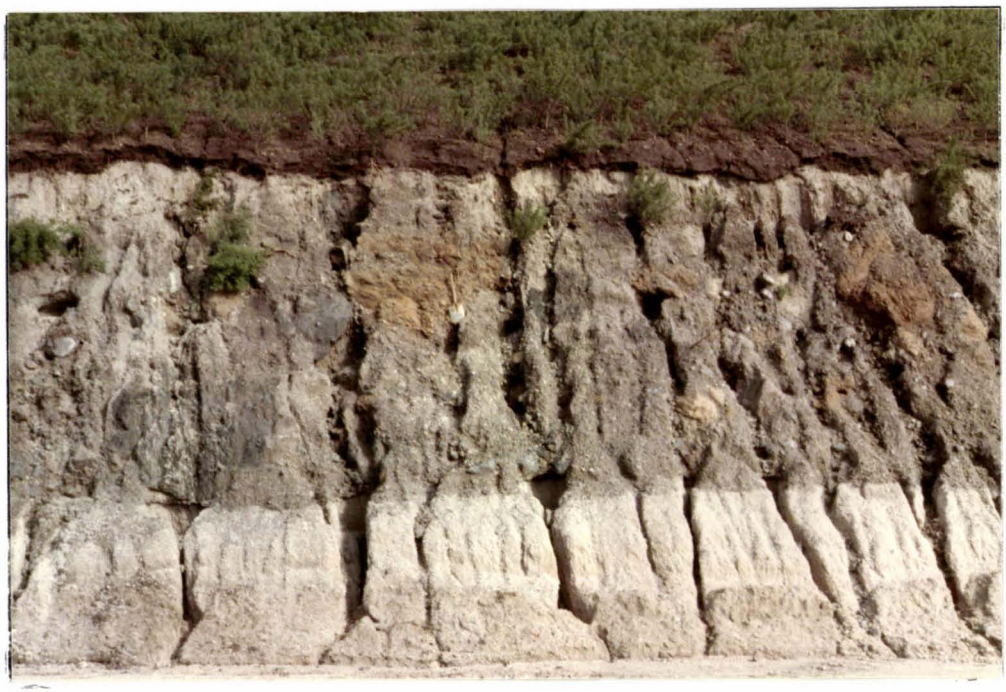

gure 4.4 : The ground layer has a maximum thickness of 3m at station 1 (6 km from the vent). The ground layer overlies the early ignimbrite flow units; note the early ignimbrite flow units and the erosive contact at the top and bottom of the ground layer. Big blocks of hydrothermally altered rhyolite are exposed. These have remained intact during transportation (spade is 0.6 for scale) (Grid ref. NZMS N94-553230).

ure 4.5 : The ground layer has a thickness of = 20 cm and overlies the Taupo Plinian Pumice at station 11 (Grid ref. N103-586080; 17 km from the vent)

They also noted that the upper and lower contacts were strongly erosional and the upper contact was planar even on irregular terrain. Healy (1964) suggested that the layer is probably formed by secondary transportation but because of the widespread nature of the "Rhyolite Block Member" he suggested as an alternative explanation that the eruption may have blasted its way through thick buried rhyolite lava which spread huge billowing clouds loaded with rhyolite blocks in to the area.

Recent studies of ignimbrites have shown that the products of ignimbrite eruptions are many and varied. Ignimbrites were often considered to be relatively homogeneous rock bodies, but detailed studies reveal that there are considerable departures from homogeneity in both physical and chemical characterstics. Sparks et al. (1973) first proposed that an ignimbrite flow unit usually contains a deposit which is rich in crystals and lithics, found between the ignimbrite proper and the pre-ignimbrite plinian pumice (Layer 1). This was interpreted as a deposit from a kind of pyroclastic surge or "ground surge" which moved outwards from the vent in advance of the pyroclastic flow itself.

Froggatt (1981) defined the same unit as the "Lithic Lag Layer" in the Taupo Ignimbrite and suggested an origin from simple sedimentation or gravity separation of the dense lithics from the pyroclastic flow. On the model presented for the deposition of pyroclastic flows Wilson and Walker (1982) gave this layer that is rich in crystals and lithics which is found at the base of the ignimbrite proper the non genetic name the "Ground Layer". An origin by sedimentation of lithics from the more fluidized nose of the pyroclastic flow head was proposed. This name will be used in this text henceforth.

4.7.2 Field occurrence

The ground layer overlies the Taupo Plinian Pumice or the Roton gaio Ash but in some near vent exposures it overlies the lower ignimbrite unit of Froggatt (1981) or the early ignimbrite flow units of Wilson (1985). The ground layer is almost always thinner than the underlying Layer 1(P) at the same locality, but it is more extensive laterally, stretching out to the distal limits of the ignimbrite although becoming very thin, fine grained and patchy beyond about 60 km from the vent. Its thickness varies from 3 m near vent to less than 1 cm in distal exposures (Fig 4.4 & Fig 4.5),

ɜure 4.6 : Lake sediment mudstone and siltstone in the ground layer (station 2 ; Grid ref. N94-495160)

ıre 4.7 : Hydrothermally altered welded tuff is broken into pieces but was emplaced intact with fine ash filling the fractures in the ground layer (station 2; Grid ref. N94-495160).

but in most sections it has a thickness of 10-30 cm. Because it is discontinuous and shows such rapid local thickness variations no attempt is made to construct an isopach map.

The average size of lithics is a function of the thickness of the ground layer. In thick exposures (station 1) rhyolite lava (some blocks are intensely hydrothermally altered), ignimbrite and lake sediment blocks as big as 1.5-2 m in diameter are found. Friable blocks of hydrothermally altered rhyolite, tuff, and lake sediments are fractured but are preserved intact and in some cases the fractures are filled with a matrix of fine ash (Fig 4.6 and 4.7). Similar blocks of rhyolite and welded tuff up to 1.5 m in size are found along the northern shore of lake Taupo (station 3), along Five Mile Beach and other localities on the eastern shore of Lake Taupo. These blocks are assumed to have been eroded out of the co-ignimbrite lag fall deposit.

The ground layer underlies both the valley ponded ignimbrite and the ignimbrite veneer deposit. On irregular terrain it almost entirely fills small hollows between ridges while on more gentle terrain it thins and becomes fine grained up slope. The ground layer has been observed to occur on slopes as steep as 60-70 degrees (Wilson and Walker, 1982).

The upper and lower contacts are erosive and are commonly sheared to generate material of intermediate grain size. Wilson (1985) notes that apart from near vent localities the ground layer or Layer 1(H) is extremely poor in fines and rich in crystals and lithics. He also notes that the ground layer is normally coarsest at or just above its base, while its upper part, immediately below Layer 2 may be rather fine grained.

4.7.3 Grain size characteristics

In near source exposures the ground layer is extremely coarse and contains boulders 2 m or more in size. Rhyolite boulders several metres across which may have been eroded out from the ground layer now lie on the surface near the NE shore of Lake Taupo at Waitahanui, Five Mile Beach and Wharewaka Point. Fig 4.1 shows the average maximum diameter of three largest lithics clasts in the ground layer over the entire extent of the Taupo Ignimbrite.

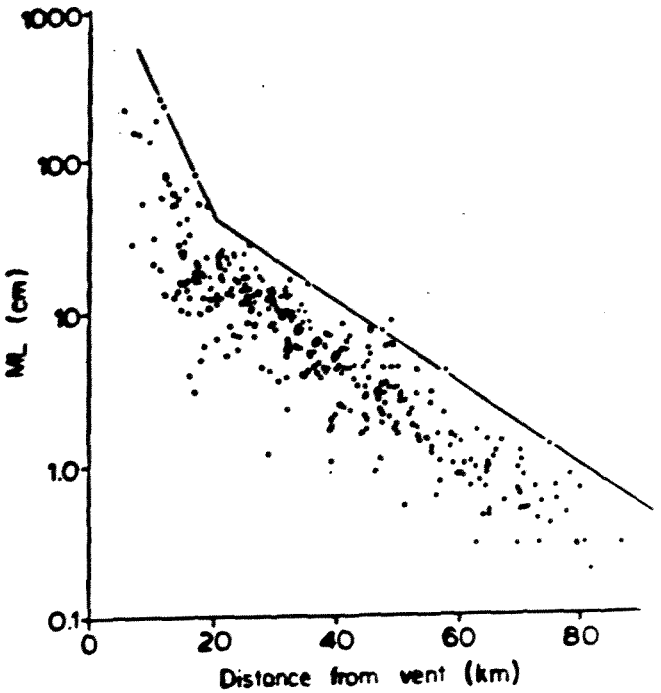

ɡure 4.8 : Plot of the average length of the 5 largest lithic clasts found in samples of the ground layer (ML), versus the distance from the vent. The two lines are hand-fitted maxima to the data. The break in continuity of the maxima at about 20 km from the vent is interpeted to represent the co-ignimbrite lag fall deposit (Adopted from Walker *et al. 1981b*)

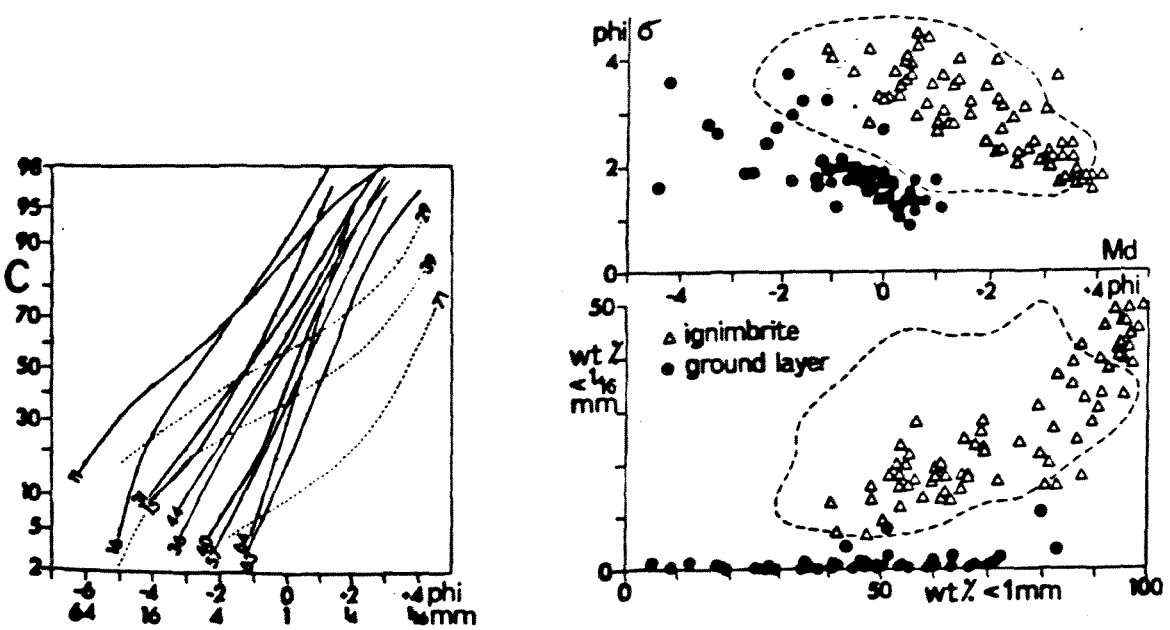

ıre 4.9 : Representative probablity curves of the ground layer samples showing the cumulative weight percentage (C) coarser than the grain size indicated. Figures give the distance from the vent in km. The dashed lines are typical samples of Taupo Ignimbrite for comaprision. (from Walker *et al. 1981b*)

ıre 4.10 : Summary and comparsion of grain size charecteristics of the Taupo Ignimbrite and its ground layer. Above is a plot of graphic standard deviation against median diameter (Md) showing that the ground layer is coarser and better sorted. The dashed line is the 1% contour for the pyroclastic fall field. Below is a grain-size plot showing the negligible content of ash finer than 1/16 mm in the ground layer samples. The dashed line is the 1% contour for the pyroclastic flow field. (From Walker *et al. 1981b*)

Walker et al. (1981b) noted that the lithic size distribution in the ground layer as well as in the pre-ignimbrite plinian pumice indicates that the vent lies within the present area of the lake, probably at or near Horomatangi Reefs.

Wilson and Walker (1982) plotted the maximum lithic size data from the ground layer against distance from the vent which showed a progressive decrease in lithic size with increasing distance from the vent, with a break in trend at about 20 km (Fig 4.8). They interpreted the steeper near-vent trend as that of a co-ignimbrite lag-fall deposit (Wright & Walker, 1977), but since it is evident in the field that all the ground layer was emplaced with some lateral flow, it was interpreted to represent a lag-fall deposit that has been carried from the vent area by the momentum of the flow. Co-ignimbrite lag-fall deposits and other proximal lag breccias can be considered to represent another kind of depositional mode which is normally confined to the immediate area of the vent, but can be extended (as at Taupo) to greater distances when a lag-fall deposit merges into the ground layer deposit. The boundary between the two may be taken at the break in slope shown in Fig 4.8.

The grain size analysis of the ground layer is characterized by a log normal size distribution (Fig 4.9, Walker et al. 1981b) of most samples analysed, but the coarsest samples have a bimodal distribution with a coarser mode of boulder-sized clasts. Fig 4.10 summarizes the grain-size characteristics of the ground layer. It is moderately well sorted (most samples falling in the pyroclastic fall field) and compared with the ignimbrite shows a noteworthy lack of fines.

4.7.4 Origin and mechanisms of formation

Several views were previously proposed on the origin of the ground layer. In view of the fact that a shower origin has been proposed; Walker et al. (1981b) presented the following evidence against an airfall origin:

1. The blocks never indent the underlying surface (whether it is plinian pumice or underlying paleosol) showing that they cannot have fallen at high velocity to their present position.

2. Some of the large blocks are relatively delicate (eg. mudstone) and could hardly have survived intact after falling from any appreciable height (Fig 4.6).

3. The area enclosed by any given isopleth (Fig 4.1) is much greater than is presently known for any deposit of proven airfall type. The 10 cm isopleth as an example, encloses 2750 km^2 as compared to 700 km^2 for the Taupo plinian pumice which is claimed to be deposited from the most powerful plinian eruption presently known (Walker, 1980). From these lines of evidence the large lithics with the associated fine material must have been carried laterally by a pyroclastic flow or a pyroclastic surge.

Walker et al. (1981b) presented two arguments against a pyroclastic surge origin:

1. All historical pyroclastic surges have developed on high and steep volcanic cones. Only on a steep cone can gravity sustain the high velocity on which the carrying power of the gas and distance reached by the surge, depends. The carrying power of a surge on flat topography such as Taupo and the present vent position being lower than any outcrop of the ignimbrite would not be capable of moving metre-sized blocks nearly 10 km.

2. The general absence of stratification and cross-stratification in the ground layer as in most ground surge deposits.

Evidence that the ground layer was deposited from the pyroclastic flow include:

1. When traced outwards from source the ignimbrite becomes at first impoverished in lithics then in crystals and towards its distal ends approaches 100% vitric material (Fig 4.11). Such a steady impoverishment in heavies must be accounted for and is best explained by the loss of heavies into the ground layer.

2. The maximum lithic size in both the ignimbrite and the ground layer steadily decreases outwards. Lithics have a much wider grain-size range than crystals in the erupted mixture, and the crystal:lithics ratio accordingly varies as the grain-size of the "heavies" in the ground layer decreases from low near source where large lithics predominate to high at the distal ends.

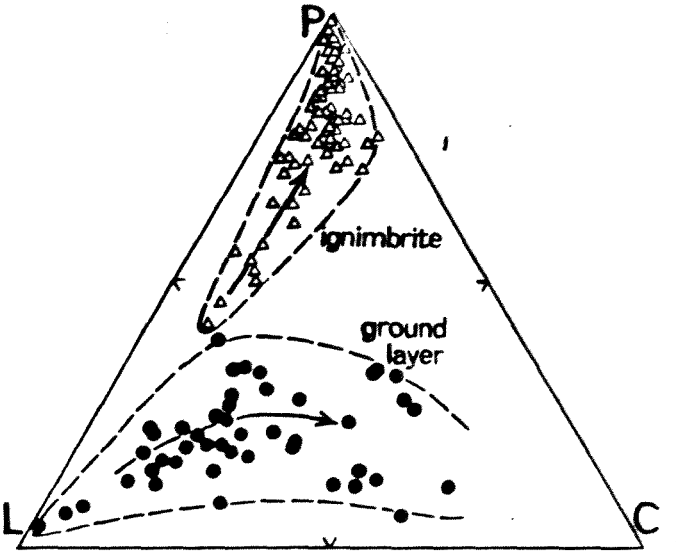

gure 4.11 : Plot of percentages of pumice (P), lithics (L) and free crystals (C) in samples of the Taupo Ignimbrite and its ground layer, for the classes 1/4mm and coarser recalculated to 100% total. The arrows indicate compositional trends with increasing distance from vents. (from Walker *et al. 1981b*).

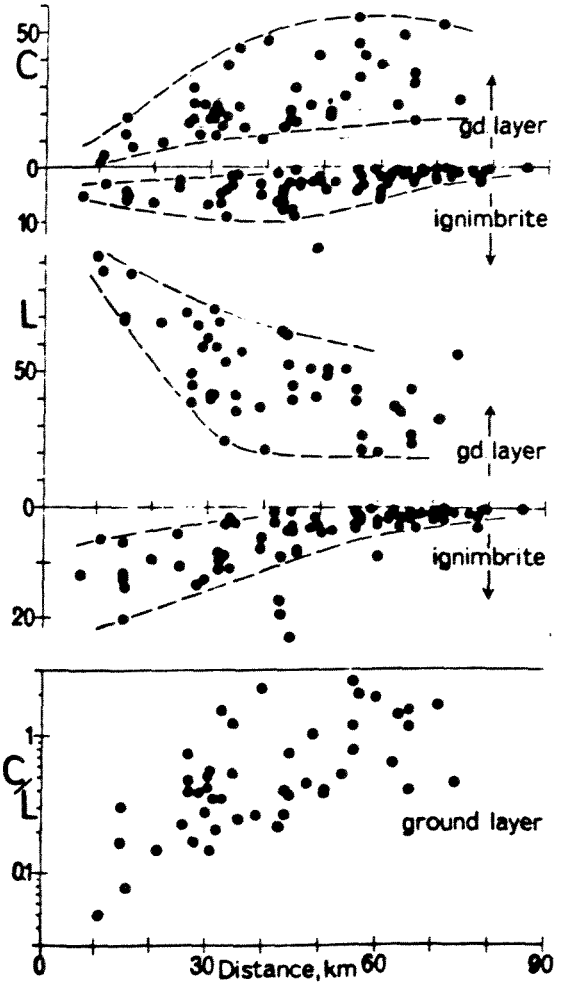

ıre 4.12 : Variation in percentages of free crystals (C) and lithics (L) against distance from vent in the ground layer, and variation in the C/L ratio in the ground layer. Note particularly the sympathetic variation of the lithic content in the ground layer and ignimbrite (After Walker *et al. 1981b*).

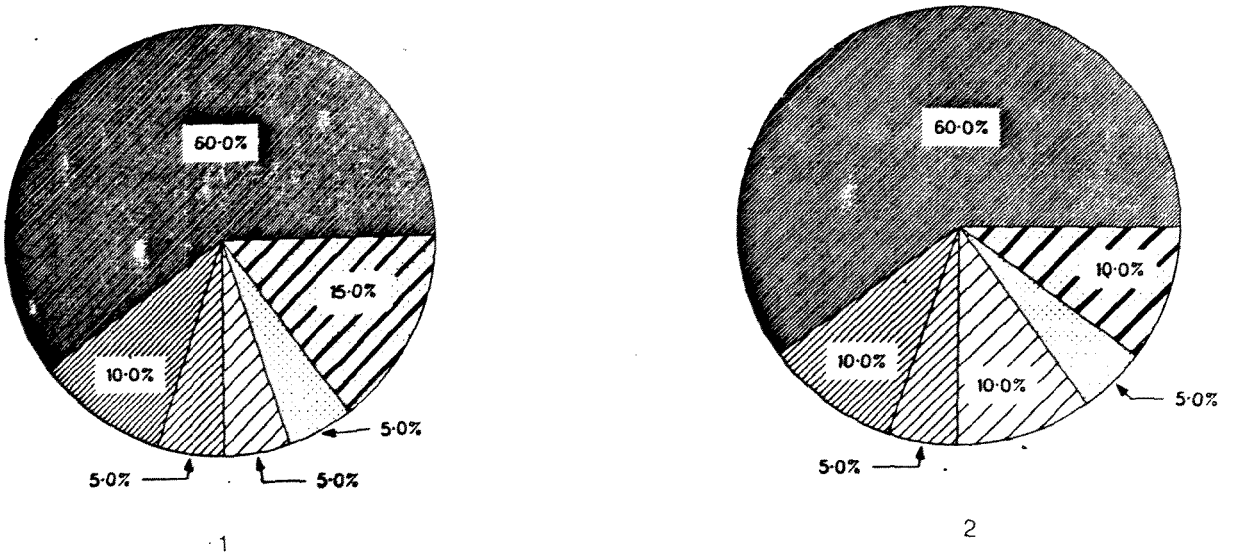

gure 4.13(a) : Proportion of the different rock types in the ground layer, estimated at two outcrops about 10km from the inferred vent position (Location of station 1 and 2 is given on Fig. 4.2 and Appendix1)

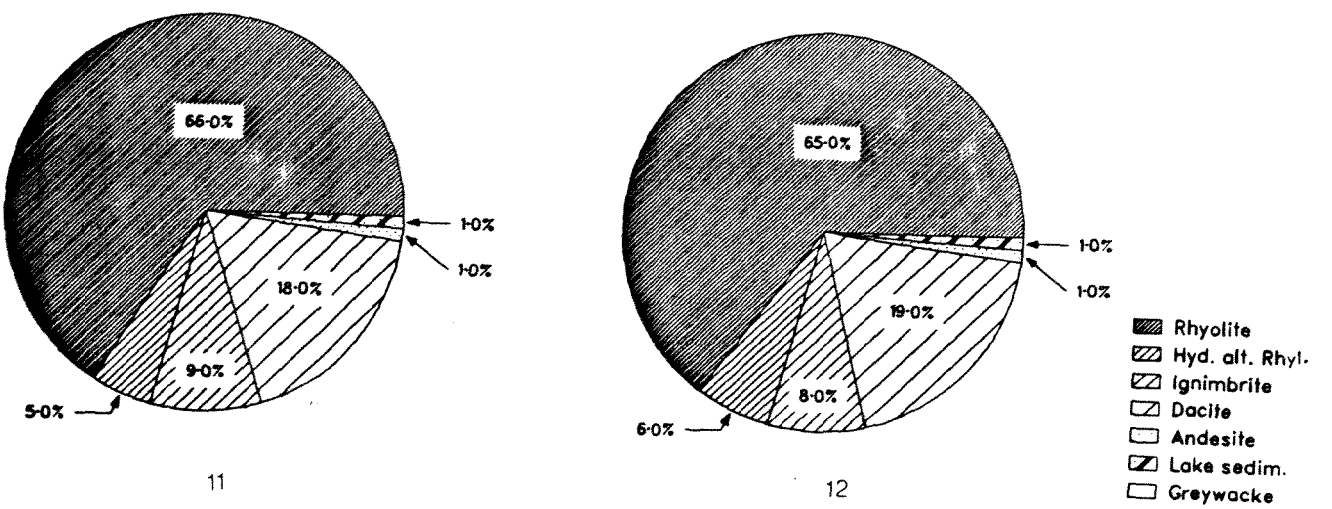

ıre 4.13(b) : Estimated proportion of the different rock types in the ground layer at a section about 20 km from the inferred vent position (stations 11 and 12).

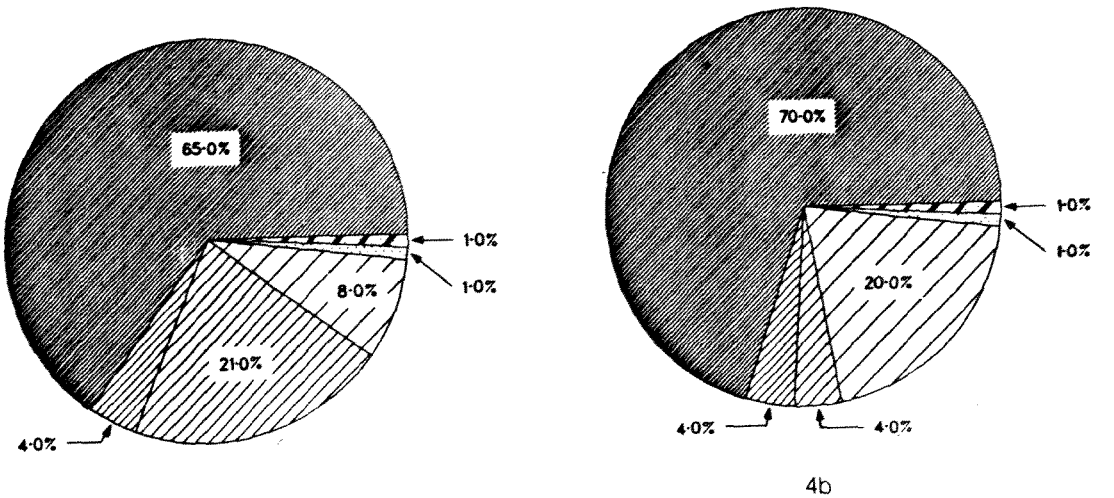

4a 4b

gure 4.13(c) : Estimated proportion of the different rock types in the ground layer at a section about 20 km from the inferred vent position (stations 4a and 4b).

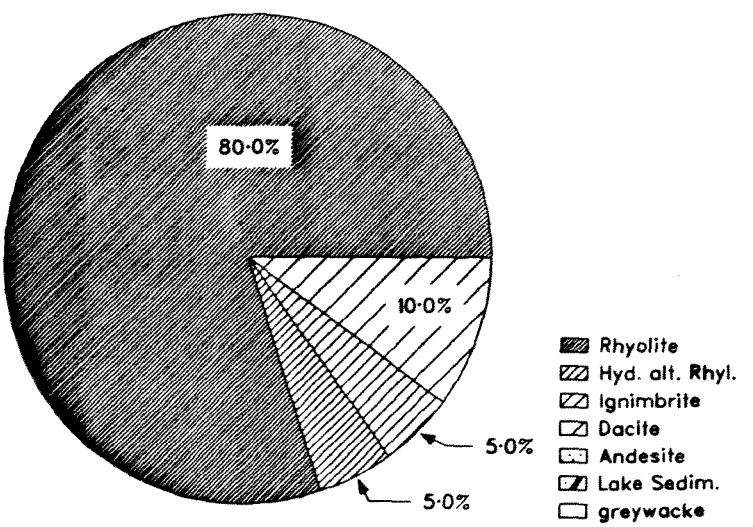

ure 4.13(d) : Estimated proportion of the different rock types in the ground layer at a section about 30 km from the inferred vent position (station 21).

3. Giant boulders of friable lake sediments, welded tuff and hydrothermally altered rhyolites were fractured during transportation but are preserved intact. This testifies that the pyroclastic flow head, despite its strongly fluidized state caused by air ingestion, had enough pressure to support such boulders from all sides, behaving like an air cushion during transportation.

4.7.5 Bulk composition and Sampling

Weight percentages of components (pumice plus shards, free crystals and lithics) have been determined down to 1/4 mm size (Fig 4.11 & Fig 4.12) (Walker et al. 1981b). A strong enrichment in dense components (lithics and crystals) is shown by the ground layer as compared to the main body of the ignimbrite. Furthermore the pumice in the ground layer has an average density about 30% higher than pumice of a corresponding size in the ignimbrite (Froggatt, 1982).

The proportion of lithic types in the ground layer was estimated by eye at two near vent thick exposures (stations 1&2, Fig 4.13a), where the ground layer was too coarse to sample. At outcrops further than 10 km from vent the thickness and grainsize of clasts in the ground layer is small enough for the estimation of the proportion of lithic types to be done on the lapilli-sized clasts in bulk samples collected from the ground layer. About 100 gm of lapilli-sized bulk samples were taken at stations which are about 10, 20 and 30 Km from the inferred vent position. A binocular microscope was used in the separation of the different types of lithics. Proportions were estimated by weighing the separated fractions. Fig 4.13(b,c,d) presents the estimated proportion of the major types of lithics in the ground layer.

In general rhyolites make up about 75% of all the lithics in the ground layer both at near vent and distant exposures. Dacites, andesites, welded ignimbrites and lake sediment mud and siltstone blocks make up the remaining 25%. Near vent exposures of the ground layer are thicker and hence the size of the blocks in the ground layer is bigger than at more distal exposures. The main difference between the near vent and distal exposures of the ground layer is that the proportion of soft and friable rocks (mudstone, siltstone, welded tuff) rapidly decreases away from the vent.

Figure 4.14 : A single giant pumiceous block enclosed within subhorizontal lake sediments. Note cooling contraction joints around the block. Similar pumiceous blocks are found at several localities around the lake and were extruded at the end of the Taupo eruption.

For the petrographic study of lithics in the ground layer, samples from 28 stations were collected. Locations of the sampling stations are shown on Fig 4.1 and the grid references are given in Appendix 1.2 with some sampling remarks. The chemistry of the lithics in the Taupo Pumice Formation is based only on the lithic blocks collected from the ground layer since lithic inclusions in other members of the Taupo Pumice Formation are generally smaller in size and fresh unaltered samples large enough for wholerock chemical analyses are rarely found.

Pumice blocks up to 5 m in size are found scattered at exposures on the eastern side of Lake Taupo, mostly associated with the cliff line of a lake level some 5 m higher than at present and postdating the pyroclastic phases of the eruption. The pumiceous blocks show cooling contraction joints (Fig 4.14). Fragments of the pumice vary slightly between negatively and positively bouyant in water, (density = 0.9 gm/cc) but field evidence suggests that they must have floated into their present position. Samples of these dense grey pumiceous blocks were collected and chemically analyzed.

Chapter V

PETROGRAPHY OF LITHIC BLOCKS

5.1 INTRODUCTION

About 100 thin sections were examined from the lithic blocks of the ground layer and lithic inclusions from the Taupo plinian pumice and Hatepe Tephra. The petrography of the main types of lithic inclusions is given in this chapter. Modal content of the main types of rocks is presented on Table 5.1 and the list of samples studied and their petrographic names are given in the Appendix 2 together with sampling localities.

5.2 RHYOLITES

Rhyolites form the major proportion of all the lithics in the Taupo Pumice Formation. In the ground layer, rhyolite blocks up to 1.5m in diameter are found in near vent exposures (station 1, Fig 4.1). The rhyolite blocks are commonly angular and appear to have been derived from within the vent. Some of the rhyolite blocks show a high degree of hydrothermal alteration, which indicates that a hydrothermal system existed at some time at or near the vent area. The hydrothermally altered rhyolites remained intact despite their highly fractured and friable nature.

Most of the rhyolite blocks are light-dark grey, show flow banding, contain spherulites and have a porphyritic texture with a glassy or cryptocrystalline groundmass. The common phenocrysts are plagioclase (andesine), hypersthene, magnetite, ilmenite, quartz, hornblende and biotite. Following the classification of Ewart (1968), the rhyolite blocks in the ground layer are here sub-divided into three groups based on their ferromagnesian phenocryst assemblages.

1.Hypersthene rhyolite

2.Hypersthene-hornblende rhyolite

3.Biotite bearing rhyolite

Table 5.1 Modal analyses of selected rock types from the lithic inclusion in the Ground Layer based on 1500 point counts.

VUWN sample	31128 1T2 (1)	31131 1M7 (2)	31127 1T1 (3)	31133 1/6 (4)	31130 1/B/6 (5)	31135 3/1 (6)	31136 4/5 (7)	31140 1/M/3 (8)	31137 1B1 (9)	31138 4/10R (10)	31134 2/1 (11)	31150 4/8 (12)	31151 4/9 (13)
Glass or Groudmass	91.6	94.0	96.1	90.0	79.6	93.1	90.5	82.6	92.6	91.7	89.0	60.2	68.0
Spherulite	-	-	-	11.2	-	-	-	-	-	-	-	-	-
Vesicle	-	-	-	-	-	-	-	-	-	-	-	-	-
Quartz	0.3	0.1	0.2	1.4	1.9	0.1	1.0	1.3	0.9	0.5	2.8	-	0.3
Plagioclase	6.7	4	2.3	6.1	4.6	4.6	5.2	8.5	3.2	3.8	6.5	29.1	23.8
Hypersthene	0.7	0.8	0.8	1.3	1.7	1.1	1.3	2.7	0.2	0.9	2.4	6.0	5.0
Augite	-	-	-	-	-	-	-	-	-	-	-	0.6	0.5
Hornblende	-	0.1	-	-	-	-	-	1.0	-	-	0.3	-	-
Biotite	0.5	0.5	-	0.1	0.1	0.1	0.8	0.5	1.1	2.1	1.1	-	-
Magnetite	0.2	0.5	0.6	1.0	0.8	1.0	1.2	0.4	1.9	0.4	0.9	1.9	2.4
Xenoliths	-	-	-	-	-	-	-	-	-	-	-	2.2	-
Total xl. content	8.4	6.0	3.9	9.9	9.1	6.9	9.5	14.4	7.3	7.7	14	39.8	32.0
Plag/Qtz ratio	22.3	40.0	11.5	4.3	2.4	46	5.2	6.5	3.6	7.6	2.3	-	-

(1-7) Hypersthene rhyolite.
(8) Hypersthene-hornblende rhyolite.
(9-11) Biotite-bearing rhyolite.
(12-13) Two-pyroxene dacite.

VUWN sample	31153 2/9 (14)	31154 1/2 (15)	31156 2/8 (16)	31151 1/4 (17)
Glass or Groudmass	50.0	51.1	54.1	52.0
Vesicle	-	-	-	-
Quartz	-	-	-	-
Plagioclase	40	19.7	18.0	22.0
Hypersthene	7.9	17.3	16.5	20.7
Augite	0.3	11.9	10.9	3.0
Hornblende	1.1	-	-	-
Biotite	-	-	-	-
Magnetite	-	-	0.3	0.6
Olivine	-	-	0.2	1.7
Xenoliths	-	-	-	-
Total xl. content	49.3	48.9	45.9	48.0
Porphyritic pyx.ratio	17.0	59.7	60.4	35.0

VUWN sample	31166 1BB7 (18)	31165 3/6 (19)	31168 11/2 (20)
Ash (matrix)s	78.1	72.4	45.9
Pumice	0.9	-	-
Vesicle	0.7	-	-
Quartz	7.0	9.0	14.1
Plagioclase	5.6	9.1	24.3
Hypersthene	0.8	2.1	4.0
Augite	-	-	-
Hornblende	-	0.1	0.7
Biotite	-	-	-
Magnetite	0.1	1.6	1.8
Lithics	4.8	5.7	9.0
Total xl. content	13.5	21.9	45.1

(14) Hornblende andesite.
(15) Plagioclase pyroxene andesite.
(16) Pyroxene andesite.
(17) Olivine andesite.
(18-19) Lithic crystal rich ignimbrite.
(20) Crystal rich ignimbrite.

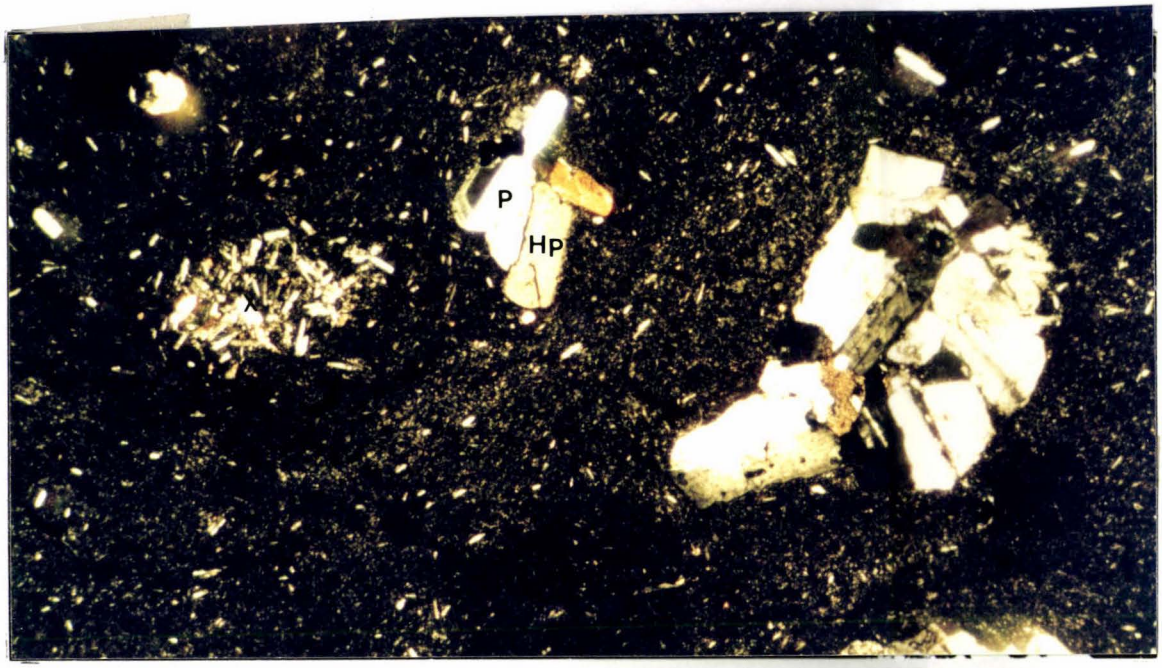

Figure 5.1 : Phenocryst aggregate of plagioclase (P), hypersthene (Hp) and Magnetite (Mg) the groundmass is glassy and microcrystalline contains laths of plagioclase. Rare xenoliths (X) are found in some of the rhyolite lava (centre left of the photo). (VUWN 31141, XPL x10)

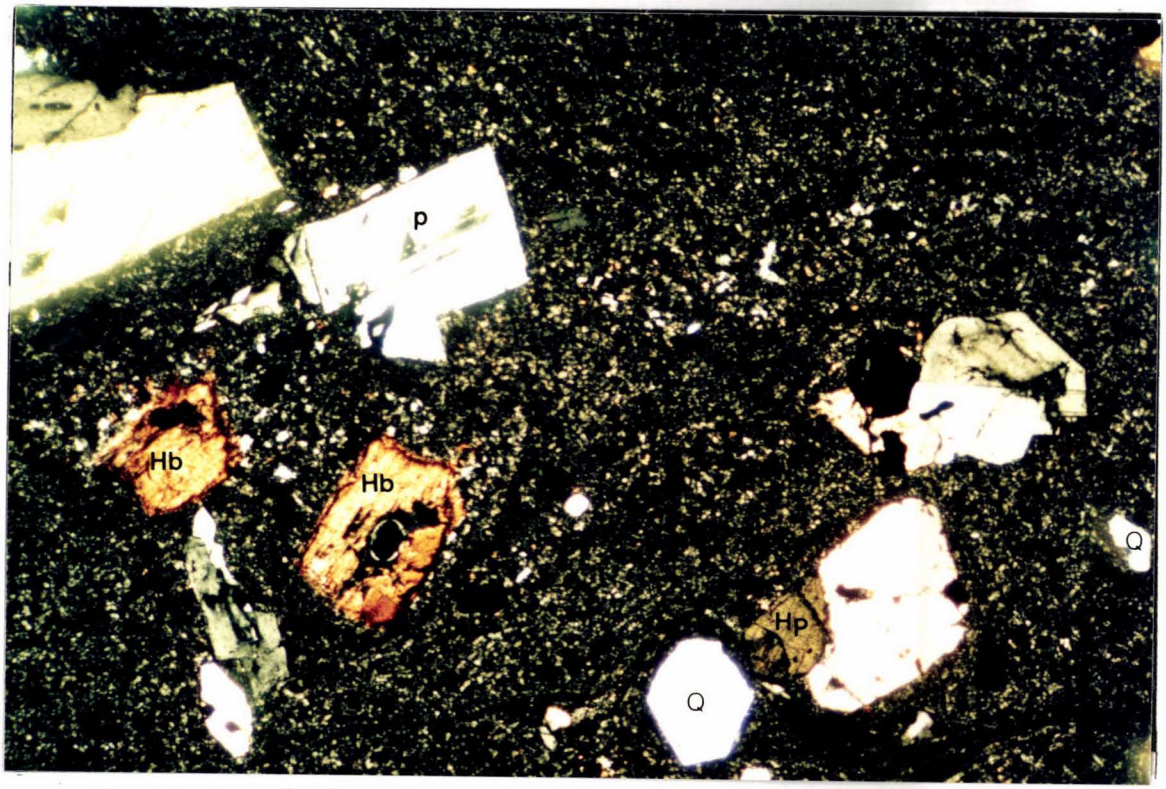

gure 5.2 : Hornblende (Hb) phenocrysts in hypersthene-hornblende rhyolite. Hypersthene (Hp) and Plagioclase (P) phenocrysts form aggregates and the groundmass is cryptocrystalline and shows flow banding. Rare resorbed Quartz (Q) occur in some samples. (VUWN 31140, XPL x10)

Hypersthene phenocrysts are very common in all of the rhyolites studied, but the rhyolites are named hypersthene-hornblende rhyolites when modal phenocrystic hornblende is > 1% and biotite bearing rhyolite when biotite phenocrysts are > 1%. When comparing the rock types a number of common features are apparent.

1. The groundmass is either completely or partly glassy and contains spherulites, cristobalite and glassy microlites which normally show a flow-line pattern.
2. Plagioclase occurs as euhedral and subhedral phenocrysts, and are sometimes found as glomeroporphyritic clusters. Oscillatory and patchy zoning is present in the plagioclase.
3. Hypersthene phenocrysts occur as fractured euhedral-anhedral crystals with inclusions of granular magnetite or as smaller euhedral-subhedral microphenocrysts in phenocryst aggregates.
4. Quartz, if present, is normally cracked and strongly resorbed.

5.2.1 Hypersthene Rhyolite

This rock type is the most abundant of the lithic blocks in the ground layer and inclusions in other members of the Taupo Pumice Formation. The rocks are grey to dark brown, and are frequently banded spherulitic and porphyritic. Plagioclase and hypersthene are the major phenocrysts (average phenocryst content is 8%) and commonly form glomeroporphyritic aggregates. Inclusions of hypersthene are common in plagioclase phenocrysts and magnetite granules occur as inclusions in both the plagioclase and hypersthene phenocrysts. The groundmass consists of isotropic glass and microcrystalline material.

Plagioclase phenocrysts are the most abundant and are commonly zoned, euhedral to subhedral, rarely broken, and have an average size of 2 mm.

The major ferromagnesian phenocryst is hypersthene which is commonly euhedral and has an average grain size of 1 mm. Many hypersthene phenocrysts are altered to opaque oxides along their margins and contain titanomagnetite inclusions. Other ferromagnesian phenocrysts include rare augite (VUWN 31129) which is < 0.5 mm in size. Rare xenoliths

(dacite and andesite?) are found in some of the hypersthene rhyolites (Fig 5.1). Accessory minerals include opaque Fe-Ti oxides and apatite.

5.2.2 *Hypersthene-hornblende Rhyolite*

This rock type forms a minor proportion of both the rhyolite blocks in the ground layer and inclusions in other members of the Taupo Pumice Formation. The rocks are dark grey, banded, spherulitic and porphyritic, rarely altered and have a phenocryst content of about 14% (Table 5.1). The main phenocrysts are plagioclase, hypersthene and brown hornblende. The groundmass consists of glass and microcrystalline material.

Phenocrysts of plagioclase (andesine) are commonly euhedral to subhedral, rarely rounded and corroded, and range from 1 mm to 3 mm in size. Oscillatory and patchy zoning are common.

Hypersthene phenocrysts are commonly euhedral although some are corroded, and are less than 1 mm in size. Some phenocrysts have magnetite rims while others are completely altered to magnetite. Hypersthene phenocrysts rarely occur as inclusions in plagioclase phenocrysts and commonly form phenocryst aggregates with occasional augite microphenocrysts (less than 0.5 mm in diameter).

Resorbed and occasionally embayed quartz and hornblende are minor phenocrysts. Hornblende forms subhedral crystals with an average size of 1 mm, strongly pleochroic from pale red to dark brown and comonly altered to opaque or brown oxides on the rims (Fig 5.2). Accessory minerals include Fe-Ti oxides and apatite.

5.2.3 *Biotite bearing Rhyolite*

The biotite-bearing rhyolites form a small proportion of the rhyolite blocks in the ground layer and inclusions in other members of the Taupo Pumice Formation. This rock is light-yellowish grey, banded and porphyritic. Phenocrysts make up about 15% of the rock; the highest phenocryst content of all the varieties of the rhyolites (Table 5.1). The groundmass consists of glass and is partly microcrystalline.

The rock contains phenocrysts of plagioclase, hypersthene, biotite, and accessory Fe-Ti oxides. Plagioclase (andesine) make the major proportion of the phenocrysts commonly euhedral have an average size of 1.5 mm and show compositional zoning.

Hypersthene phenocrysts are euhedral and have an average grain size of 0.5 mm and are commonly altered, either completely or around the rims to opaque Fe-Ti oxides. Biotite phenocrysts are found in lenticules between flow bands and as crystal aggregates about 0.5 mm in size. Quartz phenocrysts are commonly rounded and have an average grain size of 1 mm.

5.3 *DACITES*

Dacites are the second most abundant rock type and comprise about 15% of the lithic blocks in the ground layer. They commonly occur as angular to sub-angular blocks up to 30 cm in diameter in the ground layer and show various intensities of hydrothermal alteration.

Two pyroxene dacites form the major proportion of the dacite inclusions in the Taupo Pumice Formation. The rock is dense, hard, generally dark grey, greyish green or pale red in colour and is porphyritic with large phenocrysts of plagioclase, hypersthene, augite and microphenocrysts of Fe-Ti oxides commonly occuring in aggregates. The phenocrysts make up about 30% of the rock and are set in a groundmass of microcrystalline quartzofeldspathic material containing laths of plagioclase. A flow texture is indicated by the orientation of plagioclase microlites in some samples (eg. VUWN 31151, Fig. 5.3). Average size of the plagioclase in the groundmass is less than 0.2 mm. Rare diorite inclusions are also found in some of the dacites.

Plagioclase phenocrysts (andesine-labradorite) comprise the major proportion of the phenocrysts and have an average size of 1.5 mm x 3 mm. Two types of plagioclase phenocrysts are identified (Fig 5.4). The first type is euhedral to anhedral with resorbed rims and shows sieve texture or has clouded cores which are commonly jacketed by normally zoned material. The other type is euhedral to subhedral, commonly with

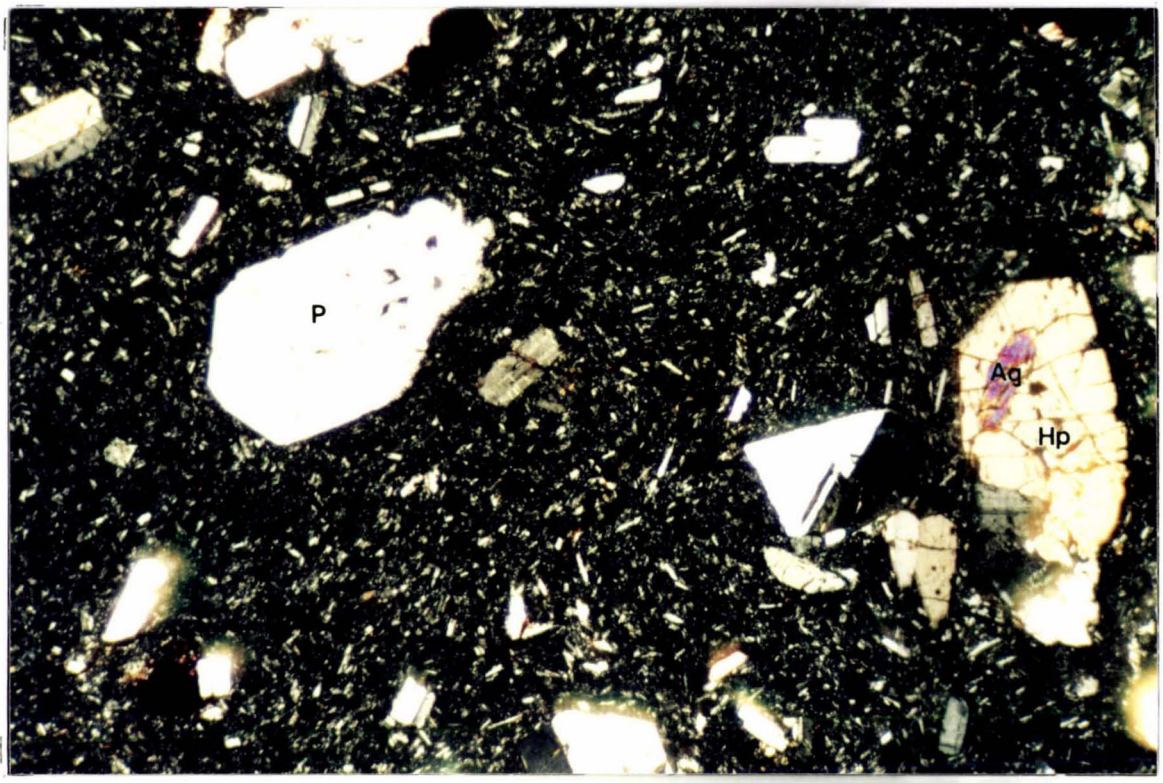

Figure 5.3 : Two pyroxene dacite, contains phenocrysts of plagioclase (P), hypersthene (Hp) and augite (Ag). Note an inclusion of augite in a hypersthene phenocryst. The groundmass is cryptocrstalline with plagioclase laths showing flow align ment. (VUWN 31151, XPL x10)

igure 5.4 : Phenocryst aggregate of plagioclase, orthopyroxene (Opx), clinopyroxene (Cpx) and magnetite (Mg) in two pyroxene dacite. Two generations of plagioclase phenocrysts are shown as P1-shows oscillatory zoning with sieve texture and glass inclusions commonly with an outer jacket of normally zoned material. P2-commonly normally, zoned euhedral with clouded cores. (VUWN 31149, XPL x10)

oscillatory zonning and rarely has clouded cores but does not contain any glass or pyroxene inclusions. The latter is the most abundant of the plagioclase phenocrysts.

Hypersthene phenocrysts are often euhedral and have an average size of 1 mm, show pleochroism from pale green to pale pink and contain inclusions of granular magnetite. Augite is present in considerable amounts as euhedral crystals but is normally smaller than the other phenocrysts. Resorbed quartz phenocrysts and rare olivine crystals are ocasionally found in some samples.

5.4 *ANDESITES*

Andesites are a minor proportion of the lithic blocks in the ground layer and in other members of the Taupo Pumice Formation. Most andesites occur as angular to subangular blocks <20 cm in size, and are grey, weathering to a rusty brown colour. Many of the blocks show various degrees of hydrothermal alteration. Some of the andesite boulders have a completely altered groundmass with rare, fresh phenocrysts. Four types of andesite lithics are identified in the ground layer:

1. Hornblende andesite
2. Plagioclase-pyroxene andesite
3. Pyroxene andesite
4. Olivine andesite

The classification of the andesites is based on the modal porphyritic pyroxene ratio of Clark (1960) which is expressed as % pyroxene phenocryst x 100 divided by % plagioclase phenocrysts + % pyroxene phenocrysts. When this ratio is less than 33% the rock is plagioclase andesite, when the ratio is 33-60% the rock is named plagioclase-pyroxene andesite and when the ratio is greater than 60% the rock is pyroxene andesite. Hornblende andesites are those with phenocrystic hornblende > 1% and olivine andesites where olivine crystals > 1%.

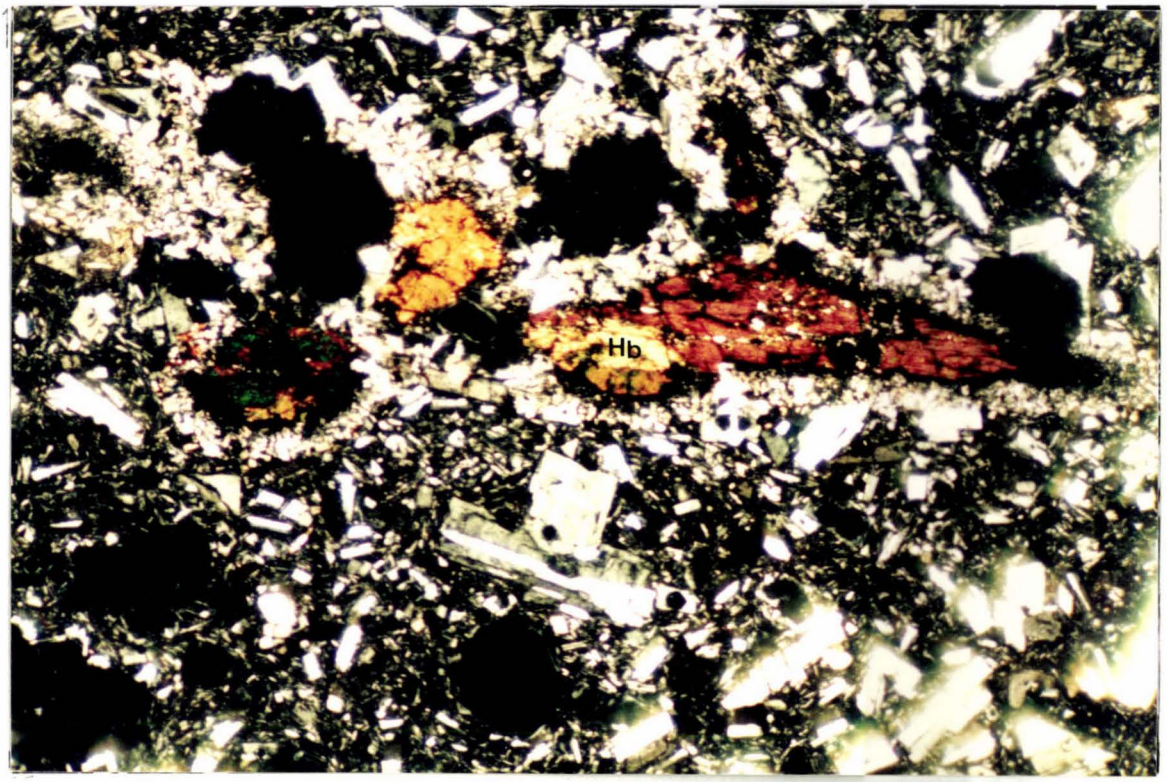

Figure 5.5 : Brown hornblende phenocryst in hornblende andesite; note that the phenocryst rims are altered to magnitite. (VUWN 31153, XPL x10)

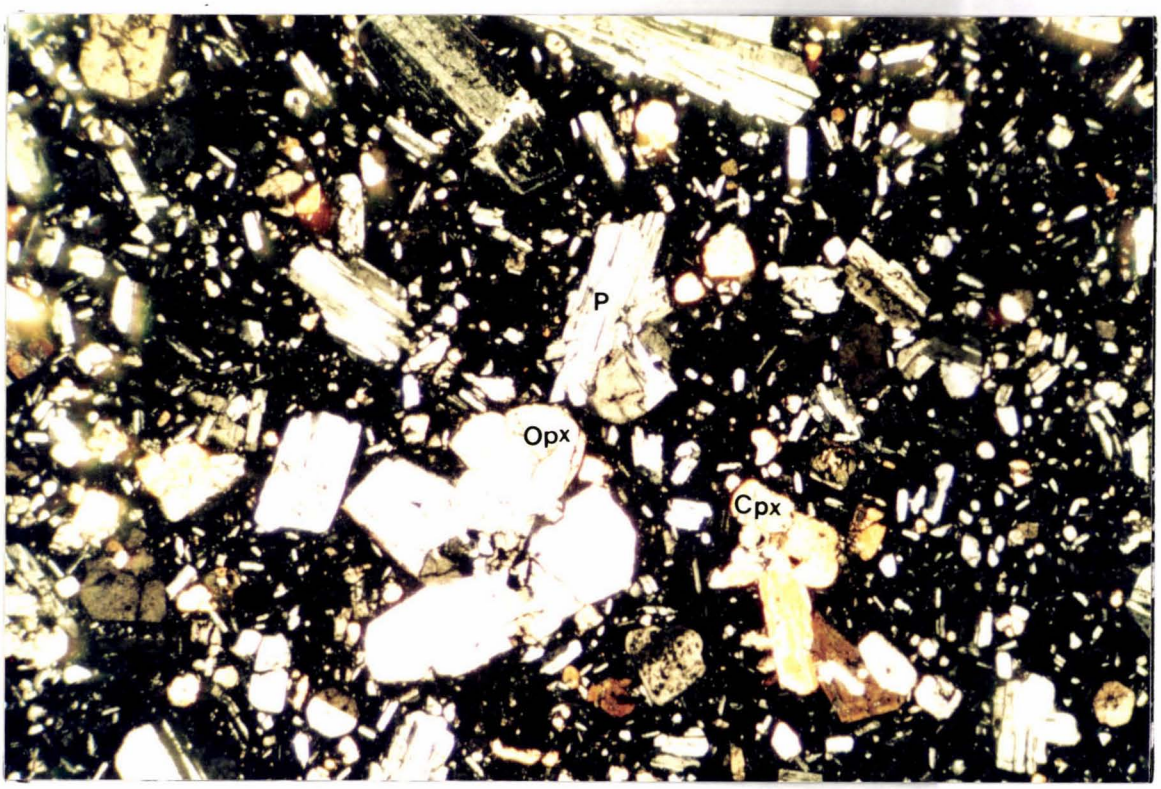

Figure 5.6 : Plagioclase-pyroxene andesite, phenocrysts of plagioclase (P) and pyroxene (Opx and Cpx) commonly forming aggregates. The groundmass is glassy and contains microcrystals of plagioclase and tridymite. (VUWN 31154, XPL x10)

5.4.1 *Hornblende Andesite*

A sample of hornblende andesite was collected from the ground layer at station 1 (Fig 4.2). The rock is red brown, with phenocrysts of plagioclase and hornblende which can be identified even in hand specimen. The rock has a seriate porphyritic texture and contains phenocrysts of plagioclase, hornblende, hypersthene and augite (in order of decreasing abundance; Table 5.1) with accessory magnetite. The phenocrysts comprise about 49% of the rock. Groundmass consists of microcrystals of plagioclase, tridymite and accessory magnetite, and apatite.

Plagioclase (labradorite) phenocrysts are euhedral to subhedral and have a maximum size of 4 mm. Larger phenocrysts of plagioclase show zoning and sieve texture and contain glass inclusions with smoothly zoned jackets of late crystallized phase. Inclusions of pyroxene, titanomagnetites, and rare tabular apatite crystals are common in the plagioclase phenocrysts.

Hornblende phenocrysts are generally subhedral, show strong pleochroism from pale yellow to red brown, and are altered to Fe oxides around the rim. They are tabular with an average length of 3 mm and commonly occur in aggregates (Fig 5.5).

Pyroxene phenocrysts are subhedral and smaller than both the plagioclase and hornblende phenocrysts. They occur as aggregates which contain granules of magnetite. Hypersthene phenocrysts are more abundant than augite.

5.4.2 *Plagioclase-pyroxene andesite*

Usually this rock is porphyritic with about 50% phenocrysts of plagioclase, hypersthene and augite and accessory magnetite. The phenocrysts are set in a microcrystalline groundmass of plagioclase, pyroxene and subordinate cristobalite (Fig 5.6).

Phenocrysts of plagioclase (labradorite-bytownite) comprise about 20% of the rock, show oscillatory and patchy zoning and have an average size of 1.5 mm. Hypersthene phenocrysts are commonly euhedral and have an average size of 1 mm.

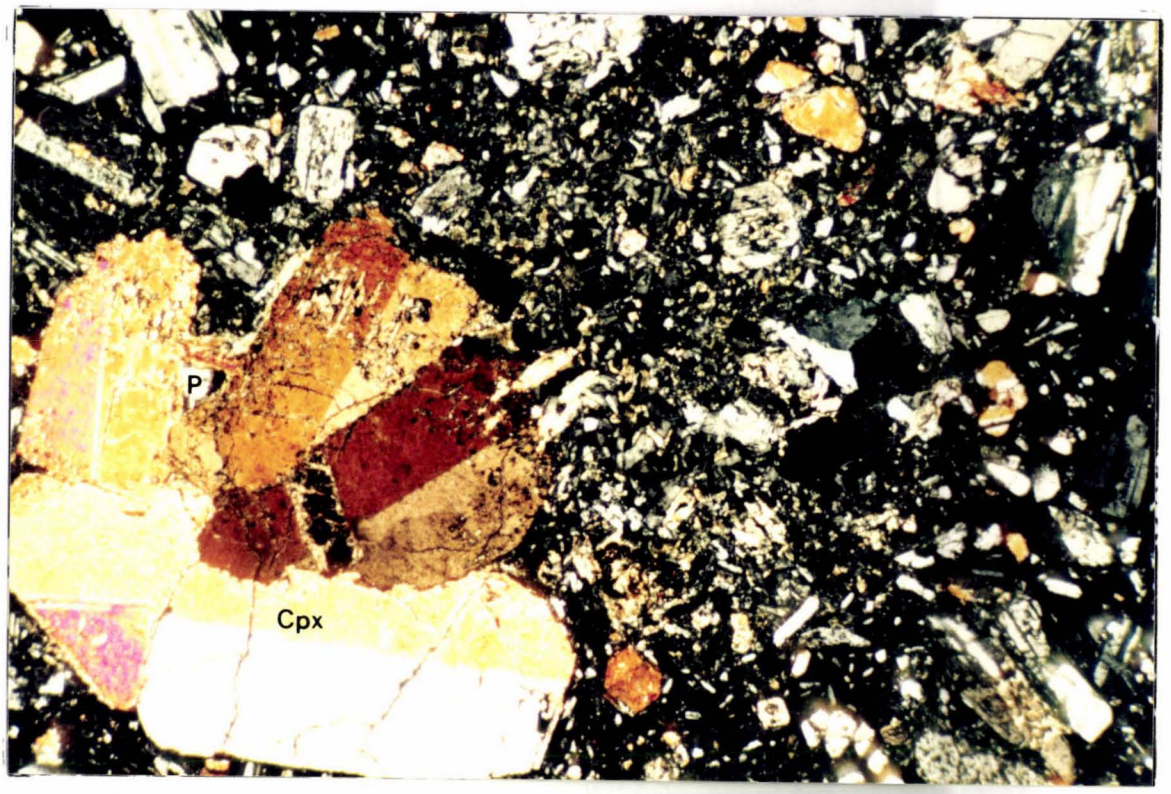

igure 5.7 : Pyroxene andesite, megaphenocrysts of clinopyroxene (Cpx) commonly form aggregates and rarely contain plagioclase (P) and orthopyroxene (Opx) inclusions; (VUWN 31156, XPL x10)

ure 5.8 : The greywacke consists of crystals of quartz and feldspar with minor hornblende, biotite and accessory sphene. (VUWN 31181, XPL x10)

Augite phenocrysts occur as euhedral microphenocrysts and larger euhedral to subhedral phenocrysts which have an average diameter of 2 mm. The pyroxene phenocrysts commonly occur in aggregates with rare magnetite inclusions. Modal analysis of a plagioclase-pyroxene andesite is presented in Table 5.1.

5.4.3 Pyroxene andesite

The rock has a porphyritic texture with phenocrysts of pyroxene, plagioclase and accessory magnetite. Pyroxene phenocrysts predominate over plagioclase phenocrysts (porphyritic pyroxene ratio of about 60%) The phenocrysts make up about 30% of the rock and are set in a microcrystalline and glassy groundmass. The rock is moderately hydrothermally altered.

Clinopyroxene phenocrysts are more abundant than orthopyroxenes. They are commonly subhedral, have an average size of 1 mm; generally bigger than plagioclase phenocrysts (Fig 5.7). Orthopyroxene phenocrysts occur as subhedral crystals with an average size of 0.5 mm and are rarely replaced by granular magnetite. The pyroxene phenocrysts commonly occur in aggregates with plagioclase and rare magnetite and olivine.

Plagioclase phenocrysts (labradorite-bytownite) are euhedral-subhedral, have an average size of 0.7 mm and show oscillatory and patchy zoning, with rare glass, pyroxene and titanomagnetite inclusions.

5.4.4 Olivine andesite

The olivine andesites have a seriate porphyritic texture with phenocrysts of plagioclase, augite, hypersthene, olivine (in order of decreasing abundance) and accessory magnetite. The phenocrysts make about 40% of the rock and are set in a fine-grained and glassy groundmass.

Plagioclase (labradorite-bytownite) phenocrysts are euhedral to subhedral < 1 mm in size and show oscilliatory and patchy zoning. Augite phenocrysts are commonly euhedral to subhedral and occur as glomerophenocrysts and microphenocrysts. Maximum size of the augite phenocrysts is 2 mm. Hypersthene phenocrysts are commonly euhedral and have an average size of 1 mm and are rarely replaced by granular magnetite.

Olivine phenocrysts are commonly anhedral, cracked and altered to a red brown iddingsite-smectite mixture along the cracks. The phenocrysts have an average size of 1.5 mm; and have a reaction coronna of orthopyroxene. Smaller crystals of olivine are found in the phenocryst aggregates with pyroxene and plagioclase.

5.5 *IGNIMBRITES*

Welded ignimbrites constitute a minor proportion of the lithics studied in the ground layer and the inclusions in other members of Taupo Pumice Formation. Two types of ignimbrites can be distinguished:

Type 1: Lithic crystal rich ignimbrite

Type 2: Crystal rich ignimbrite (Whakamaru Group type ignimbrite)

Type 1 ignimbrite is the most abundant type, while Type 2 is rare and only occurs as lapilli sized fragments. Microscopic study of Type 2 ignimbrite shows that it is very similar to the crystal rich ignimbrites of the Whakamaru Group (see chapter 3.3).

5.5.1 *Type 1: Lithic crystal rich ignimbrite*

Blocks of Type 1 ignimbrite up to 1.5 m occur in near vent exposures of the ground layer. The rock is a light brown to orange coloured, moderately welded, pumiceous lithic rich ignimbrite with vitroclastic texture. Crystals of quartz, plagioclase (oligoclase), hypersthene and hornblende (in order of decreasing abundance) make up about 25% of the rock. Xenoliths of rhyolite, dacite, andesite and rare greywacke pebbles make up about 5% of the rock. A representative modal analysis of this type of ignimbrite is given in Table 5.1.

Quartz crystals are frequently corroded and embayed, range from 0.2-2 mm in size and make up about 10% of the rock. Sodic plagioclase crystals make up about 8% of the rock. They are up to 2 mm in diameter, commonly broken and rarely show oscillatory zoning. Ferromagnesian crystals make up the remaining 7% of the rock and are frequently altered to dark brown oxide and clay minerals. Unaltered crystals of hypersthene have a subhedral shape and an average size of 0.7 mm. Hornblende crystals

are anhedral and have an average size of 0.5 mm. The matrix is light brown pumiceous ash, containing accessory magnetite.

5.5.2 *Type 2: Crystal rich ignimbrite*

Pale yellow, welded crystal rich ignimbrite, with crystals of sodic plagioclase, quartz, hypersthene and hornblende which make up about 45% of the rock. Crystals of plagioclase make up about 25% of the rock and are commonly broken and show oscillatory zoning. Quartz crystals are corroded, fractured and rarely embayed, have an average size of 2 mm and makeup about 15% of the rock. Euhedral to subhedral crystals of hypersthene (average size 1 mm) make up about 5% of the rock and are frequently altered to chlorite. Small amounts of brown hornblende and biotite are found which commonly are < 0.5 mm in size. Lithic fragments up to 2 mm in size make up about 10% of the rock, The matrix is pale yellow ash which contains accessory magnetite.

5.6 *NON VOLCANIC ROCK TYPES*

5.6.1 *Lake Sediments*

Lake sediment boulders up to 1 m in diameter are found in near vent exposures of the ground layer. The lake sediments are commonly light grey to pale brown or pink pumiceous sandstones and siltstones with abundant quartz, rhyolite lapilli, and rounded pebbles of greywacke.

5.6.2 *Greywacke*

These rocks are greenish to dark grey, dense meta-sandstones and consist of quartzo-feldspathic, poorly sorted coarse to fine sand. The greywacke occurs as subrounded to rounded pebbles in the ground layer (Fig 5.8).

Microscopic study shows that the rocks consist of angular to sub-rounded grains of plagioclase which constitute about 50% of the rock. The plagioclase is mainly albite-oligioclase and frequently shows polysynthetic twinning. Alkali feldspars (orthoclase and microcline) occur in subordinate amounts compared to the plagioclase grains,

constituting approximately 20% of the total feldspars. Both plagioclase and alkali feldspars are commonly altered to illite.

Quartz constitutes about 35% of the rock and occurs as subrounded grains and frequently shows undulose extinction.

Ferromagnesian minerals constitute about 5% of the rock and are mainly biotite and rare hornblende and accessory opaque oxides. Biotite grains are usually deformed and bent around more competent minerals, suggesting that the biotites are primary features of sedimentation and not post-depositional authigenic minerals. Lithic fragments are rare (less than 5%) and are of igneous, metamorphic and sedimentary origin. A matrix of fine grained intergranular clay minerals (mainly chlorite which is frequently altered to brown oxides) makes up to 10% of the rock.

Chapter VI

MINERAL CHEMISTRY OF LITHIC BLOCKS

6.1 INTRODUCTION

Major rock forming minerals in polished thin sections cut from seven selected rock samples from the inclusions in the Taupo Pumice Formation (four andesites, two dacites and two rhyolites) were analysed using the JXA-733 electron probe microanalyzer (EPMA) in the Research School of Earth Sciences (Victoria University of Wellington). Analytical procedures on the EPMA are described in Appendix 3. Mineral chemistry on some selected rock samples was studied to understand the differences in element distribution in similar mineral species in the rhyolites, dacites and andesites described in chapter 5 which is also reflected in the wholerock chemistry of the analysed lithic blocks from the ground layer.

6.2 OLIVINE

Olivine occurs as fractured and partially resorbed phenocrysts, rarely enclosed by either hypersthene or augite in some andesites and rarely as altered microphenocrysts in the dacites. Phenocryst cores are unaltered, but the rims and fractures are partly replaced by a brown alteration product, possibly an iddingsite-smectite mixture (Fig 6.1). Some olivine crystals contain chrome spinel inclusions.

Olivine compositions in the andesites range from $Fo_{82.2}$ to $Fo_{88.4}$ (Table 6.1). Fragmented grains are generally chemically homogeneous, but a slightly higher Fo content is shown by most analysed cores.

MnO content varies from 0.18 to 0.26 wt%, and a negative correlation exists between wt% NiO and (mol %) Fa which is consistent with observations made by Nishimura et al. (1968) and Simkin and Smith (1970).

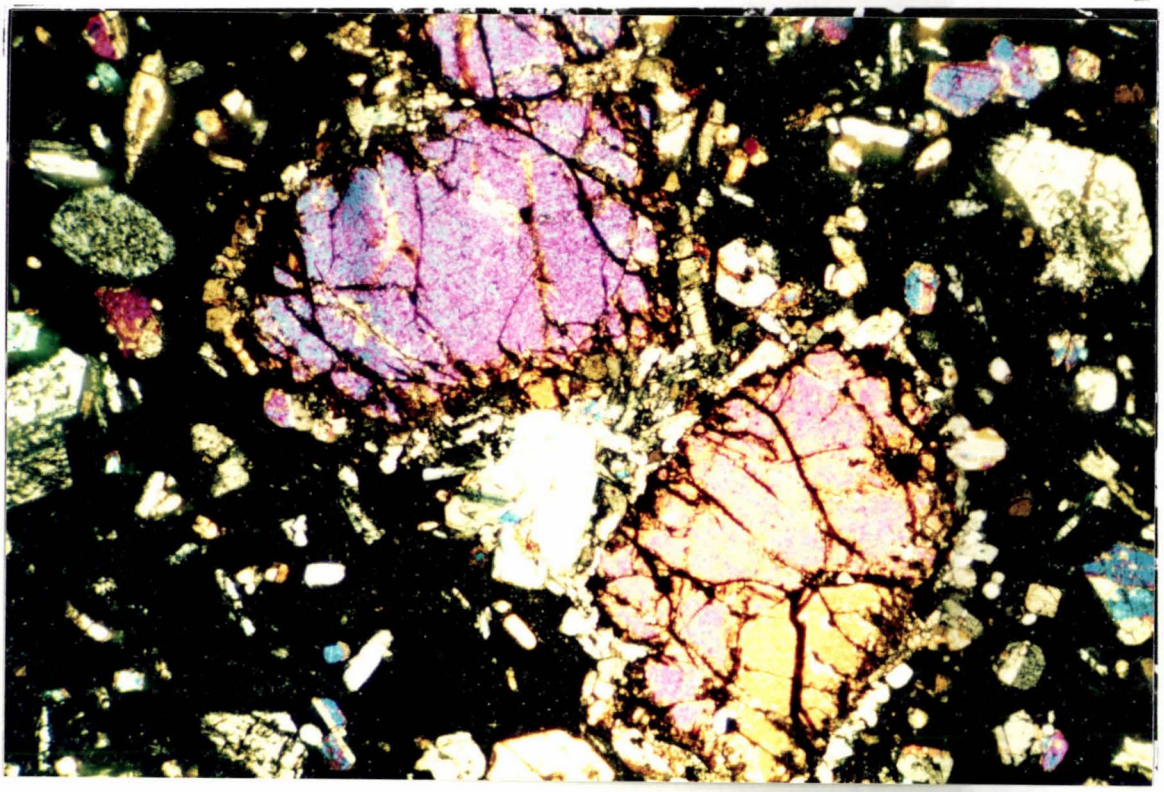

Figure 6.1 : Fractured olivine phenocryst, the fractures are filled with an iddingsite-smectite alteration product. Phenocryst rims have a reaction corona of orthopyroxene. (Olivine bearing andesite VUWN 31157, XPL x10)

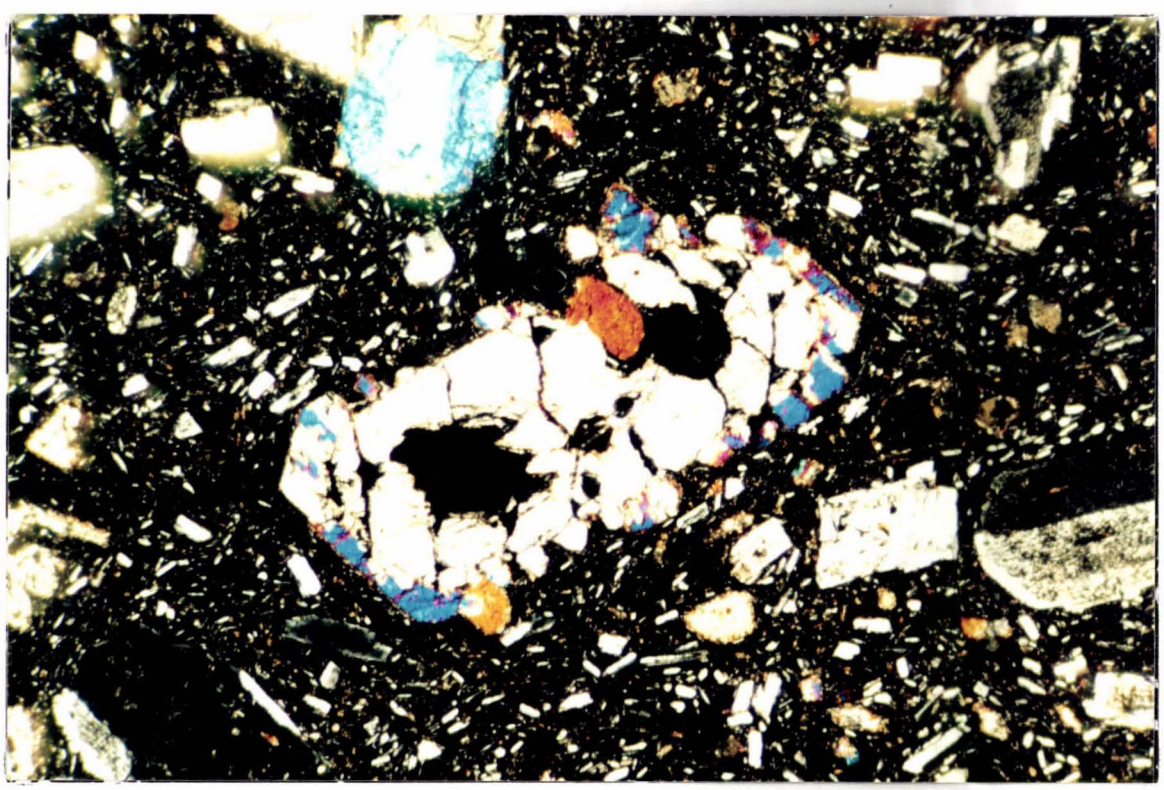

Figure 6.2 : Hypersthene phenocryst is rimmed by pigeonite in pyroxene-andesite this is among the evidence of magma mixing in the andesites. (VUWN 31157, XPL x10)

Table 6.1 : Electron microprobe analyses of olivines from the lithic blocks in the Taupo Pumice Formation.

VUW	31157	–	–	–	–	–
Sample	1/4	–	–	–	–	–
	(1)	(2)	(3)	(4)	(5)	(6)
	(C)	(R)	(R)	(C)	(C)	(R)
SiO_2	39.80	38.75	39.40	39.63	41.07	39.23
TiO_2	-	-	-	-	-	-
Al_2O_3	-	0.08	-	-	0.07	-
FeO*	12.99	15.95	15.33	13.06	11.43	16.78
MnO	0.2	0.23	0.26	0.23	0.18	0.24
MgO	46.80	43.56	43.97	45.97	47.82	43.46
CaO	0.11	0.11	0.10	0.15	0.16	0.09
Na_2O	-	-	-	-	-	-
K_2O	-	-	-	-	-	-
NiO	0.30	0.31	0.27	-	0.19	-
Total	100.20	98.99	99.33	99.04	100.92	99.80

*Total iron as FeO

Atomic Proportions, O = 4

Si	0.990	0.989	0.999	0.996	0.995	0.995
Ti	-	0.002	-	-	-	-
Al	-	-	-	-	-	-
Fe	0.270	0.341	0.325	0.274	0.232	0.356
Mn	0.004	0.005	0.006	0.005	0.004	0.005
Mg	1.735	1.658	1.662	1.722	1.763	1.644
Ca	0.003	0.003	0.003	0.004	0.004	0.002
Na	-	-	-	-	-	-
K	-	-	-	-	-	-
Ni	0.006	0.006	0.006	-	0.004	0.002
Total	3.008	3.004	3.001	3.001	3.002	3.004
bd; Fe						
Fe+Mg	0.135	0.170	0.164	0.137	0.116	0.178
En	13.5	17.1	16.4	13.7	11.6	17.8
Fs	86.5	82.9	83.6	86.3	88.4	82.2

Olivine andesite (1-6)
(C)= phenocryst core; (R)=phenocryst rim

Ca content varies from 0.09 to 0.16 wt% and is slightly higher in the more Fe-rich olivines. Simkin and Smith (1970) suggested that extrusive olivines have > 0.10 wt% CaO as opposed to plutonic olivines which have < 0.10 wt% CaO. Initial Ca content, however is dependent upon the silica activity of the magma (Stormer, 1973) and this dependence may explain the low CaO content of the analysed olivines. The iddingsite-smectite mixture probably results from a hydrothermal reaction with water present in the system (Deer et al. 1966).

Textural evidence indicates that olivine was an early and relatively minor phase in the andesites. Partial resorption of olivine phenocrysts and their occurrence only within andesites suggests that they are preserved as a relict of an earlier crystallisation environment. Hackett (1985) has suggested that coexistence with orthopyroxenes, presence of corroded olivines with orthopyroxene coronas, and the occurrence of chrome spinel inclusions in andesites all indicate that the olivines were xenocrystic and probably originated from magma mixing or the entrainment of the crystallisation product of a basaltic magma. While low Ni contents (compared with olivine field of Simkin and Smith (1970) of 1-4 wt% Ni) are probably the result of a low Ni content of the magma, low CaO contents may be due to low Si activity and are possibly due to post formational alteration.

6.3 PYROXENES

Both orthopyroxenes and clinopyroxenes are important phenocryst minerals in the studied rocks. Orthopyroxenes have a limited compositional range falling between the end members $Mg_2 Si_2 O_6$ and $Fe_2 Si_2 O_6$ with minor substitutions of other components. Clinopyroxenes have a much wider compositional range but are generally Ca-rich lying below the $CaMgSi_2 O_6$ to $CaFeSi_2 O_6$ join. Ca poor clinopyroxene (pigeonite) occurs in one olivine andesite (VUWN 31157) and in one pyroxene andesite (VUWN 31156), jacketing orthopyroxene phenocrysts and as microphenocrysts (Fig 6.2).

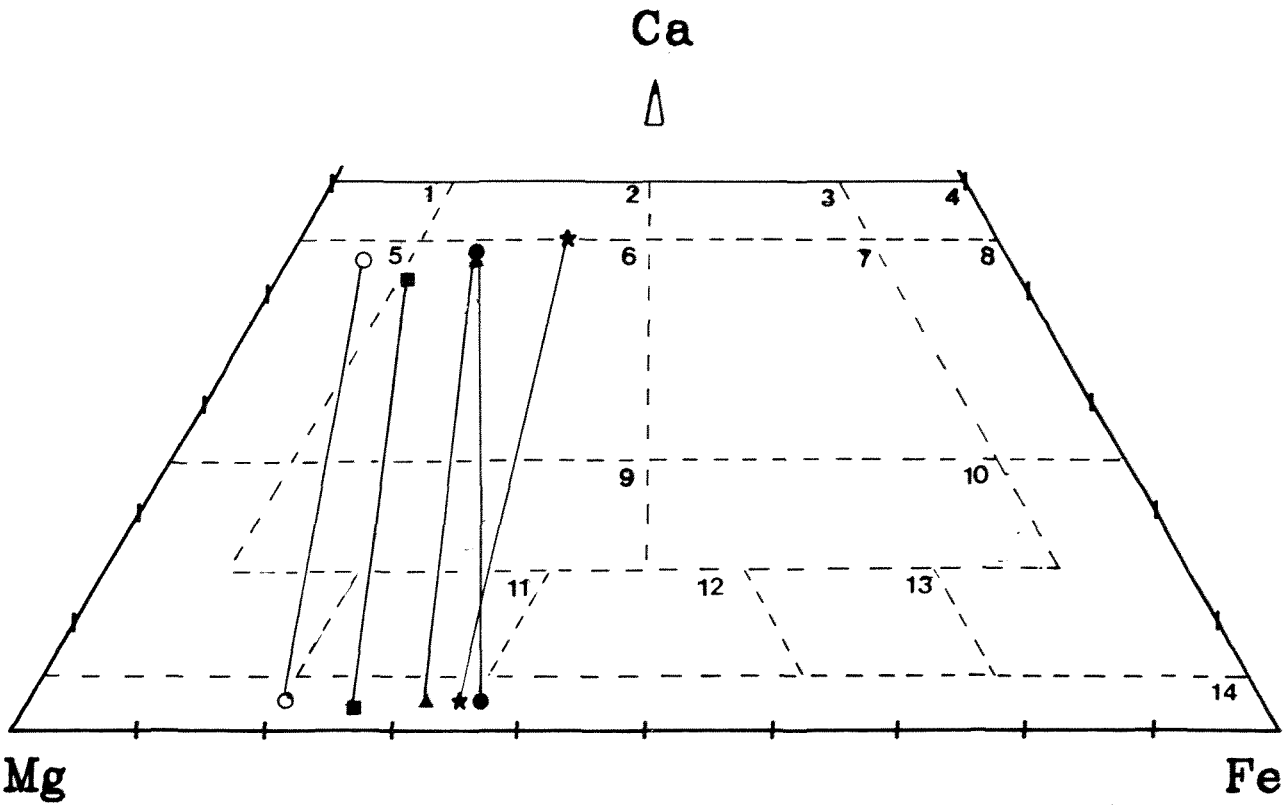

ure 6.3 : Composition of representative pyroxene analyses from the lithics in the ground layer, tie lines show coexisting orthopyroxene and clinopyroxene pairs.

1.Diopside
2.Salite
3.Ferrosalite
4.Hedenbergite
5.Endiopside
6.Augite
7.Ferroaugite
8.Ferroaugite
9.Subcalcic Augite
10.Subcalcic Ferroaugite
11.Magnesium Pigeonite
12.Intermediate Pigeonite
13.Ferriferrous Pigeonite
14.Enstatite-Orthoferrosilite series

Open circle -Pyroxene Andesite (VUWN 31153)
Square -Hornblende Andesite (VUWN 31156)
Closed circle -Two pyroxene dacite (VUWN 31146)
Star -Biotite Rhyolite (VUWN 31139)
Triangle -Olivine Andesite (VUWN 31157)

Table 6.2 : Electron microprobe analyses of orthopyroxenes from the lithic blocks in the Taupo Pumice Formation.

VUW	31139	–	–	31129	–	–	–	31155	–	–	–	31146	–	–	–	31153	–	–	–	31156
Sample	4/12	–	–	1/B/3	–	–	–	4/1	–	–	–	1/M/4	–	–	–	2/9	–	–	–	2/8
	(1)	(2)	(3)	(4)	(5)	(6)	(7)	(8) (C)	(9) (R)	(10) (C)	(11) (R)	(12) (C)	(13) (R)	(14) (C)	(15) (R)	(16) (C)	(17) (R)	(18) (C)	(19) (R)	(20) (C)
SiO_2	52.63	52.53	51.97	51.43	51.46	51.57	50.47	53.03	52.27	52.10	52.36	52.37	53.39	52.05	51.97	52.55	53.27	53.90	52.59	54.29
TiO_2	0.17	-	-	0.14	0.24	0.15	0.16	0.21	0.27	-	0.29	-	0.16	0.25	0.30	0.18	0.19	0.11	0.18	0.11
Al_2O_3	0.37	0.29	0.33	0.59	0.75	0.48	0.56	0.86	0.81	0.59	0.64	0.66	0.98	1.37	2.81	1.17	1.79	0.98	1.91	1.41
FeO*	21.11	21.22	20.93	26.83	24.92	27.20	28.12	19.14	19.99	20.91	21.11	21.10	19.28	19.62	15.86	19.08	16.44	16.60	17.57	11.69
MnO	1.89	2.03	2.37	0.96	0.69	1.01	1.04	0.57	0.81	0.93	1.02	1.05	0.72	0.79	0.45	0.55	0.42	0.44	0.45	0.27
MgO	21.89	21.60	21.85	17.59	19.85	18.00	16.77	23.20	23.85	21.92	21.97	21.85	22.74	22.37	24.62	23.43	24.67	26.05	25.37	28.83
CaO	0.97	0.92	1.35	1.30	1.05	1.31	1.24	1.56	1.20	1.21	1.06	1.07	1.38	1.30	2.03	1.18	0.20	1.12	1.14	1.81
Na_2O	-	-	-	-	-	-	-	-	-	-	-	-	-	-	-	-	-	-	0.09	
K_2O	-	-	-	-	-	-	-	0.16			-	-	-	-	-	-	-	-	-	-
Total	98.86	98.59	98.87	98.84	98.96	99.72	98.36	98.57	99.20	97.82	98.45	98.10	98.65	97.75	98.04	98.14	96.98	99.28	99.30	98.41

*Total iron as FeO

Atomic Proportions, O = 6

Si	1.985	1.991	1.971	1.991	1.970	1.981	1.981	1.981	1.953	1.981	1.979	1.984	1.990	1.967	1.924	1.969	1.972	1.971	1.934	1.959
Ti	-	-	-	0.004	0.007	0.004	0,005	0.006	0.008	0.026	0.008	0.003	0.005	0.007	0.008	0.005	0.005	0.003	0.005	0.003
Al	0.016	0.013	0.015	0.027	0.034	0.022	0.026	0.038	0.035	0.003	0.029	0.029	0.043	0.061	0.123	0.052	0.078	0.042	0.083	0.060
Fe	0.666	0.673	0.664	0.869	0.797	0.874	0.923	0.598	0.625	0.665	0.667	0.669	0.661	0.620	0.491	0.598	0.509	0.508	0.540	0.353
Mn	0.061	0.065	0.076	0.032	0.022	0.033	0.0350	0.018	0.026	0.030	0.033	0.034	0.023	0.025	0.014	0.018	0.013	0.014	0.014	0.008
Mg	1.231	1.220	1.235	1.015	1.133	1.031	0.981	1.292	1.328	1.242	1.238	1.234	1.263	1.260	1.359	1.309	1.362	1.420	1.391	1.551
Ca	0.039	0.037	0.055	0.054	0.043	0.054	0.052	0.062	0.048	0.049	0.043	0.043	0.055	0.053	0.081	0.047	0.040	0.044	0.045	0.070
Na	-	-	-	-	-	-	-	-	-	-	-	-	-	-	-	-	-	-	0.007	-
K	-	-	-	-	-	-	-	-	-	0.008	-	-	-	-	-	-	-	-	-	-
Total	3.998	3.999	4.016	3.992	3.997	3.999	4.001	3.995	4.022	4.004	3.997	3.996	4.040	3.993	4.000	3.998	3.979	4.002	4.019	4.004
Fe/Mg+Fe	0.351	0.355	0.349	0.461	0.413	0.459	0.489	0.316	0.320	0.349	0.350	0.351	0.322	0.330	0.265	0.314	0.272	0.263	0.280	0.185
FMI	62.8	61.2	60.8	53.0	58.0	53.2	50.6	67.7	67.1	64.1	63.9	62.3	65.0	64.4	69.9	68.0	72.3	73.1	71.5	81.1
Mg	63.6	63.2	63.2	52.4	58.1	52.6	50.2	66.2	66.4	63.6	63.6	63.4	65.8	65.2	70.4	66.9	71.3	72.0	70.4	78.6
Fe	34.4	34.9	34.0	44.9	40.8	44.6	47.1	30.6	31.2	34.0	34.2	34.4	31.3	32.1	25.4	30.6	26.6	25.8	27.3	17.9
Ca	2.0	1.9	2.8	1.7	1.1	2.8	2.7	3.2	2.4	2.5	2.2	2.2	2.9	2.7	4.2	2.4	2.1	2.2	2.3	3.5

FMI=FM index
(C)=phenocryst core (M)=phenocryst middle (R)=phenocryst rim
Biotite bearing rhyolite (1-3) Hypersthene Rhyolite (4-7)
Two pyroxene dacite (8-11)

FMI=FM index
(C)=phenocryst core (M)=phenocryst middle (R)=phenocryst rim
1.Two pyroxene dacite (12-15) 2.Hornblende andesite (16-19)

Table 6.2 : Electron microprobe analyses of orthopyroxenes from the lithic blocks in the Taupo Pumice Formation (continued).

VUW	31156	–	–	–	–	31157	–	–	–	–
Sample	2/8	–	–	–	–	1/4	–	–	–	–
	(21)	(22)	(23)	(24)	(25)	(26)	(27)	(28)	(29)	(30)
	(R)	(C)	(R)	(C)	(R)	(C)	(R)	(C)	(R)	(C)
SiO_2	53.14	54.82	51.98	54.18	52.60	53.51	52.61	52.65	52.64	53.66
TiO_2	0.25	0.09	0.36	-	0.18	0.19	0.17	0.22	0.20	0.17
Al_2O_3	0.94	1.41	0.85	1.46	1.45	1.46	1.95	0.75	0.64	0.13
FeO*	17.54	12.83	21.39	13.20	16.21	15.26	16.45	21.99	22.36	17.25
MnO	0.40	0.25	0.48	0.29	0.34	0.36	0.27	0.50	0.53	0.38
MgO	24.38	28.84	18.59	27.52	25.08	25.42	24.59	21.91	21.67	25.56
CaO	1.84	1.54	5.49	1.83	1.51	2.37	1.73	1.44	1.42	1.64
Na_2O	0.07	-	0.07	-	-	-	-	-	-	-
K_2O	-	0.15	-	-	-	-	-	-	-	-
Total	98.49	99.78	99.21	98.63	97.44	98.54	97.77	99.46	99.46	99.79

*Total iron as FeO

Atomic Proportions, O=6

Si	1.971	1.963	1.971	1.961	1.966	1.964	1.954	1.974	1.977	1.960
Ti	0.003	0.003	0.010	0.003	0.005	0.005	0.005	0.005	0.006	0.005
Al	0.041	0.060	0.038	0.062	0.063	0.063	0.085	0.033	0.028	0.049
Fe	0.544	0.394	0.696	0.400	0.503	0.468	0.511	0.689	0.702	0.527
Mn	0.012	0.008	0.016	0.009	0.011	0.011	0.009	0.016	0.017	0.012
Mg	1.348	1.511	1.031	1.485	1.386	1.390	1.362	1.224	1.213	1.392
Ca	0.073	0.060	0.226	0.071	0.060	0.093	0.069	0.058	0.057	0.064
Na	0.004	-	0.005	-	-	-	-	-	-	-
K	-	-	-	-	-	-	-	-	-	-
Total	3.996	3.999	3.993	3.991	3.994	3.994	3.995	4.000	4.002	4.009
Fe/Mg+Fe	0.288	0.207	0.403	0.212	0.266	-	-	-	-	-
FMI	70.8	79.0	59.2	78.4	72.9	74.4	72.4	61.6	61.0	72.0
Mg	68.6	76.9	52.8	75.9	71.1	71.2	70.1	62.1	61.5	70.2
Fe	27.7	20.1	35.6	20.5	25.8	24.0	26.3	35.0	35.6	26.6
Ca	3.7	3.1	11.6	3.6	3.1	4.8	3.6	2.9	2.9	3.2

FMI=FM index
(C)=phenocryst core (M)=phenocryst middle (R)=phenocryst rim
Pyroxene andesite (20-25) Olivine andesite (26-30)

Table 6.3 : Electron microprobe analyses of clinopyroxenes from the lithic blocks in the Taupo Pumice Formation.

VUW	31139	31146	–	31157	–	31153	–	31156	–	–
Sample	4/12	1/M/4	–	4/1	–	2/9	–	2/8	–	–
	(1)	(2)	(3)	(4)	(5)	(6)	(7)	(8)	(9)	(10)
	-	(C)	(R)	(C)	(R)	(C)	(R)	(C)	(R)	(C)
SiO_2	47.81	51.14	51.14	54.34	51.80	50.51	52.46	53.83	51.90	52.02
TiO_2	-	0.44	0.41	0.10	0.27	0.42	0.24	1.13	0.31	0.25
Al_2O_3	1.92	1.91	1.74	1.14	1.86	3.70	1.60	1.06	1.87	1.78
FeO*	12.35	9.14	9.47	5.39	9.23	6.49	7.13	4.28	10.16	5.87
MnO	2.68	0.38	0.47	0.18	0.17	0.21	0.37	0.15	0.24	-
MgO	11.06	14.37	14.72	15.87	14.58	16.92	16.96	18.16	16.01	17.11
CaO	20.43	21.04	21.04	21.58	21.23	20.16	20.04	21.67	18.63	20.63
Na_2O	1.92	0.31	0.30	0.23	0.19	0.29	0.17	0.20	0.25	0.20
K_2O	-	-	-	-	-	-	-	-	-	-
Cr_2O_3	-	-	-	0.43	-	0.42	-	0.39	-	0.48
Total	98.17	98.73	99.69	99.26	99.33	99.42	98.97	100.48	99.54	98.34

*Total iron as FeO

Atomic Proportions, O=6

Si	1.887	1.935	1.934	2.000	1.944	1.882	1.950	1.965	1.942	1.939
Ti	0.002	0.013	0.011	0.003	0.008	0.160	0.007	0.004	0.009	0.007
Al	0.090	0.085	0.077	0.049	0.082	0.012	0.070	0.046	0.083	0.078
Fe	0.409	0.289	0.297	0.166	0.290	0.201	0.221	0.134	0.326	0.183
Mn	0.090	0.012	0.015	0.006	0.005	0.007	0.012	0.005	0.008	0.004
Mg	0.651	0.811	0.823	0.871	0.816	0.934	0.940	0.970	0.865	0.951
Ca	0.864	0.853	0.846	0.651	0.854	0.800	0.798	0.859	0.757	0.824
Na	0.147	0.022	0.022	0.016	0.014	0.021	0.012	0.014	0.018	0.014
K	-	-	-	-	-	-	-	-	-	-
Cr	-	-	-	0.012	-	0.012	-	0.011-	0.013	
Total	4.140	4.020	4.016	3.962	4.013	4.030	4.010	3.997	4.008	4.000
Fe/Mg+Fe	0.385	0.263	0.265	0.160	0.262	0.177	0.191	0.121	0.274	0.164
FMI	56.6	72.9	72.5	83.5	73.4	81.8	80.1	87.5	72.1	83.6
Mg	33.8	41.6	41.8	46.1	41.6	48.3	48.0	49.4	44.4	48.6
Fe	21.3	14.8	15.1	8.8	14.8	10.4	11.3	6.8	16.7	9.4
Ca	44.9	43.6	43.1	45.1	43.6	41.3	40.7	43.8	38.9	42.0

FMI=FM index

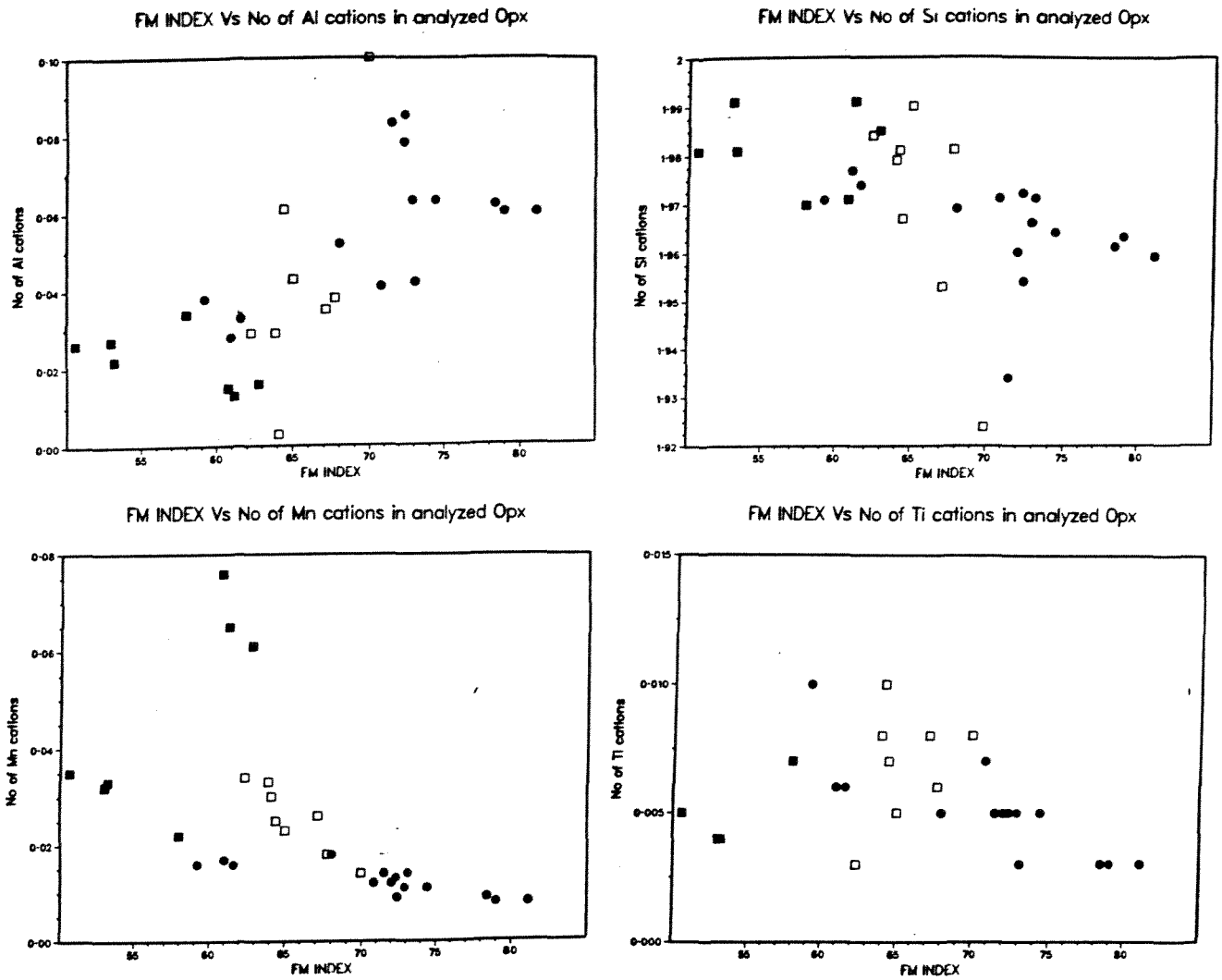

Figure 6.4 : Variation in calculated number of Si, Al, Mn and Ti cations with the FM index in the analysed orthopyroxenes.
rhyolites (filled squares); dacites (squares); andesites (circles)

The modal ratio ranges from Cpx = Opx in most of the andesites; to Opx > Cpx in the dacites and Opx >> Cpx in most of rhyolites. In most of the andesite lava groundmass Opx > Cpx. A general increase in plag : pyx and Opx : Cpx ratios with increasing SiO_2 content of bulk rocks is considered to be a result of fractional crystallization while aberrant ratios (eg. Cpx >> plag or plag >> pyx in andesites) are considered to result from accidental entrainment of igneous rock fragments from the plutonic enviroment.

6.3.1 ORTHOPYROXENES

Orthopyroxenes occur as both a phenocryst phase and a groundmass constituent in the andesitic rocks and as a phenocryst phase in the dacite and rhyolites. Orthopyroxene analyses from the andesites, dacites and rhyolites show a distinct compositional range. Orthopyroxene andesites are bronzite or hypersthene in composition, and most phenocrysts have an FM index (=100 $Mg/(Mg+Fe^{+2}+Fe^{+3}+Mn)$ ranging from 71-81% in most of the andesites (Table 6.2). Phenocrysts show a compositional zoning in core rim pairs from $Mg_{78.6}\ Fe_{17.6}\ Ca_{3.8}$ to $Mg_{68.6}\ Fe_{27.7}\ Ca_{3.7}$ and an increase in FM index is observed from core to rim in most of the analysed phenocrysts.

In the dacites and rhyolites orthopyroxene is hypersthene. It ranges in composition from $Mg_{66.3}\ Fe_{31.3}\ Ca_{2.4}$ to $Mg_{63.5}\ Fe_{34.3}\ Ca_{2.2}$ from core to rim and has an FM index of 64-67% in the dacites. In the rhyolites the hypersthene phenocrysts have an FM index of 50-58% and range in composition from $Mg_{58.6}\ Fe_{40.8}\ Ca_{1.2}$ to $Mg_{50.1}\ Fe_{47.2}\ Ca_{2.6}$

Cr and Ni occur mainly in Mg rich orthopyroxenes and high contents of Mn are found in Fe rich orthopyroxenes in igneous rocks. In most of the analysed orthopyroxenes Al is nearly always sufficient to fill the tetrahedral sites with Si and the remaining octahedrally coordinated Al is generally less than 1% of the total cations.

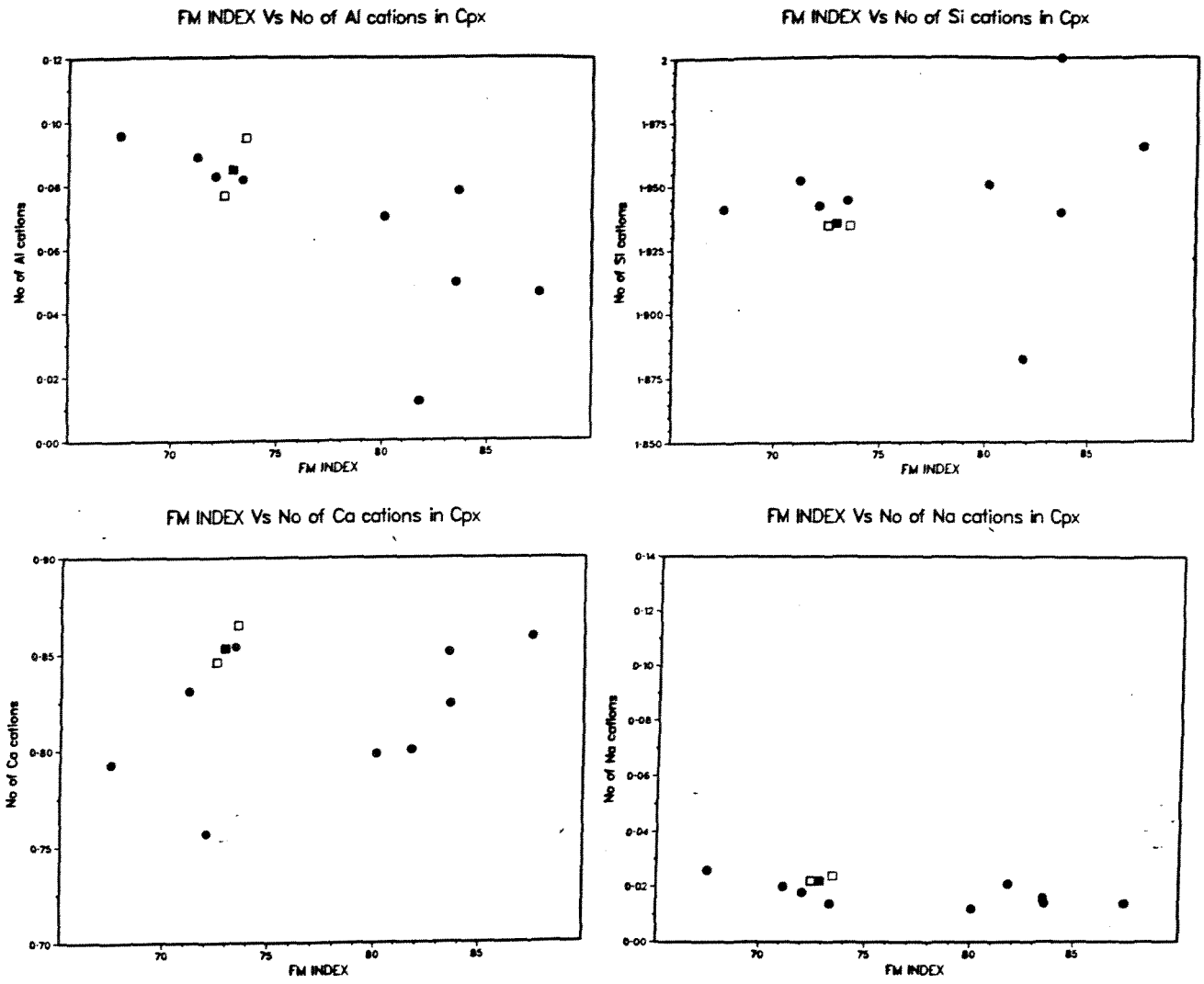

Figure 6.5 : Variation in the calculated number of Si, Al, Na, and Ca cations with the Fm index in the analysed clinopyroxenes.
rhyolites (filled squares); dacites (squares); andesites (circles)

Of the ions in the orthopyroxenes Si, Al, and Ti show little variation with changing FM index, although poorly defined trends suggest an increase in Al and a decrease in Si, Ti and Mn with increasing Mg content (Fig 6.4). Cr and Ni are not important in most of the orthopyroxenes, being present in cation proportions less than 0.01.

The orthopyroxene compositions are related to the Mg number of the parent rock. The andesitic orthopyroxenes are more magnesian rich than the rhyolitic hypersthenes as would be expected. The dacitic orthopyroxenes lie between the andesitic and rhyolitic compositions. Ca content in the orthopyroxenes is higher in the andesites and progressively decreases in the dacites and rhyolites. It is generally considered that the Ca content is related to crystallization temperatures of the individual magmas.

6.3.2 CLINOPYROXENE

Clinopyroxenes are both phenocryst and groundmass phases in the andesites and commonly contain inclusions of orthopyroxene, plagioclase and magnetite. In the dacites clinopyroxene occurs as a phenocryst phase only and is commonly smaller than the coexisting orthopyroxene phenocrysts. Rare clinopyroxene microphenocrysts occur in some of the rhyolites.

Clinopyroxenes occur in the andesites as phenocrysts, as glomeroporphyritic aggregates and as a groundmass constituent. Subhedral to euhedral clinopyroxene phenocrysts tend to be smaller than coexisting hypersthene phenocrysts. In the andesites inclusions of orthopyroxene, plagioclase, magnetite and glass are moderately common, while resorption is rare. In the dacites, clinopyroxene occurs as euhedral-subhedral phenocrysts commonly smaller in size than the orthopyroxene phenocrysts and forming aggregates. Rare clinopyroxene phenocrysts commonly less than 0.5 mm in size are found in some of the rhyolites.

Most clinopyroxenes are augites although in the andesites some have endiopside cores with an augite rim. Phenocrysts generally show a normal trend of iron enrichment ranging from $Mg_{49.4}\ Fe_{6.8}\ Ca_{43.8}$ to $Mg_{40.1}\ Fe_{18.7}\ Ca_{41.2}$ from core to rim in the andesites. Average composition in the dacites is about $Mg_{41.5}\ Fe_{14.7}\ Ca_{34.3}$ and about $Mg_{57.2}\ Fe_{8.5}\ Ca_{34.3}$ in the rhyolites.

Si content of the clinopyroxenes varies inversely with Ti and Al and increases with increasing Mg content (Fig 6.5). In most of the clinopyroxenes analysed, Al is less than 0.1 ions per formula unit. When the amount of Si is not enough to fill the Z site, Al is assigned into the tetrahedral site. In most analysed clinopyroxenes Si and Al are sufficient to fill in the tetrahedral sites, and the remaining octahedrally coordinated Al is generally less than 1% of the total cations.

Ca shows no definite relationship with Mg content of the clinopyroxenes. Mn and Na are the only minor elements of any importance and are inversely proportional to the amount of Mg. Cr is important only in clinopyroxenes of the pyroxene and olivine andesites, and shows a marked preference for high Mg cores. These compositions are explained by Seward (1971) as due to high octahedral site preference of Cr.

Most of the analysed clinopyroxenes are smoothly and normally zoned and lack zonation reversals or overgrowths, which are attributed to magma mixing. All of the analysed pyroxenes in the andesites, dacites and rhyolites show a limited Mg/Fe compositional range similar to that of the andesites and dacites of the Tongariro Volcanic Centre which was considered to result from the weak iron enrichment trend of orogenic andesites (Hackett, 1985). Fig 6.3 shows coexisting orthopyroxene and clinopyroxene pairs in the andesites and dacites. It is interesting to note that most of the more basic rocks have comparatively Mg rich clino and orthopyroxene pairs. Pyroxenes in the dacites have the least Mg content. A more important relationship about the Mg-Fe distribution between coexisting orthopyroxene and clinopyroxene pairs during crystallization can also be observed on this diagram. Mg is preferentially taken into the clinopyroxenes whereas Fe is enriched in the orthopyroxenes. Al, Ti, and Na are enriched in the clinopyroxenes, while Mn is enriched in the orthopyroxenes. This observation is in agreement with those of De Vore (1957) and Fleet (1974), who found similar element partitioning between orthopyroxene and clinopyroxene.

6.4 *HORNBLENDE*

In the andesites, euhedral to subhedral crystals (up to 3 mm in size) are strongly pleochroic, and highly oxidized with small iron oxide crystals concentrated along cleavage traces, internal fractures and outer rims (Fig 5.5). Rare hornblende crystals are found in some of the dacites where they are 0.3-0.5 mm in size. In the hornblende rhyolites hornblende phenocrysts are 1-1.5 mm in size and occur in more than accessory amounts.

The compositions of hornblendes analysed from VUWN 31153 are presented on Table 6.4. According to the classification of amphiboles proposed by Leake (1978), the analysed hornblende compositions approach that of pargasite - ferrohastingsite, with an A site occupancy of 50-60% and Fe:Mg ratios averaging 1:2. An ideal formula for paragasite is $NaCa_2\ Mg_4\ Al\ Si_6\ O_{2.2}\ (OH)_2$ Comparision of the analysed hornblendes with the ideal formula shows that they are deficient in Al and have undergone significant $Mg\text{-}Fe^{2+}$ substitution. The amount of Ti present is considerable and accounts for the dark brown colouration. No significant chemical variation between the core and rim of the hornblende phenocrysts was observed.

Presence of amphiboles in volcanic rocks shows the relatively high degree of water saturation in the magma and with it a related high fO_2 (Heltz, 1973). The low Al content suggests crystallization at relatively low pressure (Leake, 1973).

6.5 *BIOTITE*

Biotite occurs as phenocrysts of about 0.5mm in diameter and microphenocryst aggregates in the biotite-bearing rhyolites and in the hornblende-hypersthene rhyolites as an accessory phase. The biotite is brown and strongly pleochroic from light brown to dark brown. Biotite analyses are presented in Table 6.5. In most, the Mg:Fe ratio is nearly 2:1. The sum of Si and Al is usually sufficient to fill the tetrahedral position, with an excess Al of about 0.15 mol% going to the octahedral positions. Other cations include Ti and Mn which substitute for Fe and Mg.

Table 6.4 : Electron microprobe analyses of hornblende from the lithic blocks in the Taupo Pumice Formation.

VUW	31153	–	–	–	–	
Sample	2/9	–	–	–	–	
	(1)	(2)	(3)	(4)	(5)	
SiO_2	43.48	42.70	42.85	42.71	42.6	44.52
TiO_2	1.94	2.0	2.01	2.22	1.94	2.12
Al_2O_3	11.04	10.75	11.33	11.30	10.78	11.07
FeO*	11.76	11.34	11.13	11.95	12.27	12.35
MnO	0.16	-	0.16	-	0.14	0.26
MgO	14.17	13.83	14.39	14.13	13.97	14.45
CaO	11.02	11.03	11.04	11.31	11.05	11.07
Na_2O	2.12	2.02	2.19	2.32	2.11	2.29
K_2O	0.22	0.25	0.38	0.29	0.32	0.31
Total	95.91	93.92	95.48	96.23	95.18	98.44

*Total iron as FeO

Atomic Proportions, (O)=23

Si	6.471	6.481	6.404	6.360	6.425	6.466
Ti	0.217	0.228	0.226	0.248	0.219	0.231
Al	1.937	1.923	1.995	1.983	1.917	1.895
Fe	1.463	1.439	1.392	1.488	1.548	1.500
Mn	0.019	-	0.020	-	0.018	0.032
Mg	3.142	3.131	3.206	3.138	3.142	3.127
Ca	1.757	1.794	1.767	1.806	1.785	1.754
Na	0.611	0.593	0.635	0.641	0.618	0.643
K	0.041	0.048	0.072	0.056	0.062	0.056
Total	15.658	15.648	15.718	15.720	15.734	15.704
Fe/Mg+Fe	0.318	0.315	0.303	0.322	0.330	0.324

Hornblende andesite (1-5)

Table 6.5 : Electron microprobe analyses of biotite from the lithic blocks in the Taupo Pumice Formation.

VUW	31139	–	–
Sample	4/12	–	–
	(1)	(2)	(3)
SiO_2	41.54	40.50	38.86
TiO_2	1.19	1.36	1.53
Al_2O_3	10.11	10.35	10.00
FeO*	15.32	13.37	14.21
MnO	0.47	0.33	0.40
MgO	15.60	14.62	14.97
CaO	0.10	0.28	0.09
Na_2O	0.77	1.10	0.49
K_2O	7.26	7.54	8.47
Total	92.36	89.45	89.02

*Total iron as FeO

Atomic Proportions, (O)=22

Si	6.303	6.329	6.185
Ti	0.136	0.161	0.183
Al	1.807	1.907	1.876
Fe	1.944	1.745	1.892
Mn	0.061	0.044	0.053
Mg	3.530	3.406	3.553
Ca	0.016	0.048	0.015
Na	0.226	0.334	0.152
K	1.468	1.503	1.719
Total	15.491	15.477	15.628
Fe/Mg+Fe	0.355	0.339	0.347

Biotite bearing rhyolite (1-3)

Table 6.6 : Electron microprobe analyses of plagioclase from the lithic blocks in the Taupo Pumice Formation.

VUW	31139	–	–	–	–	–	31129	–	–	–	31129	31155	–	–	–	31146	–	–	–	–
Sample	4/12	–	–	–	–	–	1/B/3	–	–	–	1/B/3	1/4	–	–	–	1/M/4	–	–	–	–
	(1)	(2)	(3)	(4)	(5)	(6)	(7)	(8)	(9)	(10)	(11)	(12)	(13)	(14)	(15)	(16)	(17)	(18)	(19)	(20)
	(C)	(M)	(R)	(C)	(M)	(R)	(C)	(M1)	(M2)	(R)	(MP)	(C)	(R)	(C)	(R)	(C)	(M)	(R)	(C)	(R)
SiO_2	59.34	58.70	59.83	58.76	59.76	60.51	55.66	55.91	56.28	55.36	60.01	52.79	52.85	45.75	54.82	50.52	51.03	52.50	54.46	52.52
TiO_2	-	-	-	-	-	0.01	-	-	-	-	-	-	-	-	-	-	-	-	-	-
Al_2O_3	26.05	26.12	26.07	26.25	25.59	25.58	26.87	26.86	26.66	28.13	24.70	29.29	29.56	33.98	26.91	30.94	30.36	29.22	28.12	28.06
FeO*	0.33	0.20	0.29	0.26	0.26	0.22	0.38	0.33	0.33	0.37	0.22	0.51	0.32	0.51	0.48	0.47	0.48	0.49	0.47	0.42
MnO	-	-	-	-	-	-	-	-	-	-	-	-	-	-	-	-	-	-	-	-
MgO	-	-	-	-	-	-	-	-	-	-	-	-	-	-	-	0.06	0.04	-	0.06	0.05
CaO	8.16	8.60	7.78	8.43	7.89	7.67	9.86	10.05	9.76	10.82	6.87	12.49	11.76	17.08	10.87	13.86	14.03	12.24	11.40	12.17
Na_2O	7.03	6.34	7.22	6.83	7.09	7.05	5.87	5.66	5.77	5.50	7.17	4.57	4.83	1.74	5.34	3.43	3.64	4.47	4.93	4.54
K_2O	0.29	0.23	0.36	0.21	0.45	0.64	0.19	0.19	0.27	0.17	0.32	0.11	0.13	-	0.09	0.13	0.06	0.10	0.15	0.12
Total	101.20	100.19	101.55	100.74	101.04	101.68	99.02	99.12	99.11	100.47	99.29	99.76	99.45	99.06	98.51	99.41	99.64	99.02	99.59	97.88

*Total iron as FeO

Atomic Proportions, O = 32

Si	10.501	10.477	10.542	10.541	10.584	10.635	10.135	10.160	10.219	9.956	10.754	9.616	9.621	8.511	10.041	9.252	9.338	9.616	9.882	9.731
Ti	-	-	-	-	-	-	-	-	-	-	-	-	-	-	-	-	-	-	-	-
Al	5.434	5.495	5.414	5.502	5.342	5.299	5.766	5.753	5.702	5.963	5.217	6.287	6.342	7.452	5.810	6.679	6.548	6.308	6.013	6.127
Fe	0.049	0.029	0.042	0.038	0.038	0.033	0.058	0.050	0.050	0.055	0.333	0.078	0.049	0.079	0.074	0.072	0.074	0.075	0.072	0.064
Mn	-	-	-	-	-	-	-	-	-	-	-	-	-	-	-	-	-	-	-	-
Mg	-	-	-	-	-	-	0.021	0.008	0.011	0.005	-	-	-	-	-	0.017	0.011	0.011	0.017	0.014
Ca	1.547	1.645	1.468	1.604	1.497	1.439	1.924	1.957	1.898	2.085	1.318	2.437	2.294	3.405	2.133	2.720	2.751	2.402	2.216	2.416
Na	2.413	2.195	2.468	2.355	2.434	2.401	2.073	1.995	2.031	1.919	2.493	1.614	1.703	0.628	1.897	1.218	1.292	1.589	1.734	1.632
K	0.066	0.053	0.081	0.048	0.102	0.144	0.044	0.043	0.059	0.043	0.074	0.026	0.030	-	0.015	0.030	0.014	0.024	0.034	0.025
Total	20.010	19.894	20.015	20.088	19.997	19.951	20.021	19.966	19.970	20.026	20.189	20.058	20.039	20.075	19.970	19.988	20.028	20.025	19.968	20.009
mole %																				
An	38.5	42.2	36.6	40.1	37.1	36.1	47.6	49.0	47.6	51.5	33.9	59.8	57.0	84.4	52.7	68.5	67.9	59.9	55.6	59.3
Ab	59.9	56.4	61.4	58.8	60.4	60.3	51.3	50.0	51.0	47.4	64.2	39.6	42.3	16.6	46.9	30.7	31.8	39.6	43.5	40.1
Or	1.6	1.4	2.0	1.2	2.5	3.6	1.1	1.0	1.4	1.1	1.9	0.6	0.7	-	0.4	0.8	0.3	0.5	0.9	0.6

Biotite Bearing Rhyolite (1-6); Hypersthene Rhylite (7-11)
(C)= Phenocryst core (M)=Phenocryst middle (R)=Phenocryst rim
(PA)=Phenocryst aggregate (MP)=microphenocryst (GM)=Groundmass

Two pyroxene dacite (12-15)
Two pyroxene dacite (16-20)

Table 6.6 : Electron microprobe analyses of plagioclase from the lithic blocks in the Taupo Pumice Formation (continued).

VUW	31156	–	–	–	–	–	31153	–	–	–	31153	–	–	–	–	31157	–	–	–	–
Sample	2/8	–	–	–	–	–	2/9	–	–	–	2/9	–	–	–	–	1/4	–	–	–	–
	(21)	(22)	(23)	(24)	(25)	(26)	(27)	(28)	(29)	(30)	(31)	(32)	(33)	(34)	(35)	(36)	(37)	(38)	(39)	(40)
	(C)	(M)	(R)	(C)	(M)	(R)	(C)	(M1)	(M2)	(M3)	(R)	(C)	(R)	(C)	(R)	(C)	(M1)	(R)	(PA)	(MP)
SiO_2	47.25	51.93	51.81	51.07	48.06	49.32	53.44	54.33	52.67	55.20	53.10	50.13	54.11	48.82	52.25	45.87	47.01	46.75	47.57	47.56
TiO_2	-	-	-	-	-	-	-	-	-	0.14	-	-	-	-	-	-	-	-	-	-
Al_2O_3	32.11	28.89	28.66	30.30	32.94	30.67	28.51	27.89	29.06	27.35	28.14	31.07	29.30	31.62	29.80	32.56	33.54	34.25	33.85	32.84
FeO*	0.54	0.55	0.85	0.78	0.53	0.82	0.43	0.46	0.39	0.39	0.48	0.48	0.38	0.50	0.56	0.62	0.74	0.79	0.84	0.36
MnO	-	-	-	-	-	-	-	-	-	-	-	-	-	-	-	-	-	-	-	-
MgO	0.07	0.11	0.15	0.09	-	0.13	0.04	0.07	0.06	0.07	0.07	-	-	-	-	-	-	-	-	-
CaO	16.99	13.47	13.67	14.34	16.87	15.17	11.55	10.91	12.32	10.27	11.64	14.78	12.16	15.50	13.24	17.30	17.35	17.78	17.01	17.02
Na_2O	1.96	4.02	3.97	2.99	2.23	2.82	4.96	5.18	4.68	5.57	4.97	3.36	4.70	2.88	4.08	1.63	1.75	1.75	1.67	2.07
K_2O	0.09	0.19	0.15	-	-	-	0.15	0.23	0.19	-	0.21	0.11	0.19	0.09	0.16	0.06	0.09	-	-	-
Total	99.01	99.16	99.26	99.57	100.63	98.93	99.08	99.07	99.37	98.99	98.61	99.93	100.84	99.41	100.09	98.04	100.48	101.32	100.94	99.85

*Total iron as FeO

Atomic Proportions, O = 32

Si	8.791	9.544	9.537	9.344	8.782	9.126	9.909	9.772	9.621	10.042	9.772	9.177	9.724	8.998	9.495	8.634	8.623	8.522	8.672	8.757
Ti	-	-	-	-	-	-	-	-	-	0.019	-	-	-	-	-	-	-	-	-	-
Al	7.041	5.981	6.218	6.533	7.095	6.688	5.995	6.144	6.257	5.863	6.103	6.703	6.207	6.869	6.382	7.221	7.250	7.358	7.275	7.126
Fe	0.083	0.005	0.131	0.120	0.081	0.126	0.069	0.066	0.059	0.059	0.073	0.073	0.057	0.078	0.008	0.098	0.114	0.120	0.128	0.055
Mn	-	-	-	-	-	-	-	-	-	-	-	-	-	-	-	-	-	-	-	-
Mg	0.020	0.030	0.040	0.026	0.004	0.036	0.018	0.011	0.015	0.018	0.015	0.010	-	0.019	0.017	-	-	-	-	-
Ca	3.386	2.652	2.696	2.811	3.303	2.009	2.132	2.263	2.411	2.002	2.295	2.899	2.342	3.061	2.578	3.489	3.409	3.472	3.323	3.357
Na	0.706	1.430	1.416	1.059	0.789	1.013	1.831	1.758	1.659	1.965	1.773	1.193	1.638	1.029	1.438	0.594	0.622	0.618	0.587	0.738
K	0.020	0.043	0.035	0.020	-	0.019	0.053	0.035	0.045	0.028	0.050	0.026	0.044	0.020	0.036	0.014	0.020	-	0.011	0.010
Total	20.047	19.685	20.073	19.914	20.054	19.021	20.007	20.049	20.067	19.996	20.081	20.081	20.012	20.074	19.954	20.050	20.038	20.090	19.993	19.379
mole %																				
An	82.4	64.3	65.0	72.3	80.7	74.5	55.8	53.1	58.6	50.1	55.7	70.4	58.2	74.5	63.6	85.2	84.2	84.9	84.7	81.8
Ab	17.2	34.7	34.2	27.2	19.3	25.1	43.3	45.6	40.3	49.2	43.1	29.0	40.7	25.0	35.5	14.5	15.4	15.1	15.0	18.0
Or	0.5	1.0	0.8	0.5	-	0.4	0.8	1.3	1.1	0.7	1.2	0.6	1.09	0.5	0.8	0.3	0.5	-	0.3	0.2

Pyroxene andesite (21-26)
Hornblende andesite (27-30)
Hornblende andesite (31-35);
Olivine andesite (36-40)
(C)=phenocryst core; (M)=phenocryst middle
(MP)=microphenocryst; (PA)=phenocrystagregate

6.6 PLAGIOCLASE

Plagioclase is the dominant phenocryst and groundmass mineral in the andesites, and a dominant phenocryst phase in the dacites and rhyolites. Plagioclase analyses from selected rock samples are presented in Table 6.6. Plagioclase compositions are calculated in terms of percentage Ab-An-Or and are plotted on Fig 6.6. Plagioclase is often complexly zoned, nearly always oscillatory zoned, and in most analysed phenocrysts a general trend of normal zoning is superimposed on their outer rims. Plagioclase rim compositions are similar to groundmass plagioclase compositions. Inclusions of glass, titanomagnetite, pyroxene and tabular apatite are common.

Plagioclase phenocryst compositions in the andesites usually have a composition of An_{65-82} with phenocryst cores commonly having the highest anorthite content. Only one hornblende andesite has plagioclase phenocrysts which are dominantly labradorite (An_{53-70}). Plagioclase phenocrysts in the dacites are generally labradorite (An_{52-69}), while those of the rhyolites are andesine (An_{33-50}).

K_2O contents in all the plagioclases are low (less than 0.2 wt%). Calculated %Or in the andesites and dacites is unifomly < 1%; whereas it is 1-2% in the rhyolites.

FeO content in the plagioclase is moderately high (0.22-0.8 wt%), while Mg and Ti are also present as minor components. In general, FeO increases and K_2O decreases with increasing An content (Fig 6.7). Mg is very low or below the detection limit of the analysis in the sodic plagioclase and does not show any distinct trend with increasing An mol%, however a poorly defined trend shows an increase in the An molecular percent. MgO is more dependent on the bulk compositions of the rock from which the plagioclase has crystallized. Fe in plagioclase exists as both divalent and trivalent ions, with most of the Fe^{3+} substituting for Si in the tetrahedral site, as may also be the case for Ti (Smith, 1977).

The plagioclase phenocrysts analyzed are more calcic than the corresponding normative feldspars of bulk rocks, which suggests that potassium and to a lesser extent sodium are concentrated in finely crystalline to glassy matrices. Plagioclase is often complexly zoned, and nearly always oscilliatory zoned.

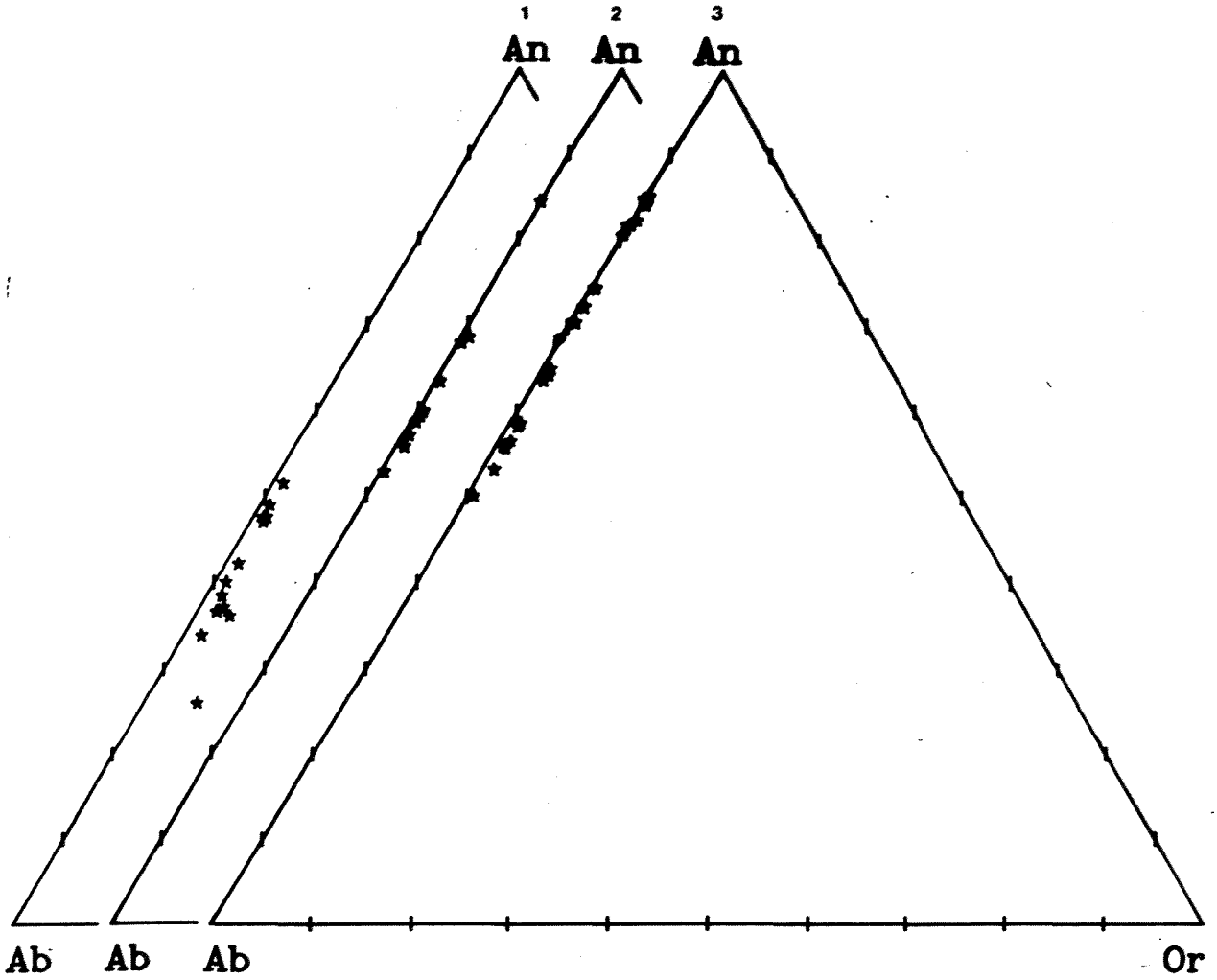

Figure 6.6 : Mole% of Or, Ab, and An in analyzed plagioclase in the rhyolites (1), dacites (2) and andesites (3).

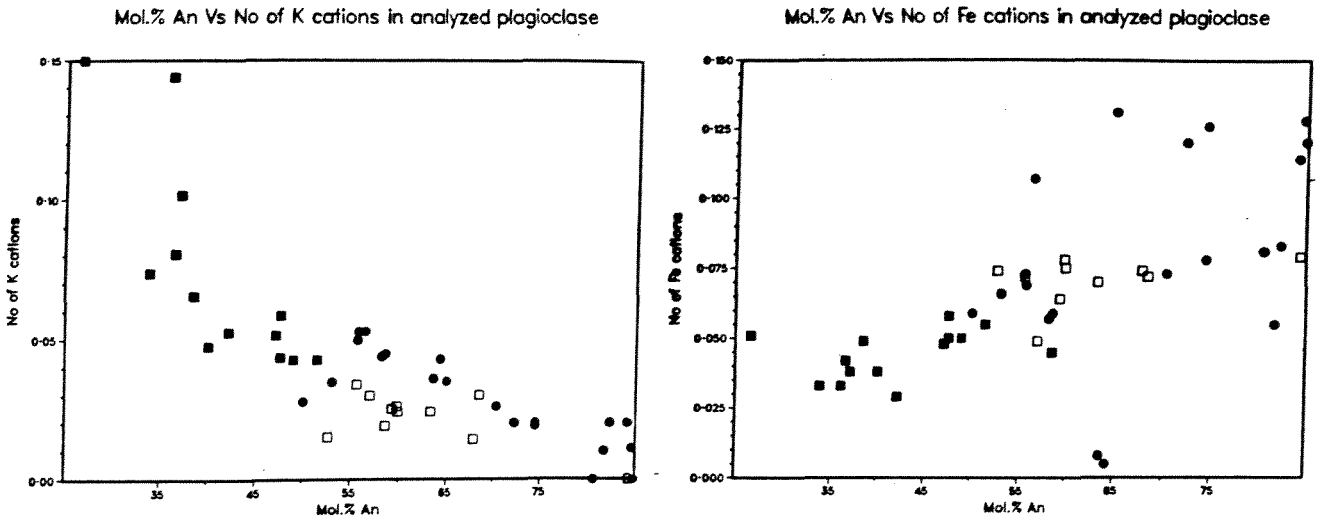

Figure 6.7 : Variation in number of Fe and K cations calculated on the basis of 32(O) in the analysed plagioclase in the andesites, dacites and rhyolites. rhyolites (filled squares); dacites (squares); andesites (circles)

Thus the textural feature of the plagioclase shows that they have crystallized in a closed system, together with pyroxene and oxides from the melt whose residue comprises the groundmass, with a variety of evidences for thermal and compositional disequilibrium in the course of this crystallization (cf. reverse zoning, seive texture etc.). Partial alteration of plagioclase cores, evident in some samples, may be due to sudden pressure change at the time of the eruption creating a disequilibrium between phenocrysts and the surrounding liquid.

Plagioclase is the most important feldspar in volcanic rocks of the calk-alkaline series and in particular in the volcanic rocks of the TVZ. Rare alkali feldspar phenocrysts are found in some of the rhyolite lava and ignimbrite inclusions in the Taupo Pumice Formation.

6.7 QUARTZ

Quartz occurs as a phenocryst mineral in most of the rhyolites, ignimbrites, and some of the dacites and is commonly resorbed and/or embayed. Microscopic tridymite prisms occur as linings to shear cavities in some of the rhyolite, dacite, and andesite lava flows. Tridymite is formed from vapour phase crystallization.

The amount of quartz phenocrysts correlates with the abundance of plagioclase phenocrysts and total phenocryst content in the rhyolites of the TVZ (Ewart, 1968). The three ferromagnesian assemblages were statistically correlated with both total phenocryst content and modal plagioclase to quartz ratio. The hypersthene and hypersthene hornblende rhyolites are low in quartz and the majority are quartz free. The biotite-bearing rhyolites contain the highest phenocryst content and commonly contain quartz phenocrysts. This indicates that the biotite-bearing rhyolites were formed at a comparatively low temprature. Quartz crystals in the dacites could be xenocrysts.

Table 6.7 : Electron microprobe analyses of magnetite from the lithic blocks in the Taupo Pumice Formation.

VUW	31139	31146	–	–	31153	–
Sample	4/12	1/M/4	–	–	2/9	–
	(1)	(2)	(3)	(4)	(5)	(6)
SiO_2	-	0.12	0.14	0.16	2.33	0.09
TiO_2	16.57	10.61	8.99	10.40	3.76	0.67
Al_2O_3	1.96	2.55	2.62	2.65	3.39	3.53
FeO*	69.75	75.13	76.57	76.04	72.88	80.24
MnO	1.09	0.42	0.33	0.35	-	-
MgO	0.51	1.24	1.65	1.66	1.88	1.54
CaO	-	-	-	-	0.78	-
Na_2O	-	-	-	-	-	-
K_2O	-	-	-	-	-	-
Cr_2O_3	-	-	-	-	0.22	-
Total	89.88	90.07	90.30	91.26	85.39	86.07

*Total iron as FeO

Atomic Proportions, (O)=32

Si	-	0.043	0.054	0.059	0.917	0.036
Ti	4.492	2.978	2.537	2.875	1.109	0.205
Al	0.835	1.123	1.159	1.147	1.568	1.729
Fe	21.030	23.454	24.006	23.381	24.011	27.880
Mn	0.330	0.132	1.105	0.112	0.021	0.953
Mg	0.27	0.687	0.992	0.912	1.009	-
Ca	-	-	-	-	0.331	-
Na	-	-	-	-	-	-
K	-	-	-	-	-	-
Cr	-	-	-	-	0.064	-
Total	26.957	28.417	28.853	28.486	29.030	28.803
Fe/(Mg+Fe)	0.987	0.972	0.963	0.962	0.956	0.967

Biotite bearing rhyolite (1) Hypersthene dacite (2-4)
Hornblende andesite (5,6)

Table 6.7 : (continued) Electron microprobe analyses of ilmenite and chrome-spinel from the lithic blocks.

VUW	31129	–	31139	–	31157
Sample	1/B/3/	-	4/12	-	4/1
	(1)	(2)	(3)	(4)	(5)
SiO_2	-	-	-	-	0.10
TiO_2	49.54	49.01	45.20	46.20	0.50
Al_2O_3	-	-	0.93	0.95	7.13
FeO*	46.8	48.36	50.51	49.50	26.67
MnO	0.88	0.77	1.03	1.10	-
MgO	1.27	1.30	1.32	1.55	8.25
CaO	-	-	-	-	-
Na_2O	-	-	-	-	-
K_2O	-	-	-	-	-
Cr_2O_3	-	-	-	-	54.89
Total	98.49	99.44	98.99	99.30	97.54

*Total iron as FeO

Atomic Proportions, (O)=6

Si	-	-	-	-	0.005
Ti	1.917	1.889	1.778	1.799	0.020
Al	-	-	0.057	0.056	0.044
Fe	2.015	2.073	2.209	2.134	1.179
Mn	0.038	0.033	0.046	0.048	0.004
Mg	0.097	0.099	0.103	0.119	0.650
Ca	-	-	-	-	-
Na	-	-	-	-	-
K	-	-	-	-	-
Cr	-	-	-	-	2.294
Total	4.067	4.094	4.193	4.156	4.196
Fe/(Mg+Fe)	0.954	0.954	0.955	0.947	0.644

Hypersthene rhyolite (1,2) Biotite bearing rhyolite (3,4)
Olivine andesite-Chrome spinel(5)

6.8 ACCESSORY MINERALS

The most common accessory minerals in the lithic inclusions of the Taupo Pumice Formation are opaque Fe-Ti oxides. Oxide minerals are ubiquitous microphenocrysts in the groundmass and inclusions in silicate phenocrysts in the andesites, dacites and rhyolites. The three oxides which occur as primary minerals in these rocks are titanomagnetite and rare ilmenite and chrome spinel.

6.8.1 Titanomagnetite

Iron oxides are found as accessory minerals in the rhyolites, dacites and andesites and appear as discrete grains up to 0.7 mm in length, as inclusions in pyroxene and plagioclase phenocrysts and as alteration rims around hornblende and rarely pyroxene phenocrysts. Iron oxides are commonly concentrated in glomeroporphyritic aggregates of hypersthene, augite and occasionally plagioclase and may form symplectic intergrowths with pyroxene.

Iron oxide analyses from the rhyolites, dacites and andesites in selected samples are presented in Table 6.7 . The analyses show that most of the iron-oxides are titaniferous magnetites (titanomagnetites). The titanomagnetites contain between 5 and 20 wt% TiO_2 with minor substitutions of Si, Al, Mn, Mg, and Cr. In most analyzed samples, ilmenite was not found together with titanomagnetite. The stoichiometry of magnetite allows up to 33 wt% TiO_2 in the structure. This together with the rarity of coexisting ilmenite in most of the samples reflects the Ti-poor bulk compositions of the host rocks.

6.8.2 Ilmenite

Ilmenite occurs as a minor accessory in many volcanic rocks. Ilmenite commonly occurs as microphenocrysts in the more acidic members of the rock series. Analyses of ilmenite from the rhyolites are presented in Table 6.7. The analysed ilmenite phenocrysts contain between 41-49 Wt% TiO_2. Ilmenite rarely coexists with titanomagnetite due to Ti poor melt compositions, hence the magnetite- ilmenite geothermometer could not be used on the rhyolite blocks.

6.8.3 *Chrome Spinel*

Chrome spinel occurs as microscopic subhedral inclusions in forsteritic olivines of olivine bearing andesites. One analysis of chrome spinel in an olivine is presented in Table 6.7. Hackett (1985) has described chrome spinel inclusions from the olivine andesites of the Tongariro Volcanic Centre which are TiO_2 -FeO-Fe_2O_3 poor and rich in Cr_2O_3 -MgO-Al_2O_3 and have compositions similar to refractory chrome spinels from boninites, peridotite nodules, alpine peridotites and layered basic intrusions.

6.8.4 *Apatite*

Apatite is a common accessory mineral in the rhyolites, dacites and andesites; and commonly forms elongated rectangular crystals. Apatite occurs both in the groundmass and as inclusions in plagioclase phenocrysts.

Chapter VII

WHOLE ROCK CHEMISTRY OF LITHIC BLOCKS

7.1 INTRODUCTION

Major and trace element analyses of 15 rhyolites, 5 dacites and 4 andesite samples from the ground layer of the Taupo Ignimbrite are presented in Table 7.1 together with the CIPW norms. The petrographic name of all the analysed rocks is given in Appendix 2. Major and trace element analyses were made using a Siemens SRS-1 automatic X-ray spectrometer, analytical procedures are discribed in Appendix 3.

7.2 NORMATIVE MINERALOGY

CIPW Norms were calculated using a computer program in the Research School of Earth Sciences (Victoria University of Wellington) and incorporated all major element data (Appendix 3). A ratio of 0.2 was taken for FeO : Fe_2 O_3 of the total Fe for the norm calculations. All norms were recalculated to 100% anhydrous (Table 7.1). All samples are oversaturated with respect to silica but considerable variation is apparent within the analysed rocks in the proportion of the individual normative minerals.

7.3 CLASSIFICATION

All analysed rocks are calc-alkaline and fall within the series basalt-andesite-dacite-rhyolite. Division within this series is usually based on silica content (normalized volatile free basis) using the division of Taylor (1969) and Gill (1981).

<53% SiO_2 - basalts

53-57% SiO_2 - basic andesites

57-63% SiO_2 - acid andesite

63-67% SiO_2 - dacite

>67% SiO_2 - rhyolite

Table 7.1 Representative chemical analyses of lithics from the Taupo Pumice Formation.

VUW	31127	31128	31133	31131	31132	31129	31140	31138	31170	31171	31141	31142
Sample	1T1	1T2	1/6	1M7	1/5	1B3	1M3	4/10R	2/11	1BB0	1BB2	1BB4
	(1)	(2)	(3)	(4)	(5)	(6)	(7)	(8)	(9)	(10)	(11)	(12)
Major Elements												
SiO_2	74.68	73.98	73.96	74.10	74.90	74.14	73.99	74.33	73.77	74.53	73.21	74.27
TiO_2	0.25	0.28	0.28	0.27	0.22	0.25	0.26	0.24	0.28	0.23	0.28	0.28
Al_2O_3	13.15	13.46	13.46	13.50	13.10	13.62	13.35	13.23	13.30	13.10	13.76	13.48
Fe_2O_3	0.34	1.96	0.79	0.65	0.21	0.81	0.44	0.45	2.14	0.95	1.39	1.60
FeO	1.72	0.34	1.45	1.56	1.74	1.27	1.72	1.52	0.24	1.17	0.96	0.79
MnO	0.09	0.10	0.10	0.10	0.07	0.06	0.07	0.09	0.10	0.09	0.06	0.09
MgO	0.33	0.38	0.37	0.40	0.27	0.39	0.39	0.27	0.35	0.29	0.48	0.41
CaO	1.61	1.71	1.73	1.71	1.37	1.96	1.95	1.57	1.61	1.43	2.17	1.66
Na_2O	4.48	4.59	4.47	4.61	4.19	4.17	4.27	4.45	4.47	4.06	4.21	4.42
K_2O	2.88	2.74	2.80	2.75	2.90	2.84	2.91	2.86	2.71	3.21	2.77	2.70
P_2O_5	0.02	0.04	0.05	0.05	0.04	0.04	0.03	0.03	0.04	0.03	0.06	0.04
Loss	0.33	0.44	0.28	0.37	0.49	0.59	0.69	0.40	0.88	0.54	0.38	0.29
Total	100.04	100.02	99.74	100.07	99.51	100.14	100.07	99.44	99.89	99.60	99.73	100.03
CIPW norms												
Q	32.80	31.67	32.04	31.51	35.41	33.36	32.49	33.00	32.77	34.34	31.89	32.99
C	–	–	0.05	–	0.68	0.22	–	0.03	0.22	0.42	0.03	0.37
Or	17.10	16.29	16.64	16.31	17.31	16.87	17.31	17.07	16.21	19.16	16.49	16.02
Ab	38.09	39.07	38.05	39.14	35.81	35.46	36.36	38.03	38.11	34.69	35.89	37.55
An	7.30	8.08	8.30	8.05	6.60	9.51	8.72	7.67	7.82	6.96	10.45	8.00
Di	0.51	0.16	–	0.12	–	–	0.70	–	–	–	–	–
Hy	3.19	3.59	3.73	3.72	3.20	3.52	3.33	3.20	3.71	3.41	4.01	3.90
Ol	–	–	–	–	–	–	–	–	–	–	–	–
Mt	0.50	0.52	0.53	0.53	0.48	0.49	0.52	0.48	0.54	0.44	0.54	0.53
Il	0.48	0.53	0.53	0.51	0.42	0.48	0.50	0.46	0.54	0.44	0.54	0.53
Ap	0.05	0.09	0.12	0.12	0.09	0.09	0.07	0.07	0.09	0.07	0.14	0.09
$\frac{An}{An+Ab}$	16.08	17.14	17.92	17.06	15.56	21.15	19.34	16.78	17.02	16.72	22.55	17.57
TTDI	87.99	87.02	86.74	86.95	88.53	85.69	86.16	88.09	87.08	88.19	84.24	86.55
Mg no.	25.61	27.51	26.48	28.20	22.77	29.10	27.94	22.77	25.34	23.15	31.32	27.87
Trace Elements (ppm)												
Ba	588	567	565	571	578	578	564	578	564	581	560	560
Cr	2	8	4	3	2	8	6	2	5	3	5	4
Cu	–	–	–	–	–	–	–	–	–	–	–	–
Ga	15	15	16	15	16	16	15	16	17	16	15	18
Nb	8	8	7	7	7	6	7	7	7	6	6	8
Ni	–	2	–	2	–	–	18	2	3	–	3	2
Pb	16	16	16	17	18	17	16	15	19	20	16	16
Rb	103	97	110	97	102	105	106	105	102	129	101	97
Sc	10	9	10	11	9	8	9	10	10	9	9	10
Sr	139	160	163	160	125	141	140	141	159	131	150	161
Th	11	12	10	na	na	na	na	na	na	na	na	na
U	–	3	–	na	na	na	na	na	na	na	na	na
V	4	5	4	4	3	11	12	6	4	3	16	7
Y	29	32	33	36	34	34	32	31	36	36	33	35
Zn	54	63	65	86	54	47	42	49	72	69	51	66
Zr	221	221	217	215	209	218	219	219	214	220	219	212

Loss= loss on ignition corrected for FeO oxidation.
TTDI= Thornton Tuttle differntiation index (text)
< 2 ppm (–) not analyzed (na)
Hypersthene Rhyolite (1-6,11,12); Hornblende Rhyolite (7);
Biotite bearing Rhyolite (8); Rhyolite (obsidian) (9-10)

Table 7.1 Representative chemical analyses of lithics from the Taupo Pumice Formation (continued).

VUW	31143	31172	31173	31146	31147	31174	31155	31153	31157	31154	31156	31158
Sample	1BB5	2/12	GPB1	1M4	1B4	4/10D	4a/1	2/9	1/4	1/2	2/8	1/12
	(13)	(14)	(15)	(16)	(17)	(18)	(19)	(20)	(21)	(22)	(23)	(24)
Major Elements												
SiO_2	74.38	71.78	73.18	63.52	63.09	65.33	63.26	61.41	59.80	58.30	58.00	59.13
TiO_2	0.28	0.28	0.31	0.76	0.76	0.76	0.71	0.51	0.55	0.55	0.54	0.51
Al_2O_3	13.52	13.03	13.48	15.95	15.76	15.41	15.71	17.08	14.90	14.82	14.28	14.57
Fe_2O_3	1.00	0.85	0.79	3.28	2.68	3.72	2.85	3.66	3.59	4.62	1.38	2.73
FeO	1.34	1.32	1.62	2.47	3.09	1.80	2.48	1.87	3.03	2.77	5.71	3.81
MnO	0.10	0.09	0.10	0.13	0.14	0.11	0.13	0.11	0.14	0.12	0.15	0.13
MgO	0.46	0.43	0.46	2.05	2.11	1.62	1.98	3.33	5.03	6.04	6.76	5.13
CaO	1.65	1.60	1.78	5.32	5.30	4.52	4.95	5.89	7.85	8.68	8.87	7.68
Na_2O	4.38	4.10	4.33	3.93	3.92	3.80	3.15	3.34	2.75	2.39	2.37	2.63
K_2O	2.70	2.65	2.66	1.61	1.66	1.98	2.14	1.05	1.14	0.94	0.92	1.12
P_2O_5	0.05	0.05	0.07	0.17	0.17	0.20	0.16	0.13	0.09	0.09	0.09	0.09
Loss	0.31	3.32	1.01	1.08	1.19	0.74	2.11	1.77	1.19	0.83	1.20	2.52
Total	100.14	99.60	99.79	100.27	99.87	99.99	99.63	99.96	100.06	100.15	100.27	100.05
CIPW norms												
Q	33.23	33.96	32.56	18.58	18.10	21.92	21.62	18.05	14.73	12.78	11.61	15.11
C	0.51	0.65	0.41	–	–	–	–	0.05	–	–	–	–
Or	15.99	16.29	15.92	9.62	9.96	11.82	12.99	6.33	6.83	5.61	5.49	6.80
Ab	37.14	36.09	37.11	21.35	33.68	32.49	27.39	28.81	23.60	20.43	20.25	22.86
An	7.88	7.92	8.48	21.35	20.82	19.34	23.02	28.92	25.30	27.21	25.85	25.31
Di	–	–	–	3.51	3.96	1.67	0.95	–	11.10	12.78	14.59	10.78
Hy	4.05	3.88	4.17	10.14	10.25	9.54	10.98	15.25	15.62	18.19	19.23	16.35
Ol	–	–	–	–	–	–	–	–	–	–	–	–
Mt	0.55	0.53	0.58	1.35	1.37	1.28	1.27	1.29	1.56	1.72	1.73	1.58
Il	0.53	0.55	0.60	1.46	1.47	1.46	1.39	0.99	1.06	1.06	1.04	0.99
Ap	0.12	0.12	0.16	0.40	0.40	0.47	0.38	0.31	0.21	0.21	0.21	0.21
An / An+Ab	17.49	17.99	18.60	38.85	38.20	37.32	45.67	50.10	51.74	57.11	56.08	52.55
TTDI	86.36	86.34	85.59	61.81	61.73	66.24	62.02	53.19	45.16	38.85	37.35	44.76
Mg no.	30.15	30.22	29.33	44.31	44.66	39.82	45.20	57.59	62.81	64.70	67.14	63.27
Trace Elements (ppm)												
Ba	558	545	561	385	408	449	404	442	317	281	240	306
Cr	4	4	3	11	10	11	12	40	184	221	304	179
Cu	–	–	–	5.2	2.4	5.3	3.8	22.8	28.6	28.5	65.9	18.7
Ga	16	16	17	17	18	18	17	17	16	15	14	16
Nb	6	6.3	6.7	5.5	5.4	5.8	5.4	3.0	2.5	2.8	2.6	2.6
Ni	–	–	2.1	–	–	7.5	2.6	19	22	32	41.6	25.4
Pb	21	19	18	8	10	11	10	58	5	6	6	7
Rb	96	99	99	58	61	73	57	35	42	33	33	38
Sc	10	10	10	19	20	16	17	16	25	27	30	24
Sr	163	159	168	262	264	252	258	289	398	270	270	401
Th	na	na	na	7	7	9	na	na	4	5	5	na
U	na	na	na	–	–	–	na	na	–	–	–	na
V	5	6	7	137	137	101	113	113	171	185	199	165
Y	37	36	35	27	27	27	24	17	19	18	18	19
Zn	104	72	72	71	69	68	71	59	67	70	79	68
Zr	218	207	210	201	199	184	199	83	92	84	84	90

Loss= Loss on ignition corrected for FeO oxidation.
TTDI= Thornton Tuttle differntiation index (text).
< 2 ppm (–) not analyzed (na)
Hypersthene Rhyolite (13); Pumice blocks (14,15)
Dacites (16-19); Andesites (20-24).

Table 7.1 Representative chemical analyses of lithics and some members of the Taupo Pumice Formation (continued)

VUW	31175	31176	50222	50223	50224	50225	50226
Sample	1/11	1/10	–	–	–	–	–
	(25)	(26)	(27)	(28)	(29)	(30)	(31)
				Major Elements			
SiO_2	70.90	66.04	74.31	74.47	74.06	74.51	74.58
TiO_2	0.25	0.18	0.29	0.29	0.31	0.28	0.28
Al_2O_3	13.41	12.17	13.55	13.53	13.56	13.60	13.47
Fe_2O_3	2.54	1.72	2.53	2.55	2.71	2.51	2.44
MnO	0.05	0.04	0.09	0.09	0.08	0.08	0.10
MgO	0.68	0.56	0.43	0.44	0.42	0.39	0.36
CaO	1.65	1.87	1.74	1.70	1.82	1.67	1.66
Na_2O	3.03	2.74	4.18	4.01	4.13	4.10	4.23
K_2O	2.72	2.40	2.84	2.87	2.82	2.85	2.84
P_2O_5	0.04	0.02	0.05	0.05	0.08	0.02	0.04
Loss	4.06	12.44	2.98	2.93	1.07	3.89	2.70
Total	99.33	100.18	100.12	99.62	99.94	99.35	99.67
				Trace Elements (ppm)			
Ba	571	556	570	568	577	572	581
Cr	14	8	36	24	10	–	50
Cu	12.3	2.5	7	22	6	15	15
Ga	14	12	na	na	na	na	na
Nb	4.2	4.2	na	na	na	na	na
Ni	7.1	2.4	4	4	3	6	8
Pb	18	12	14	16	16	15	17
Rb	104	109	90	92	96	93	96
Sc	8	6	na	na	na	na	na
Sr	123	138	152	166	178	160	157
Th	na	na	9.9	9.7	8.9	8.3	10.6
U	na	na	2.5	2.7	3.0	2.1	1.3
V	42	15	3	4	4	2	2
Y	28	24	30	32	28	31	33
Zn	56.7	41.0	73	75	64	69	75
Zr	135	125	217	225	226	226	222

Loss= Loss on ignition corrected for FeO oxidation.
Hydrothermally altered rhyolite (25)
Hydrothermally altered dacite (26)
Taupo Ignimbrite (27)
Taupo Lapilli (28)
Rotongaio Ash (29)
Hatepe Ash (30)
Hatepe Lapilli (31)

Analayses 27-31, (VUW 50222-50226) are tephra whole rock analyses from Froggatt (1982)

7.4 MAJOR ELEMENTS

The weight percentage of some of the major element oxides of the analysed rocks are plotted against SiO_2 wt% in Fig 7.1. The analyses shows that a smooth variation exists for most analysed element oxides. Steiner (1958) and Clark (1960) considered that such a smooth variation probably indicates the strong genetic relationships between the analysed rocks. Two major breaks in the continuity of the SiO_2 wt% can be observed from the variation diagram at the dacite-andesite boundary and between the rhyolite and the dacites. Cole (1979) has used similar characteristics to distinguish between the volcanic rock series from different regions in the TVZ, and has shown that chemically, there is a complete gradation from andesite to dacite in the Bay of Plenty region, the boundary being arbitrarily taken at 63 wt% SiO_2 . In the Rotorua-Taupo region there is a complete gradation from dacite to rhyolite with the boundary equally arbitrarily taken at 67 wt% SiO_2 .

Lavas of TVZ are chemically distinctive in having $Na_2 O > K_2 O$. Fig. 7.1 shows that $K_2 O$ and $Na_2 O$ increase with increasing SiO_2 . content, while CaO, MgO, $Fe_2 O_3$ t, TiO_2 , and MnO decrease with increasing SiO_2 . $P_2 O_5$ shows no significant variation throughout the series. $Al_2 O_3$ is relatively enriched in the andesites and is most abundant in the dacites.

A silica potash diagram (after Gill, 1961) shows that the analysed andesite blocks from the ground layer are medium-K orogenic andesites. The dacite contain significantly less $K_2 O$ than dacite lavas from the Tongariro Volcanic Centre (Fig 7.2).

7.5 TRACE ELEMENTS

Trace element analyses for all the analysed rocks are presented in Table 7.1. All the trace element contents analysed fall within a reasonable range of concentrations of average andesite, dacite, and rhyolite from the TVZ (Cole, 1979) and show a compositional continuity from andesite to rhyolite, similar to that of Ewart (1968). Most of the incompatible trace elements like Pb, Rb, Ba, Zr, Nb and Y show a postive correlation with SiO_2 wt% (Fig 7.3).

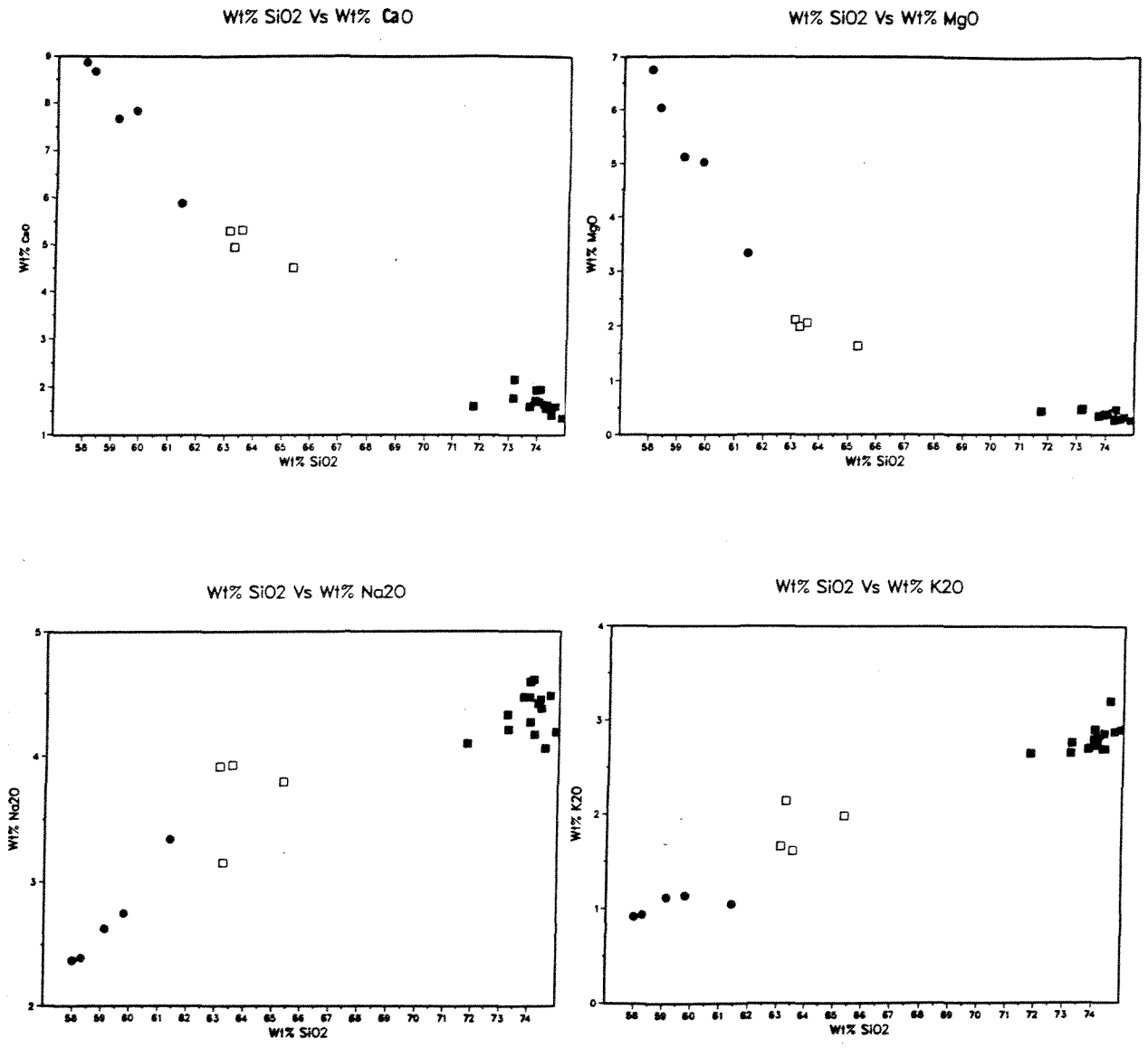

Figure 7.1 : Variation in Wt% MgO, CaO, Na2O, and K2O with SiO2 Wt% in the analysed lithic blocks in the ground layer.
rhyolites (filled squares); dacites (squares); andesites (circles)

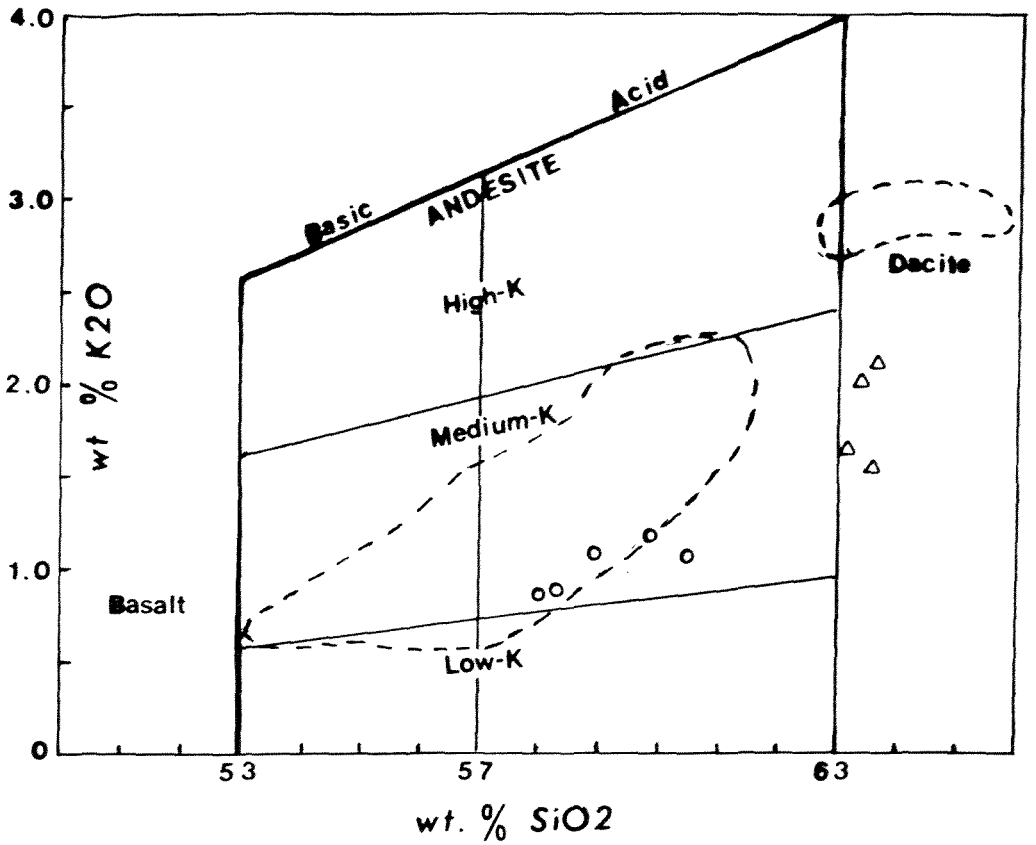

igure 7.2 : Silica potash diagram (after Gill, 1961) for the analysed andesite and dacite blocks in the ground layer. Field for orogenic andesites is the bold trapezoid at the centre of the figure. The area bounded by broken lines shows where 144 analyses from the Tongariro Volcanic Centre plot (Hackett, 1985). dacites (triangles); andesites (circles)

Rb is readily taken up in potassium-bearing minerals because it has a similar charge and radius. But K-bearing minerals are very rare in most of the analysed rocks (as can be observed by the low K_2O wt% of bulk rock analysis) so Rb behaves incompatibly (Fig 7.4).

Zr seldom substitutes for any element in most rock forming minerals hence zirconium behaves as an incompatible element and shows a postive linear correlation with rubidium. Zr commonly occurs in the mineral zircon ($ZrSiO_4$) which is an accessory mineral in many igneous rocks. Y and Nb also behave incompatibly in many igneous rock series.

Ba correlates postively with Rb, and SiO_2 High barium values are characteristic of the calc-alkaline series. Hackett (1985) has shown that even basalts from the Tongariro Volcanic Centre have 100-200 ppm Ba which is 2-10 times the abundunce reported for oceanic tholeiites.

U and Th behave incompatibly because the large and highly charged U^{4+} and Th^{4+} are not readily accommodated in the common rock forming minerals. Like the REE elements they tend to concentrate in accessory minerals such as apatite, ziricon, and sphene.

Sr, Sc, Cr, Ni, V, and Zn behave compatibly. Sr and Sc are readily taken in the plagioclase structure and since the plagioclase phenocrysts are more abundant in the andesites these elements are relatively enriched in the more basic end members. Cr, Ni, V and Zn are usually taken in the ferromagnesian minerals. Cr and Ni are especially accomodated in the Mg rich cores of olivines and pyroxenes and hence are enriched in the andesite.

Because the radius of cations Ga^{3+} and Al^{3+} is quite similar, Ga can be taken readily in the Al structure. The ratio of the two elements remains relatively uniform in the andesites, dacites and rhyolites.

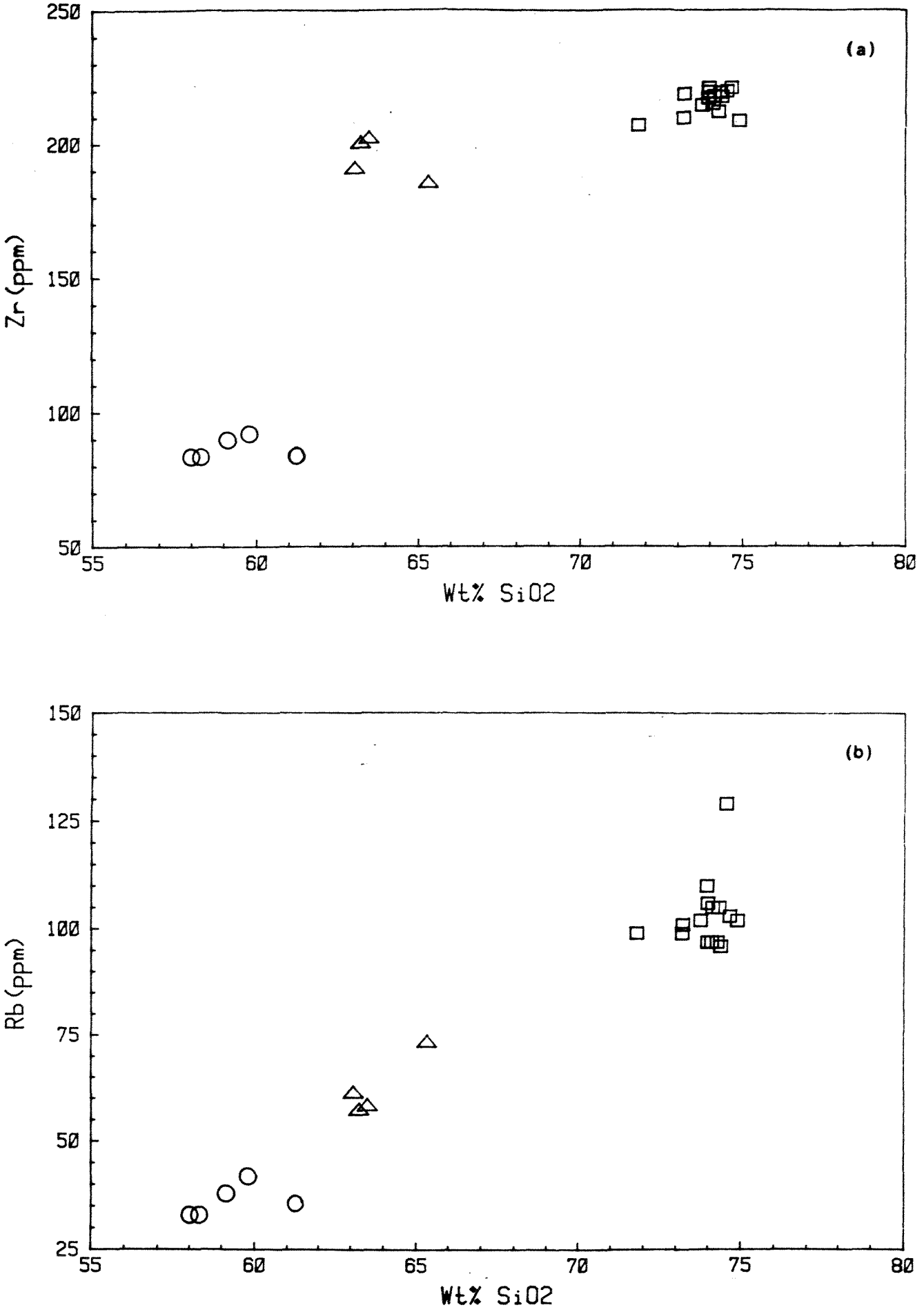

Figure 7.3 : Variation in some incompatible trace elements with wt% SiO2 (a) Zr, (b) Rb in the analysed blocks of volcanic rocks in the ground layer of the Taupo Ignimbrite.
rhyolite (squares); dacite (triangles); andesite (circles)

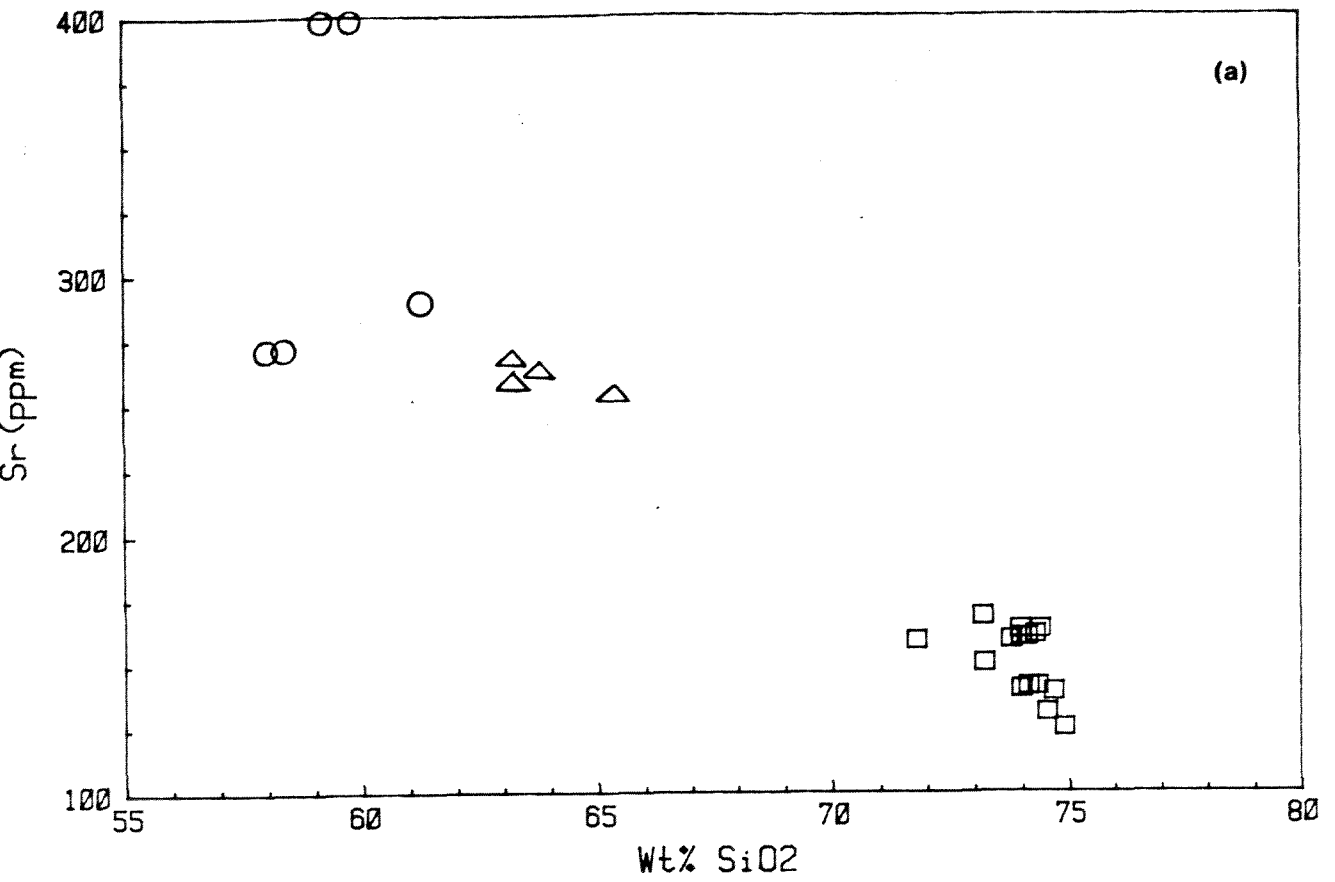

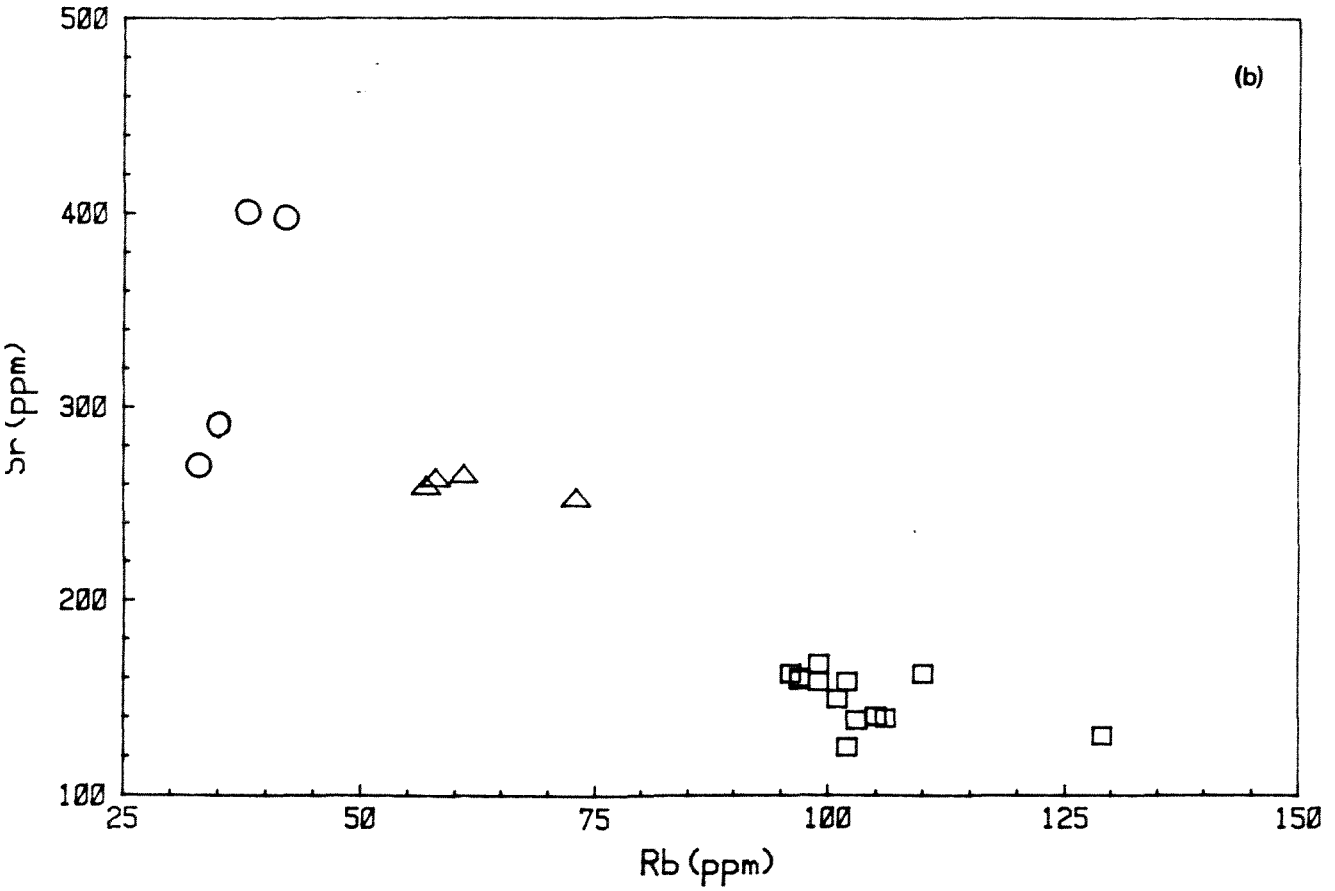

gure 7.4 : Sr behaves compatibly and shows a negative correlation with increasing wt% SiO2(a) and Rb(ppm)(b).
rhyolite (squares); dacite (triangles); andesite (circles)

Chapter VIII

CORRELATION

8.1 RHYOLITES

The rhyolite lavas in the vicinity of the Taupo Volcanic Centre were originally divided into younger and older dome building phases by Grindley (1960), mainly on their degree of erosion. Detailed work by Ewart (1968) later resulted in further subdivisions on the basis of mineralogy, field association and relative percentages of the ferromagnesian phenocryst assemblages. At Wairakei, rhyolites encountered by drilling (Haparangi Rhyolites) were classified on the basis of presence or absence of quartz phenocrysts (Steiner, 1977). Fig 8.1 shows the areal distribution of the different types of rhyolite lavas in the vicinity of Lake Taupo and it is evident that hypersthene rhyolite is the dominant type. Rhyolite lavas make up about 75% of the lithic inclusions in the Taupo Pumice Formation and petrographic study has shown that there are three types of rhyolite inclusions (chapter 4). The rhyolite inclusions in order of decreasing abundunce are hypersthene, hypersthene-hornblende and biotite-bearing rhyolites.

Froggatt (1982) has characterized the different members of the Lake Taupo Group tephras on the basis of the proportion of mafic minerals present in the tephra and has shown that the Taupo Subgroup tephras (tephra formations erupted from vents on the eastern side of Lake Taupo; (Vucetich and Pullar, 1973; Froggatt 1982; in the last 10 ka) contain dominantly hypersthene as a mafic mineral. The dominance of hypersthene rhyolites as inclusions in the Taupo Pumice Formation shows that some of the rhyolite blocks are probably genetically related to the Taupo Subgroup.

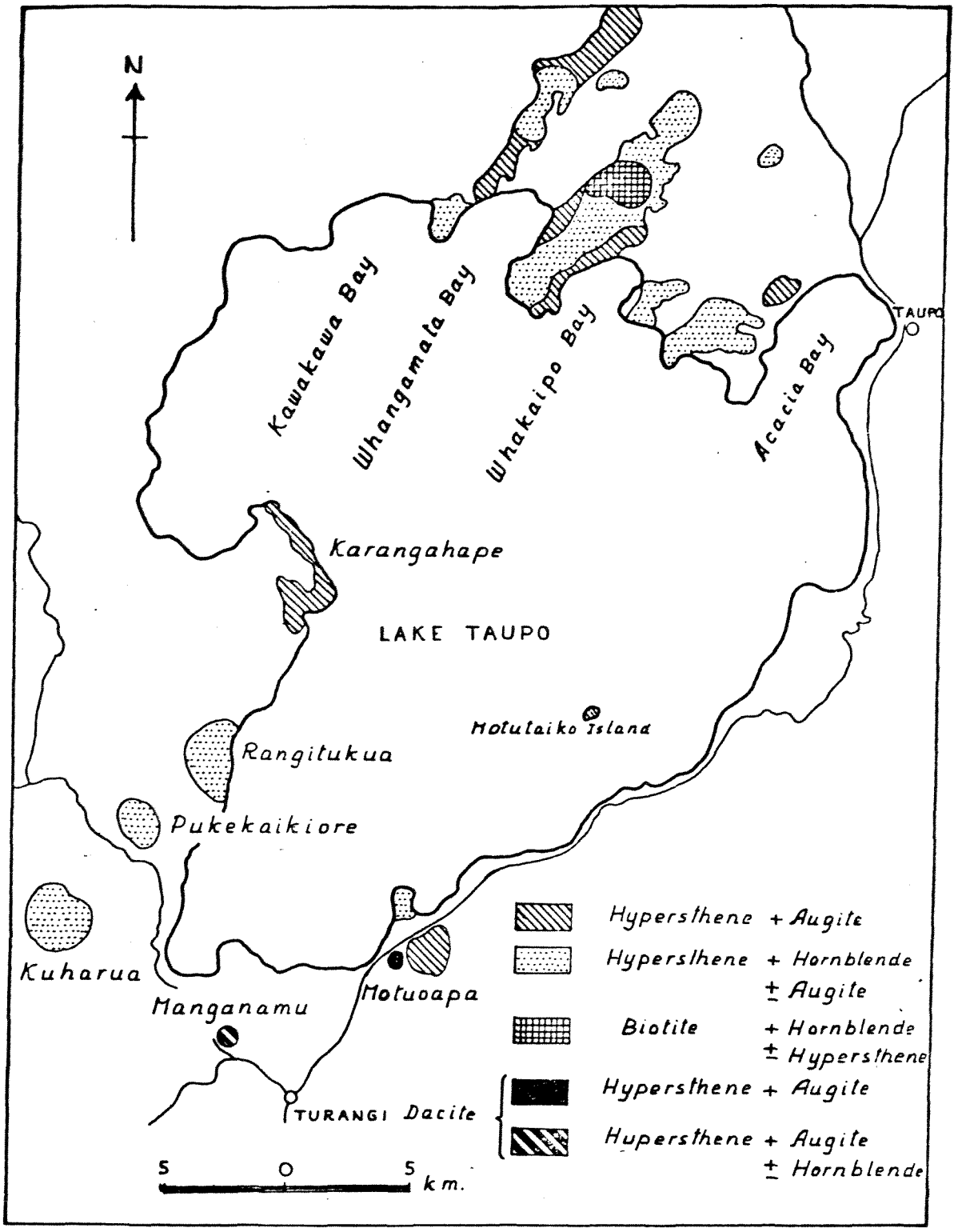

Figure 8.1 : Rhyolite domes and flows of the Taupo Volcanic Centre showing aerial variation of ferromagnesian phenocryst assemblages. (From Daorerk, 1972)

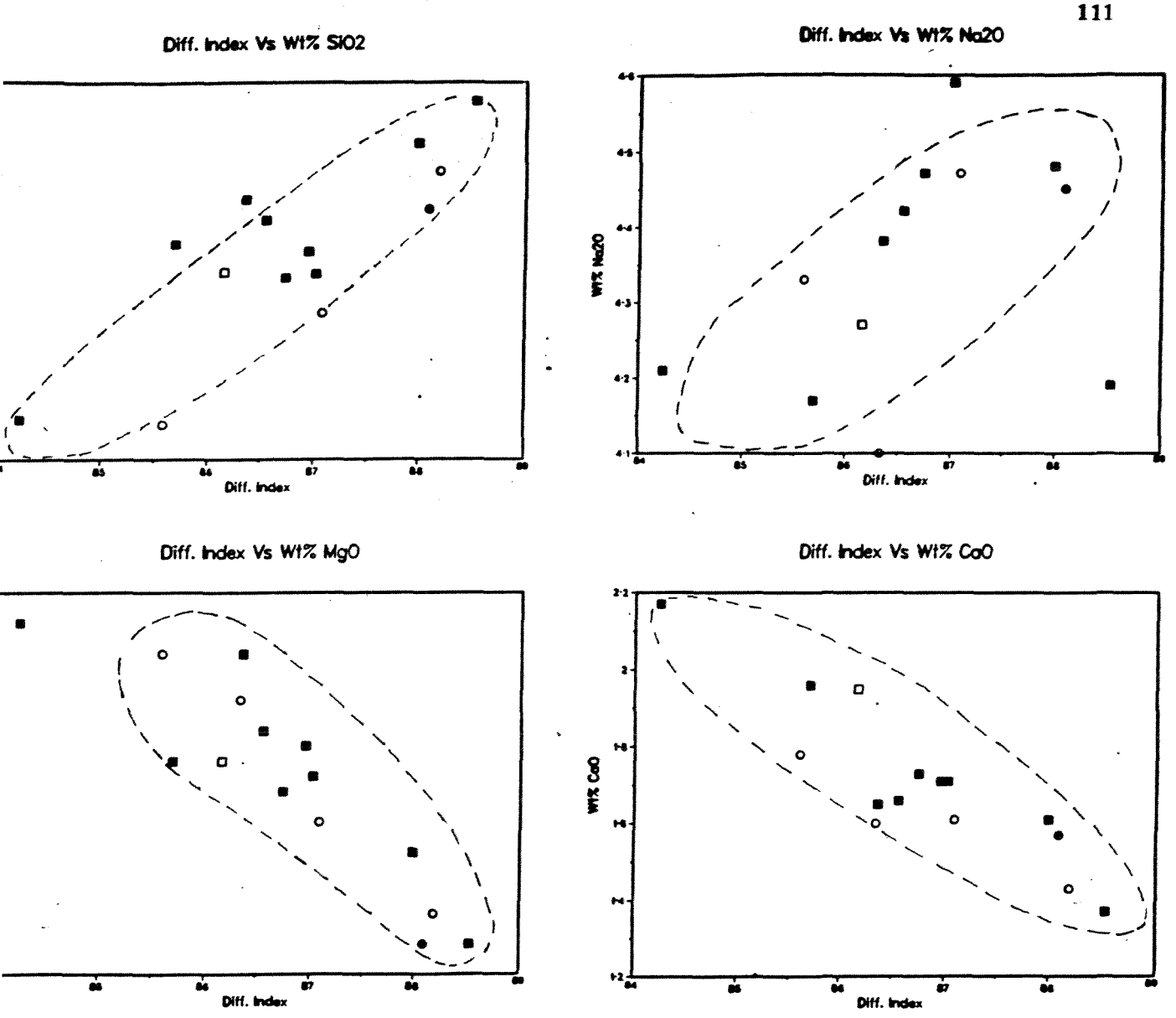

igure 8.2 : Plot of wt% SiO2, Na2O, CaO, and MgO Vs differentiation index for the analysed rhyolite blocks in the ground layer; most of the elements show a linear trend of variation similar to whole rock analyses of Taupo Sub-group tephra (Froggatt, 1982) shown as areas in the broken lines.

Obsidian and Pumice blocks (open circles); Biotite-bearing rhyolite (open squares)

Hornblende-hypersthene Rhyolite (closed circle); Hypersthene rhyolite (filled squares).

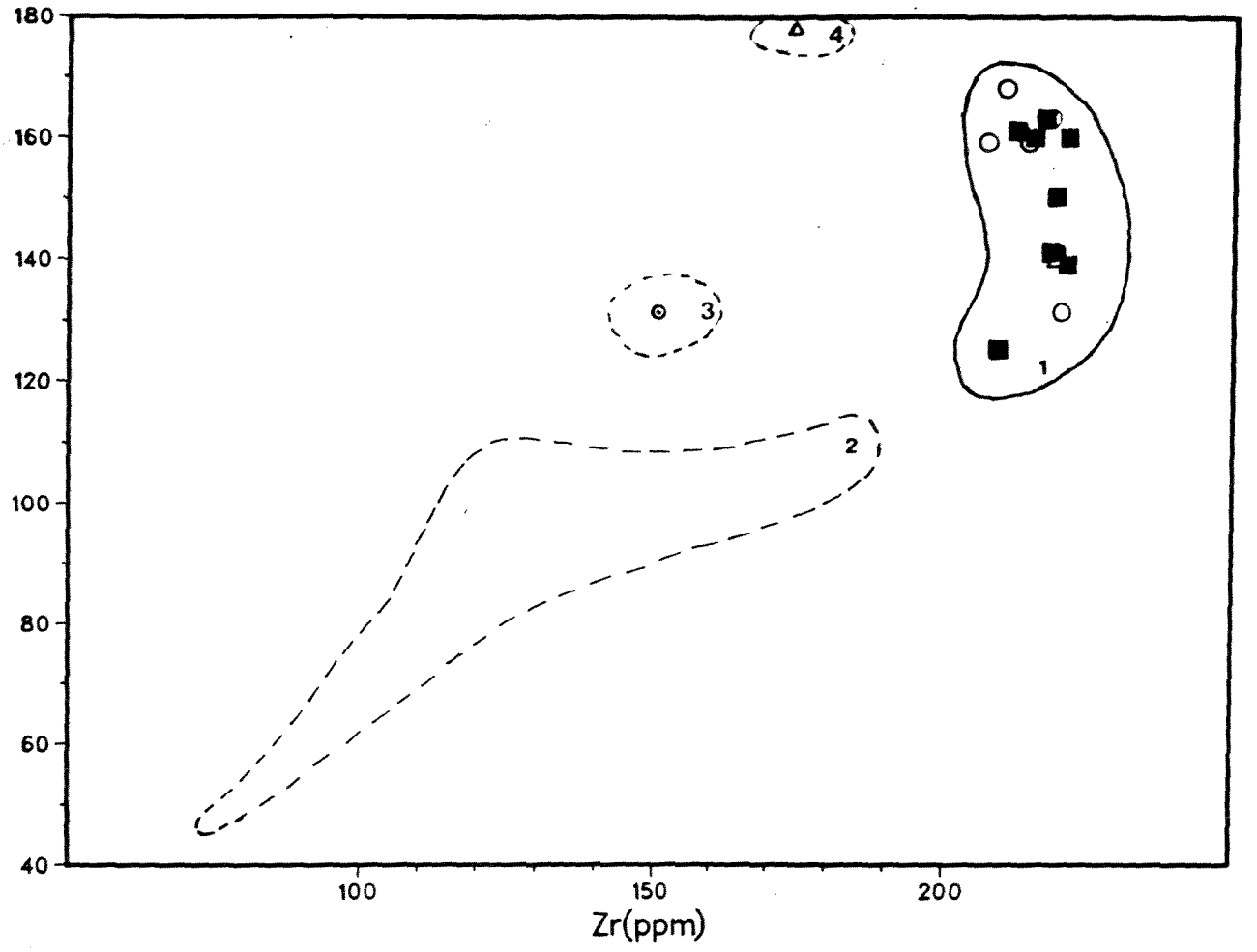

Figure 8.3 : Sr Vs Zr plot of the analysed rhyolite blocks in the ground layer, Tephra from the Taupo and Okataina Volcanic Centre are ploted for comparision.
Hypersthene rhyolite (filled squares)
Biotite-bearing rhyolite (sqares)
Hornblende hypersthene rhyolite (filled circles)
Obsidian and pumice blocks (circles)
Area 1 -Kawakawa Tephra Formation (Froggatt, 1982)
Area 2 -Tephra from the Taupo Sub-Group (Froggatt, 1982)
Area 3 -Mt Curl Tephra (Froggatt, 1982)
Area 4 -Tephra from Okataina Volcanic Centre (Lloyd, 1972)

The major element data of the analysed rhyolite blocks from the ground layer of the Taupo Ignimbrite were compared to whole rock analyses of the tephra erupted from the Taupo Volcanic Centre (Table 7.1). Froggatt (1982) showed that the Taupo Sub-group tephras form a general linear trend of major element components with increasing Thornton-Tuttle Differentiation Index (normative quartz + orthoclase + albite) and can be subdivided into three groups on the basis of age and differences in D.I. values; Taupo Ignimbrite to Mapara, Whakaipo to Motutere, and Opepe to Karapiti. A plot of selected element oxides against differentiation index for the analysed rhyolite blocks from the ground layer of the Taupo Pumice Formation (Fig 8.2) showed a similar linear trend and most of the blocks plot in the area of the tephra erupted from the Taupo Volcanic Centre in the last 10 Ka.

The trace element analyses of the rhyolite blocks from the ground layer of the Taupo Ignimbrite are compared with whole rock trace element analyses of members of the Taupo sub-group tephras. Froggatt (1982) has shown that the trace elements exhibit little variation between these tephras except for Rb, Sr, and Zr, and that Sr and Zr are useful aids in 'finger printing' tephra units. A plot of Sr and Zr distinguishes the same three groups of tephras as indicated by the major elements (Fig 8.3). Included for comparision are analyses of Rotorua sub-group Tephras from the Okataina Volcanic Centre, each of which plot in distinctive areas. The Kawakawa Tephra Formation shows different trace element characteristics from the Taupo Subgroup tephras. All of the analysed rhyolite blocks from the ground layer lie in the zone of the Taupo Sub-group tephras. And interestingly most of the analysed hypersthene-rhyolites are in the youngest Taupo to Mapara group.

Analysed hornblende-hypersthene rhyolites and biotite-bearing rhyolites do not show significant difference in chemistry to those of the hypersthene rhyolites. Hypersthen-hornblende rhyolites are mapped at Motutaiko Island close to the Horomatangi Reefs vent and at several localities to the north and south of the lake. Biotite-bearing rhyolites are mapped north of the lake (Fig 8.1) Considering that the

rhyolite inclusions in the Taupo Pumice Formation can be of cognate, accessory or accidental origin, only some of the hypersthene rhyolite blocks can be of cognate origin. Most of the rhyolite blocks are therefore either accessory or accidental.

Wilson (1985, pers. comm.) has also explained the predominance of rhyolite inclusions in the Taupo Pumice Formation by their derivation from rhyolite domes and flows extruded from the Taupo Volcanic Centre in the last 20 ka of activity. The chemistry of the rhyolite blocks show that most of the hypersthene rhyolites are probably from lava dome extrusions associated with the post 10 ka tephra erupted from the centre, since most of the tephras erupted during this period contain hypersthene as a dominant ferromagnesian phenocryst and show similar major and trace element charecteristics. The hornblende-hypersthene and biotite-bearing rhyolites are definitely accessory and accidental lithics from the pre-10 ka activity in the centre. It has been noted that the latest stage of many plinian and ignimbrite forming eruptions is extrusion of a lava dome due to degassing and volatile escape during the pyroclastic phases. Many of the rhyolite domes in the Taupo Volcanic Centre are therefore late stage magma extrusions related to the pyroclastic activity.

8.2 DACITES

Dacites make up the second most abundant lithics in the Taupo Pumice Formation. Dacite inclusions are found not only in the ground layer but also in the Taupo Plinian Pumice and Hatepe Plinian Pumice in minor proportion and in sections both to the east and west of the lake. All the studied dacite inclusions are two pyroxene dacites. Outcrops of dacite are rare in the Taupo Volcanic Centre and are only known at Tauhara (10 km east of Taupo township) and two smaller dacite domes are mapped south of Lake Taupo at Manganamu and Motuoapa (Daorerk, 1972). Hornblende hypersthene dacite, similar to that of Tauhara volcano has been mapped (Grindley, 1960) about 5 km south west of Tauhara. However drilling for geothermal steam in the area immediately north of Taupo Volcanic Centre (Wairakei, Rotokawa, and Tauhara geothermal fields) has shown no subsurface occurrence of dacites (Steiner, 1977; Grindley, 1965; Browne and Lloyd 1986).

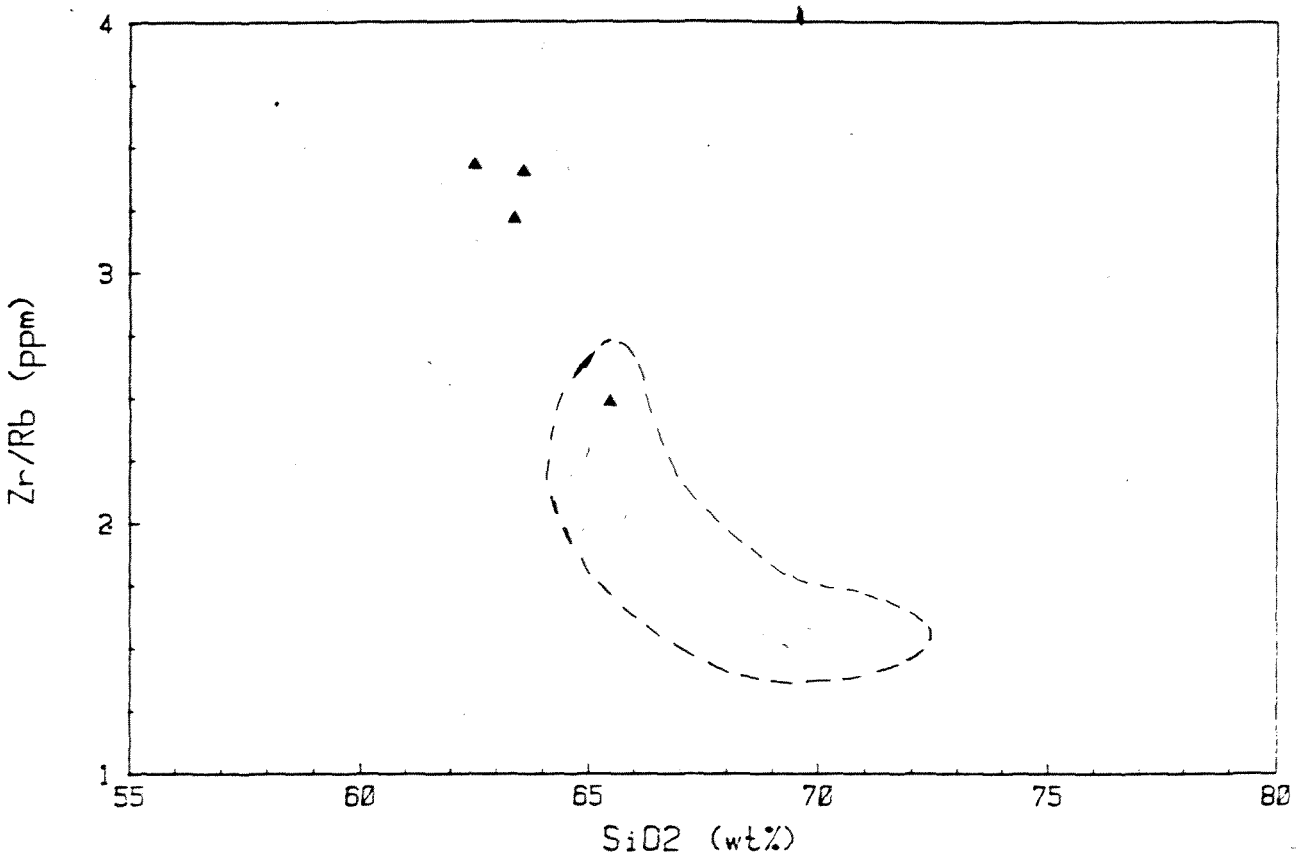

Figure 8.4 : Zr/Rb Vs SiO2 plot of the analysed lithics in the ground layer. Filled triangles represent the dacite lithics from the ground layer, the field shown represents the dacite domes and flows of the Tauhara volcanic complex (Worthington, 1985) The dacite lithics show a similar major element content to the domes and flows of Tauhara except their lower SiO2 content. Trace element ratios like Zr/Rb distinguish most of the dacite lithics from those of Tauhara.

The Tauhara dacites show several differences in mineralogy and chemistry to those found as inclusions in the Taupo Pumice Formation. Tauhara dacites contain a diverse phenocryst assemblage of plagioclase (An_{25-40} and An_{75-90}), orthopyroxene (En_{45-55} and En_{70-80}), clinopyroxenes (two morphologically distinct types), hornblende, biotite, quartz, olivine (Fo_{82}) and biotite with accessory magnetite, apatite and cristobalite. Hornblende forms 6-26% of the total phenocryst content in all of the dacites. The phenocrysts are not in equilibrium with either the groundmass or with each other, and an origin by magma mixing has been suggested for these domes (Worthington, 1985).

The petrography of all the dacite inclusions is quite distinct from those of the Tauhara dacites described above. Furthermore, the dacite inclusions show no mineralogical evidence of magma mixing (chap 5). Chemically, most of the Tauhara dacite domes contain > 65 wt% SiO_2 and relative to other dacites in the Taupo Volcanic Zone are MgO, Ni, and Sr-rich and K_2O poor (Worthington, 1985), making them distinct from the analysed dacite inclusions. Rb/Sr and Zn/Nb ratios of the dacite inclusions show more than 10% difference to those of the Tauhara dacites (Fig 8.4). The presence of a dominantly hypersthene-augite dacite as inclusions in the Taupo Pumice Formation suggests the presence of subsurface dacite flows in the near vent area. This dacite does not have any known surface correlative in the area.

8.3 ANDESITES

The most important nearby andesite lava occurrence is at the Tongariro Volcanic Centre. The Volcanic Centre comprises four major andesite massifs, Kakaramea, Pihanga, Tongariro and Ruapehu and four smaller cones and flows, Maungakatote, Pukeonake, Hauhungatahi and Ohakune. Older lavas from Kakaramea, Pihanga and Tongariro were erupted from a series of vents aligned NW-SE and more recent lavas from vents aligned NNE-SSW.

The most voluminous lava types in the centre are labradorite and labradorite-pyroxene andesites containing phenocrysts of plagioclase (An_{68-48}),

orthopyroxene (mainly bronzite) and clinopyroxene in a fine grained groundmass. Smaller amounts of pyroxene andesite (from Pihanga), olivine andesite and hornblende andesite also occur at the centre.

Most andesites of the Tongariro Volcanic Centre are acid or basic, low K andesites. Major element analysis of the andesites largely reflects variation in phenocryst content. Cole (1978) has suggested that the lavas which are more silicic have a lower ferromagnesian phenocryst content and that most of the basic andesites are pyroxene or olivine bearing. With increasing modal content of the ferromagnesian minerals, the lavas have progressively higher FeO(t), MnO, MgO, and CaO and correspondingly lower Al_2O_3, Na_2O, and K_2O. The analysed andesite blocks from the ground layer lie very close to those of the andesites of the Tongariro Volcanic Centre. Trace element concentrations are very similar and are within the range of the andesites of the Tongariro Volcanic Centre (Cole, 1978).

An eroded andesite cone occurs at Rolles Peak, north-east of Tauhara (Grindley, 1961) close to the Kaingaroa Fault. Petrographically the rock is holocrystalline, containing sparse phenocrysts of plagioclase and subordinate hypersthene, set in a groundmass consisting of augite, hypersthene and labradorite with accessory magnetite and tridymite. Chemically this andesite is calc-alkaline and is significantly richer in Al_2O_3 and Sr and has lower K_2O compared to many TVZ andesites (Worthington, 1985). The Sr rich nature of Rolles Peak andesites is specially noteworthy (919-1035 ppm Sr compared to less than 300 ppm for most TVZ andesites). None of the analysed andesite inclusions from the Taupo Pumice Formation contain such high Sr concentrations.

Andesite lava flows up to 180 m thick have been encountered in several drillholes at Wairakei, interbedded with the sediments of the Waiora Formation and rarely resting directly on the Whakamaru Group Ignimbrites (Grindley 1965, Steiner 1970). This andesite contains numerous large, partly or completely altered andesine phenocrysts and comparatively small pseudomorphs after ferromagnesian minerals, with accessory magnetite. The groundmass is either cryptocrystalline or hyalopilitic and is commonly altered.

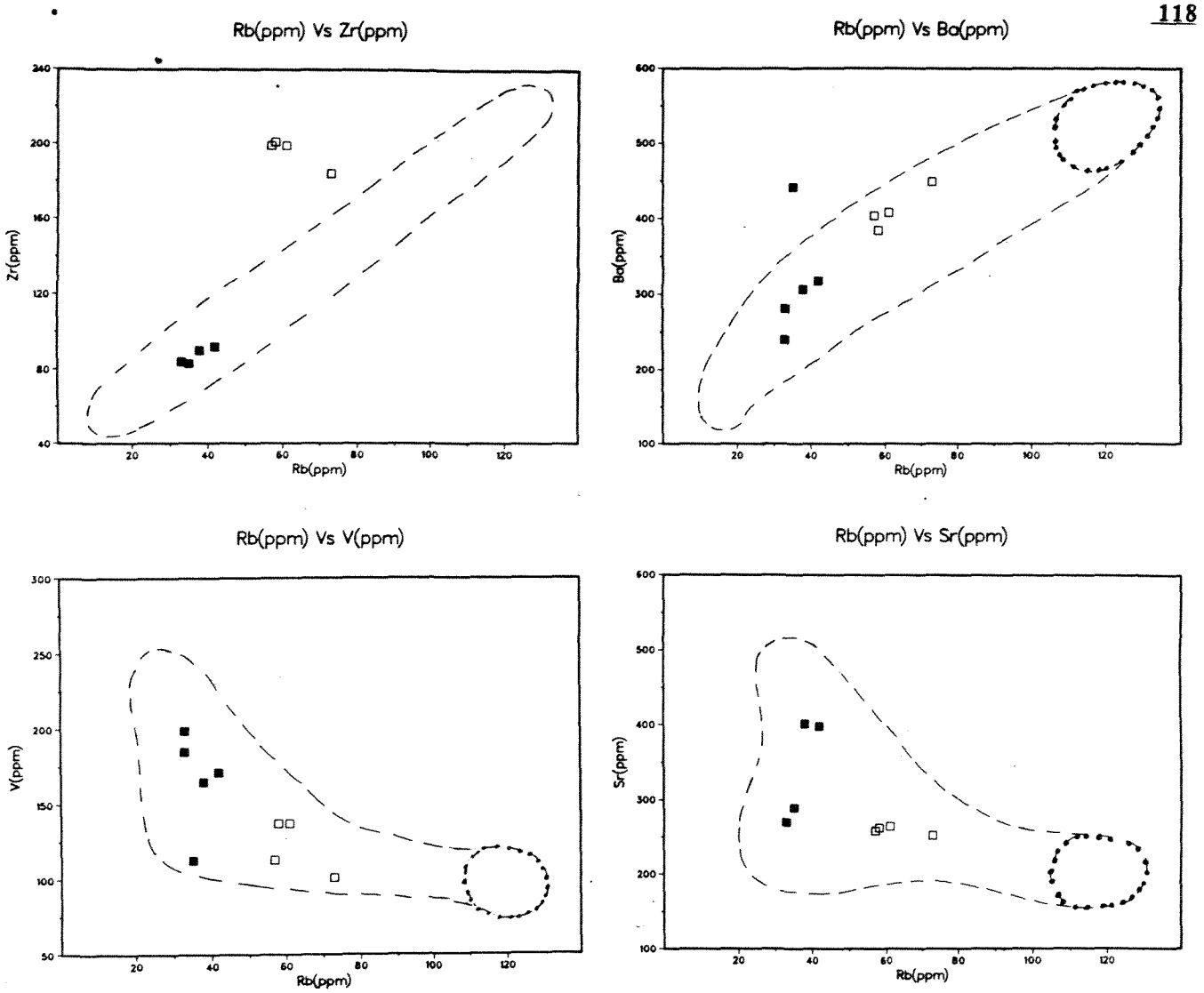

Figure 8.5 : Trace element variation of the analysed dacite (open squares) and andesite (filled squares) lithics in the ground layer. Areas bounded by broken lines represent the zone where 144 analyses of andesite lavas of the Tongariro Volcanic Centre plotted. Smaller areas bounded by dotted lines represent dacites from the centre (Hackett, 1985). All the analysed andesite lithics from the ground layer show similar trace element content to those of Tongariro Volcanic Centre a marked difference can be observed in Zr and Rb content of the dacite lithics compared to those of the Tongariro Volcanic Centre.

The petrography of the andesite inclusions shows that they have not been subject to intensive hydrothermal alteration, which indicates that they do not represent intercalations of andesite lava flows in the sediments similar to those encountered by drilling at Wairakei. The four types of andesite inclusions found in the Taupo Pumice Formation (ie. pyroxene andesite, plagioclase-pyroxene andesites, olivine andesites and hornblende andesites) have very similar petrography and mineralogy to those described for the lavas of the Tongariro Volcanic Centre (Cole, 1978 ; Hackett, 1985). Trace element variation diagrams of the analysed andesite blocks from the ground layer (Fig 8.5) shows that they plot in the area where 144 analyses from the Tongariro Volcanic Centre plotted (Hackett, 1985). However it is important to notice that there is a marked difference in Zr and Rb contents of the dacite blocks from the ground layer compared to those of the Tongariro Volcanic Centre.

Most of the andesite blocks found in the ground layer of the Taupo Ignimbrite are subangular, and could have been transported as alluvium or lahars into the lake basin and incorporated in the lake sediments before being explosively transported by the pyroclastic flow. The proximity of the Tongariro Volcanic Centre to the lake basin, and its present topographic (drainage) relation to the lake basin indicates that the andesite inclusions can easily be transported from the centre.

8.4 IGNIMBRITE

Most ignimbrite units are highly inhomogeneous rock units, showing a considerable variation in texture, degree of welding and crystallization, mineralogy and chemistry both laterally and vertically within the same unit. Correlation of the ignimbrite inclusions with a particuar ignimbrite unit in the area is therefore difficult.

There is seismic evidence that the upper surface of the ignimbrite which crops out to the east and west of Lake Taupo extends beneath the lake at depths of about 1 km. Northey (1985) presents evidence of at least two units in the ignimbrite flows, an upper unit with a seismic velocity of 2.2 km/s, overlying one of 3.8 km/s. The upper unit is

about 400 m thick near Kawakawa Point and its upper surface is about 500 m below lake level (Fig 8.6). Northey (1985) correlates these flow units to the Whakamaru Ignimbrites. Wilson et al. (1984) have presented field evidence which show that there has been one major post-Whakamaru Group and pre 50 ka ignimbrite eruption from a vent within Lake Taupo. A higher velocity unit underlying Whakamaru Group Ignimbrite seen at Western Bay at depths of about 900 m may relate to the ignimbrite and pumice breccia of the Ohakuri Group of Grindley (1960).

The lithic crystal rich ignimbrite (Type 1) is characteristically pale brown to orange and is the most abundant welded ignimbrite inclusion in the Taupo Pumice Formation. Blocks of this type of ignimbrite as big as 1-1.5 m in diameter are found in many near vent localities in the ground layer. Wilson et al. (1984) have described a similar ignimbrite at the NE end of Lake Taupo and have suggested that the ignimbrite may be a product of a post-Whakamaru Group eruption (100 ka) from the Taupo Volcanic Centre. The lithic crystal rich ignimbrite may thus be correlated with the ignimbrite of this period from the Taupo Volcanic Centre.

The northern part of Lake Taupo is a caldera structure in which depth to basement is estimated on geophysical grounds to be about 5 km below the surface. The older pyroclastics and volcaniclastic sedimentary units are expected to be deeply buried in the lake basin during the volcanotectonic activity in the centre. Intensive hydrothermal alteration would probably have completely changed the original features of the rocks. Most of the Whakamaru Group ignimbrites are considered to be below 2 km from the Lake bottom and are underlain by a thick sequence of volcaniclastic deposits (Ohakuri Group) which rest directly on the basement (greywacke?) Some of the hydrothermally altered blocks of rhyolite and tuff could have possibly been derived from the pre-Whakamaru Group volcaniclastic deposits and Whakamru Group Ignimbrites. Crystal rich ignimbrites similar to the surface outcrops of the Whakamaru Group Ignimbrites do not occur in a significant quantity in the ground layer or as inclusions in other members of the Taupo Pumice Formation. Rare lapilli-sized crystal-rich ignimbrite (Type 2) inclusions are tentatively correlated with the Whakamaru Group Ignimbrites.

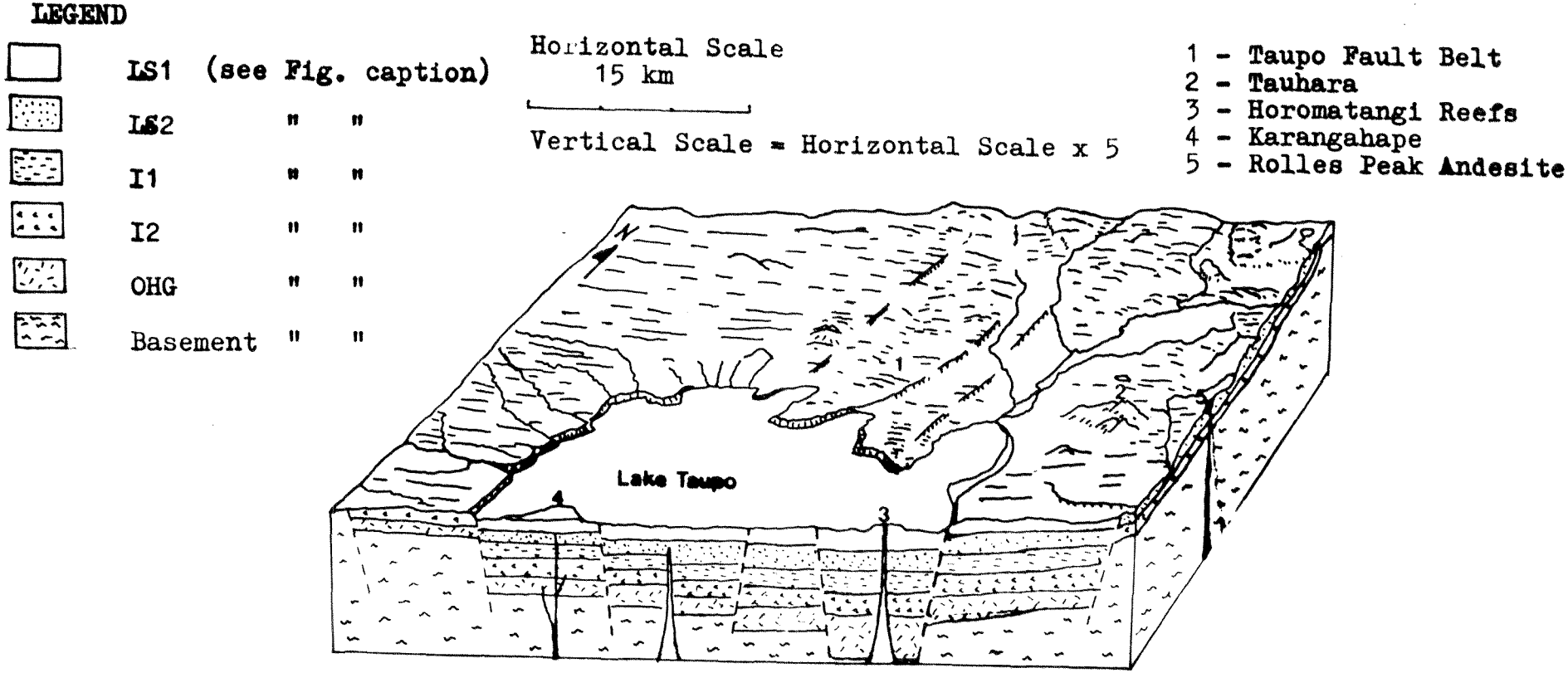

Figure 8.6 : Schematic block diagram to show the sub-bottom structure of Lake Taupo. Two major sedimentary units with intercalated tephra and lava flows are shown, underlain by two major ignimbrite layers as defined by seismic studies (Northey, 1983). The ignimbrites overlie older volcaniclastic sediments of the Ohakuri Group (Grindley, 1961) which directly rest on the basement.

LS1- includes Huka Falls Formation interbedded with Lake Taupo Group tephra, Haparangi Rhyolites.

LS2- includes Waiora Formation interbedded with Haparangi Rhyolites Waiora Valley Andesites and other undifferentiated tephra from the Tongariro Volcanic Centre.

I1- Undifferentiated (=100Ka) ignimbrite from Taupo Volcanic Centre.

I2- Whakamaru Group Ignimbrites.

OHG-Pre Whakamaru Group Volcanic deposts (Ohakuri Group) Basement-Greywacke and Granitic Plutons?

8.5 LAKE SEDIMENTS

A wide variety of lake sediments (from coarse dominantly volcaniclastic sediments to diatomaceous and carbonaceous mudstone and siltstone) occur in the Taupo Basin. The diversity of sedimentary rocks in the Huka Falls Formation and the Waiora Formation, and the absence of reliable diagnostic characteristics of the two major volcanogenic sedimentary formations makes correlation of these sedimentary boulders to known stratigraphic units difficult. Furthermore the Taupo Basin has been an active sedimentary basin in post-Huka Falls Formation time (i.e.Holocene to Recent), further complicating the correlation of the sedimentary boulders. Northey (1983) distinguished two sedimentary units: an upper unit with a seismic velocity of 1.5 km/s and a lower thicker unit with a seismic velocity of 1.7 km/s.

The lake sediment boulders are all found in near vent exposures of the ground layer and are as big as 1-1.5 m in diameter. From the highly fragile nature of these rocks it is not physically possible that they have travelled far in the eruption columun and were most probably incorporated in the pyroclastic flow by widening of the vent during the eruption. All are near surface vent derived blocks, some of the lake sediments may be correlated with the upper Huka Falls Formation, but most of the lake sediment boulders probably belong to Holocene deposits on the lake bottom.

The greywacke pebbles found as inclusions in the Taupo Pumice Formation are probably derived from alluvium deposited in the lake basin and were incorporated in the lake sediments before being explosively carried out of the vent area and transported with the pyroclastic flow.

The greywacke bordering on, and underlying some parts of the TVZ belong to the Torlesse Subgroup (eastern greywacke of Reid (1982)) and are distinguished from basement rocks cropping out on the western side of the TVZ on petrographic, geochemical and isotopic differences. The sandstones of the western basement are generally poorly sorted volcanogenic meta-sedimentary rocks and contain significantly less quartz, more ferromagnesian minerals and volcanogenic lithics than those of the eastern basement rocks.

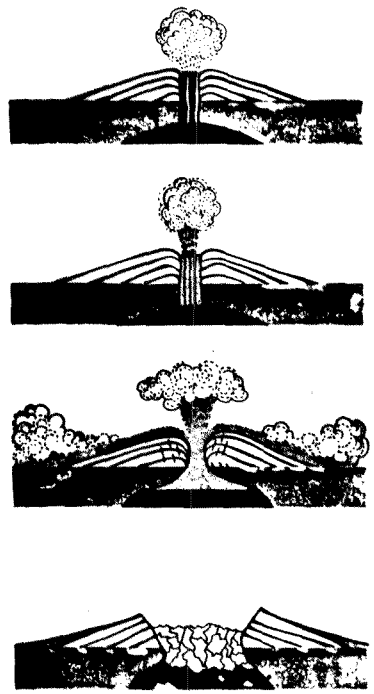

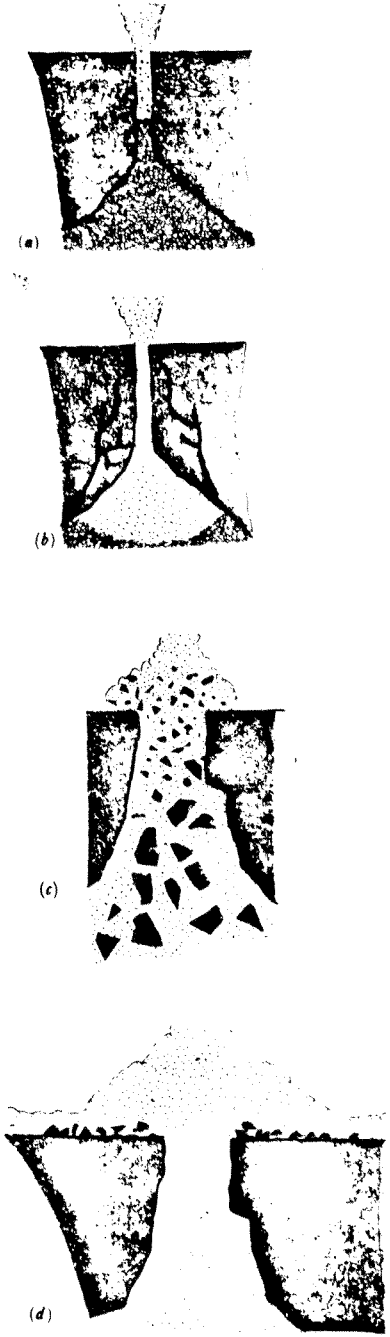

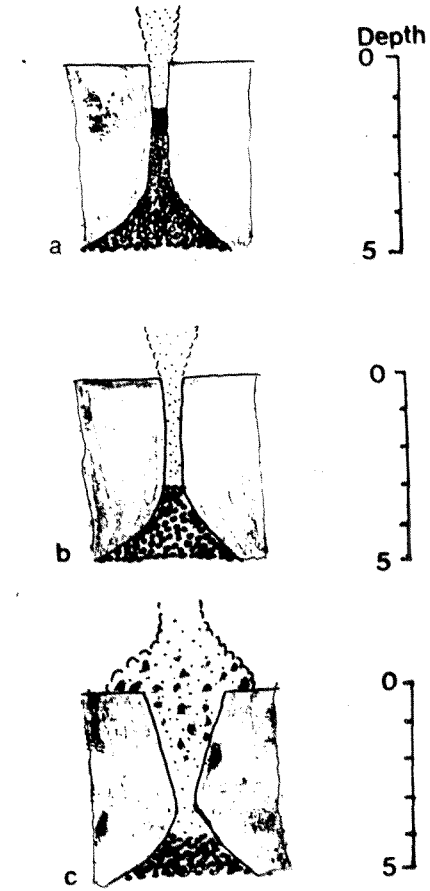

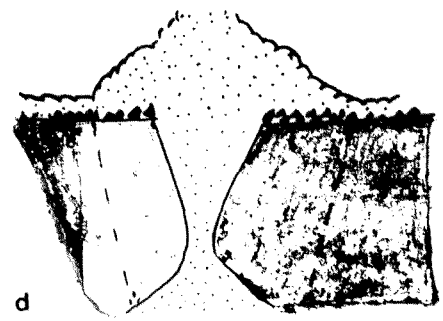

Figure 8.7 :

Schematic diagrams to show the inferred sequence of events which lead to the eruption of the Taupo ignimbrite and its ground layer.

(1) The collapse of the roof the magma chamber caused by the lack of support caused by the downward movement of the magma level resulting in the formation of a caldera is presented for comprision (Williams and McBirney, 1979).

(2) Collapse of the roof of the magma chamber caused by the lowering of the fragmentation surface is suggested to explain the high lithic content of the ground layer (Wilson and Walker, 1985)

(3) The high lithic content in the ground layer is shown to result from simple vent flaring caused by both the increase in discharge rate of pyroclastic material and lowering of the fragmentation surface. Collapse of the roof of the magma chamber which occurred at the end of the eruption resulted the Taupo eruption caldera.

Petrographically the greywacke pebbles in the ground layer of the Taupo Ignimbrite similar to the eastern basement rocks. Furthermore, the proximity of the Taupo Basin to eastern greywacke ranges (Kaimanawa Ranges), and their outcrops being within the basin catchment shows that the greywacke pebbles incorporated with the lake sediments were probably derived by erosion from the eastern basement. No sample of unreworked, angular basement rocks (greywacke) occur as lithic inclusions in the Taupo Pumice Formation.

8.6 *DISCUSSION ON AN ERUPTION MODEL*

Rhyolite magma which produce ash flow tuff similar to the Taupo Pumice Formation is commonly generated at depths in excess of 10 km in the crust and forms magma chambers at higher levels. Smith (1979) has discussed the relationship between the volumes of ash flow eruptions, size of calderas and magma chambers and zonation in magma columns. Silicic magma chambers are believed to be less than 10 km thick, with larger chambers being more slab-like and the smaller ones more cylindrical, and not more than 1/10 of the chamber volume may be erupted during any one pyroclastic eruption. The depth to which the magma is erupted from a magma chamber during a single episode is termed the depth of drawdown and is directly proportional to the volume of the magma chamber and the volume of pyroclastic material erupted. The volume of pyroclastics erupted is also found to be directly proportional to the diameter of the caldera resulting from the eruption which commonly approximates the diameter of the underlying magma chambers.

Froggatt (1982) has suggested two main physiographic features which have resulted from the Taupo eruption. A 'saucer-like' land form which has a centre about 2 km north of the Horomatangi Reefs is suggested to be from a post Taupo Pumice subsidence, that is radially symmetrical about a centre north of Horomatangi Reef . The saucer shape forms only about a 90° sector. Bathymetry of Lake Taupo (Irvin, 1972) shows a nearly rectangular flat-bottomed depression with Horomatangi Reefs in the south east corner and lying about 40 m below the floor of the remaining lake. By

approximating the area of caldera subsidence to a rectangle (8 km x 10 km x 40 m) and an inverted cone (radius 15 km, central hieght 400 m, and 90° segment) the maximum total volume of subsidence is about 27 km^3 , together with other subsidence which has occurred offshore after the eruption. Froggatt (1982) suggested that the total volume of the Taupo Pumice 'caldera' subsidence was about 28.5 km^3 which is close to the estimated erupted magma volume.

Depth to basement greywacke in most volcanic centres and depressions in the TVZ is inferred to be about 5 km on geophysical grounds. It has also been postulated that the greywacke basement has been so extended beneath the TVZ that it is probably absent beneath most of the rhyolitic volcanic centres. The lavas of the TVZ do not have a simple genetic relationship to each other. Petrologic studies on the origin of rhyolite lava in the TVZ have indicated a derivation by about 30% partial melting of the greywacke and argillite sediments at depths in excess of 10 km along the central axis of the TVZ. The chemistry of the lava, in particular the lower abundunce of K (2.69 wt%), Rb (average 108 ppm), Sr (125 ppm), U (2.53 ppm) and Th (11.3 ppm) shows a marked contrast from an acid end member derived by fractional crystallization (Cole, 1979). Froggatt (1982) presented a model where only a third of the magma generated is erupted, the remainder being intruded into the crust to compensate for spreading of the TVZ. The crustal structure of the zone is thus greywacke "blocks" separated by granitic intrusions.

Using the empirical relationships of erupted magma volume, depth of magma chamber and drawdown and resulting caldera diameter, suggested by Smith (1979) the magma chamber of the Taupo Pumice Formation is estimated to have a depth of 3-5 km from the surface, with a depth of drawdown of about 3 km below the roof of the magma chamber. Fig 8.7 is a schematic cross section of the upper crust through the Taupo Volcanic Centre. Seismic studies (Northey, 1983) have shown that there are two sedimentary structures beneath Lake Taupo with seismic velocities of 1.5 and 1.7 km/s in the central part of the lake. The lake sediments are underlain by two major ignimbrite layers with seismic velocities of 2.2 and 3.8 km/s in most parts of the lake. Onshore

geologic studies and drillhole information (Grindley, 1960, 1961, 1965) show that the ignimbrites of the Whakamaru Group are underlain by the Ohakuri Group volcaniclastic sediments whose full thickness was not penetrated by drilling at Wairakei.

Several pyroclastic eruptions have occurred from vents in Lake Taupo in the last 50 ka. Since most pyroclastic eruptions are followed by extrusion of a rhyolite dome, several rhyolite domes and flows are expected to be intercalated with the upper sedimentary unit (Huka Falls Formation?) and probably the lower sediments (Waiora Formation?). However some of the rhyolite inclusions in the Taupo Pumice Formation can be correlated with older Haparangi Rhyolites which are mapped onshore north of Lake Taupo. From the occurrence of dacite inclusions in considerable proportions in most members of the Taupo Pumice Formation it is inferred that dacite flows exist in the vent area. This dacite probably belongs to the post 50 ka period, and can be of similar age to the dacites of the Tauhara dome complex despite their petrographic differences. It has been proved from heat flow measurements at the bottom of Lake Taupo (Northey, 1983) that an active hydrothermal system exists near the Horomatangi Reefs, and the age of this hydrothermal system is not exactly known. Some of the hydrothermally altered blocks in the ground layer are derived from the geothermal reservoir, however some of the blocks were probably derived from an older vent or vents which existed prior to the Taupo eruption.

It has been suggested that the large quantity of boulders of rhyolites, ignimbrites and lake sediments as big as 2 m in diameter in near vent exposures of the ground layer probably result from the collapse of the vent area, unroofing the magma chamber at the beginning of the ignimbrite eruption (Fig 8.8). As a result, the catastrophic eruption first produced material containing a large quantity of coarse lithics (the ground layer); later material having smaller and less lithics. This collapse is likely to have resulted from the downward movement of the fragmentation surface (i.e. the boundary between coherent, vesicular magma and fragmented material) during the Taupo plinian phase; eventually leaving the vent area unsupported (Wilson and Walker, 1985).

However similar collapse of the roof of the magma chamber caused by the downward movement of the fragmentation surface and/or the magma level deep into the chamber is known to have resulted caldera structures and volcanotectonic depressions which accompany major ignimbrite eruptions (Fig 8.8 a) (eg. Toba caldera, Sumatra; Bullard, 1976). A model which involves the collapse of the roof of the magma chamber (Fig 8,8 b) proposed by Wilson and Walker (1985) to explain the large quantity of boulders of rhyolite lava, welded tuff and lake sediments does not appear physically possible considering the time span and energy envolved in breaking such crustal blocks in to a pyroclastic material.

A simple collapse and flaring of the vent area which resulted from the downward movement of the fragmentation surface at the begining of the ignimbrite eruption best explains the lithic content in the ground layer. The absence of unreworked (primary) basement rock inclusions in the Taupo Pumice Formation probably indicates that the magma chamber is located at a higher level in the crust and conform with the fact that the lithics are derived by the widening of the vent.

The lithics in the Taupo Pumice Formation are mainly a product of the explosive disruption of the country rock around the vent during the eruption. Primary xenoliths from depths of magma generation were not found, and the maximum depth of incorporation of lithics in the Taupo Pumice Formation is to a depth of 3-4 km (ie. down to the Whakamaru Group Ignimbrites).

Chapter IX

SUMMARY AND CONCLUSIONS

1. Taupo Volcano is the southernmost of the dominantly rhyolitic volcanic centres in the TVZ. The volcano is a negative feature most of which is covered by Lake Taupo and is complex consisting of several caldera structures superimposed on the regional NNE trending faults of the Taupo Fault Belt. Central and western Lake Taupo are calderas related to the Holocene and Pleistocene tephra eruptions. The central Lake Taupo caldera is suggested to have resulted from the Taupo eruption of ca. 1800a. The northern bays and southern Lake Taupo are graben structures related to the Taupo Fault Belt. Most of the faults show significant displacement with throws in excess of 500 m.

2. The Taupo Pumice Formation is the product of one of the largest explosive sequence of volcanic eruptions in the world in the last 7000 years. The vent area for the eruption is in Lake Taupo at or near the Horomatangi Reefs as indicated by several isopach and isograde maps. The eruption showed a complex interplay between wet and dry vent conditions resulting in phreatoplinian (and/or phreatomagmatic) ash deposits and plinian pumice deposits producing three phreatoplinian ash deposits, two plinian pumice deposits (one of which; the Taupo Plinian Pumice is possibly the most widely dispersed fall deposit currently known) and a low-aspect ratio and low-grade ignimbrite which covered most of the North Island of New Zealand. Volume estimates on the tephra show that the eruption volume increased together with the mass eruption rate (dischage rate) reaching a climax at the end of the eruption to produce the Taupo Ignimbrite. The Ignimbrite was produced by the collapse of the plinian eruption column which resulted from vent widening and collapse of the vent area. The most important factors which control the energy and characteristics of an eruption are gas content of magma, vent radius and

shape, mass eruption rate and volume of magma erupted. The Taupo eruption, despite the modest volume of its products was energetic due to its high volatile content and discharge rate.

3. Lithic content within the three phreatomagmatic ash deposits in all studied sections is negligible. The lithic content within the two plinian pumice deposits is less than 10% by volume in most sections. The main body of the ignimbrite contains variable amount of lithics, usually less than 20% by volume, and a decrease in lithic content and increase in crystal and pumice contents was observed away from the vent. This is considered to have resulted from the gravitational separation and sedimentation of the heavies from the pyroclastic flow.

4. Lithic blocks in the Taupo Pumice Formation are mostly concentrated in the ground layer which forms the base of the the ignimbrite. The ground layer contains blocks of rhyolite, lake sediments and welded tuff up to 2 m in size in near vent exposures where it is up to 3 m thick. These big boulders are considered to constitute the co-ignimbrite lag-fall deposit which was transported laterally by the momentum of the flow. In most exposures further away from the vent (20 km or more) the ground layer has a thickness of 10-30 cm. The erosive upper and lower contacts suggest that sedimentation of 'heavies' took place in the more strongly fluidized head of the pyroclastic flow. Giant friable boulders of lake sediments, welded tuff and intensely hydrothermally altered rhyolite are highly fractured but are exposed intact in the ground layer. This shows that the fluid pyroclastic material mixture provided sufficient support during transportation.

5. Estimation of the proportion of the lithic types in the ground layer shows that rhyolites make up about 75% by weight of the lithics in most sections. Dacites, andesites, welded ignimbrite and lake sediments (pumiceous mudstones and siltstones) make up the remaining 25% of the lithics. The main type of lateral variation in the proportion of lithic types in the ground layer is that the soft and friable rocks rapidly decreases away from the vent.

6. A study of the stratigraphy of the area shows that the units in the vent area consist of predominantly silicic volcanics and derivative sedimentary rocks of late Tertiary to Pleistocene age. Three volcaniclastic sedimentary units from the oldest to the youngest are Ohakuri Group, Waiora Formation and Huka Fall Formation intercalated with pyroclastic units erupted from vents in the Taupo Volcanic Centre which include some of the most widespread ignimbrite units in the Central Volcanic Region (Whakamaru Group Ignimbrites). These ignimbrites are described as the Whakamaru Group Ignimbrites, and another undifferentiated younger ignimbrite, Okaia Sub-group, Kawakawa Tephra Formation and Lake Taupo Sub-group. Lava extrusions and intrusions intercalated with these sediments and pyroclastics in the vicinity of the Taupo Volcanic Centre are dominantly rhyolitic with minor dacite and rare andesite and basalt. These are the Haparangi Rhyolites, Tauhara Dacites, Waiora Valley Andesites and K-trig Basalts.

7. Three types of rhyolite lithics; hypersthene rhyolite, hypersthene-hornblende rhyolite and biotite bearing rhyolite (in order of decreasing abundance were found in the Taupo Pumice Formation. The rhyolite inclusions are generally porphyritic (with phenocryst content commonly <15 modal%) and contain phenocrysts of plagioclase (An_{27-50}), hypersthene ($Mg_{58}\ Fe_{41}\ Ca_{1}$ to $Mg_{50}\ Fe_{47}\ Ca_{3}$), quartz, brown hornblende, biotite and accessory magnetite and apatite. The phenocrysts rarely form aggregates and occur in a cryptocrystalline groundmass which is partly or completely glassy and contains spherulites, cristobalite and glassy microlites which normally show flow banding. Hypersthene is the dominant mafic phenocryst in the rhyolite lithics in the Taupo Pumice Formation and also forms the major mafic mineral in the Taupo Sub-group Tephras. Whole rock analyses of Taupo Sub-group tephras show a similar trend in major element oxides to those of the rhyolite lithics in the ground layer. Furthermore a Sr Vs Zr plot shows that the rhyolite inclusions are very similar to the Taupo Sub-group tephras. This indicates that the accessory and accidental lithics in the Taupo Pumice Formation are probably derived from the lava extrusions associated with the pyroclastic eruptions from the Taupo Volcanic Centre in the last 10 ka. Lithics derived from older rhyolite lava

(Haparangi Rhyolites) are probably represented by the intensly hydrothermally altered rhyolite blocks in the Taupo Pumice Formation.

8. Dacites are the second most important type of lithics in the Taupo Pumice Formation and comprise about 15 weight % of the lithic blocks in the ground layer at many sections. The dacites are always porphyritic and contain phenocrysts of plagioclase (An_{52-80} which commonly occur in two generations), orthopyroxenes (Mg_{66} Fe_{47} Ca_3 to (Mg_{64} Fe_{34} Ca_2 hypersthene), clinopyroxene (augite; Mg_{41} Fe_{15} Ca_{44}) and accessory Fe-Ti oxides and apatite. Resorbed quartz and rare olivine phenocrysts are found in some of the dacites. The groundmass consists of a quartzo-feldspathic cryptocrysalline material and laths of plagioclase which occasionally show a flow texture. Whole rock chemical analyses of the dacites shows that most of them contain 63-65 wt% SiO_2 where as most dacite analyses from the Tauhara dacite dome complex (Worthington, 1985) contain > 65 wt% SiO_2 . Rb/Sr and Zn/Nb ratios from the dacite inclusions show a significant difference from Tauhara dacites. This indicates that most of the dacite inclusions are not genetically related to the Tauhara dacites, and suggests the presence of other dacite flows in the vicinity of the vent area covered by the pyroclastics and their derivative lake sediments. The presence of dacite lithics in the Taupo Pumice Formation in most localities indicates an accessary origin for the lithics.

9.Four types of andesite blocks hornblende andesite, plagioclase-pyroxene andesite, pyroxene andesite and olivine andesite were studied from the ground layer. Hornblende andesites contain phenocrysts of plagioclase (An_{53-70}), orthopyroxene (hypersthene-bronzite), clinopyroxene (augite), and hornblende (paragasite-ferrohasingsite). The ground mass consists of microcrystals of plagioclase, tridymite and is commonly cryptocrystalline. Except for the presence of hornblende the other andesites have a similar mineralogy and texture. Plagioclase compositions are An_{65-80} in the plagioclase-pyroxene andesite and An_{85-52} in the pyroxene and olivine andesites. Orthopyroxenes are mainly bronzite in the latter three types of andesites. Clinopyroxene with an endiopside core and augite rim are found in

the pyroxene and olivine andesites. Olivine (Fo_{82-84}) crystals in the olivine andesites are xenocrystic and probably originated by mixing of the crysallization product of a basaltic magma. Other evidence of magma mixing is observed in the pyroxene andesite which contain hypersthene phenocrysts jacketted by pigeonite. All the andesites contain accessory titanomagnetite, ilmenite, and apatite. Chrome spinel occurs as inclusions in the olivine phenocrysts in the olivine andesites. Based on the Gill (1981) classification of intermediate volcanic rocks, the wholerock chemistry of these rocks shows that they are calc-alkaline, medium-K orogenic andesites and show similar major and trace element concentrations to the andesites of the Tongariro Volcanic Centre (Cole, 1978; Hackett,1985). The petrography and available wholerock chemistry of the andesite lithic differ from those encountered by drilling at Wairakei (Grindley, 1965) and from the andesite cone at Rolles Peak. The Rolles Peak andesites in particular are distinct from most TVZ andesites in their high Sr content (919-1035 ppm compared to less than 300 ppm for TVZ andesites). Most of the andesite blocks found in the ground layer of the Taupo ignimbrite are sub-angular and could have been transported as alluvium or lahars into the lake basin and incoporated in the lake sediments before being explosively transported by the pyroclastic flow.

10. Two types of welded ignimbrite inclusions were found as lithics in the Taupo Pumice Formation; these are described as Type 1- Lithic crystal-rich ignimbrite and Type 2- Crystal rich ignimbrite. Type 1 ignimbrite is light brown to orange, pumiceous, relatively lithic rich, ignimbrite which contains about 25% crystals .quartz, plagioclase (oligioclase), hypersthene and hornblende in order of decreasing abundunce] in a matrix of fine glass and ash. Type 1 ignimbrite is correlated on the basis of its petrography with an ignimbrite cropping out north of Lake Taupo, which has erupted from a vent in the Taupo Volcanic Centre in a post Whakamaru Group and pre-50 ka (100 ka) period. Boulders as big as 1.5 m of type 1 ignimbrite are found in near vent exposures of the ground layer which indicates type 1 ignimbrite forms a major stratigraphic unit in the vent area for the 1800 ka Taupo eruption. Type 2 ignimbrite forms a minor proportion

of ignimbrite lithics in the Taupo Pumice Formation and contains crystals of quartz, sodic plagioclase, hypersthene, and rare hornblende which make up about 45% of the rock. The crystals and a minor amount of lithics occur in a matrix of yellow ash. From the crysal rich nature of this ignimbrite it is tentatively correlated with the Whakamaru Group Ignimbrites.

11. A variety of non-volcanic rock types are found in near vent exposures of the ground layer. These includes lake sediments (pumiceous mudstone, siltstone and sandstone) and reworked greywacke pebbles. The lake sediment boulders in the ground layer are near surface vent derived lithics and probably correlate with either the Huka Falls Formation or younger Holocene sediments. The petrography and roundness of the greywacke pebbles in the ground layer shows that they are derived from the Eastern basement ranges and were incorporated in the lake sediments after being transported by rivers into the basin.

12. The study of the lithic content in the Taupo Pumice Formation shows that there is an increase in volume and size of lithic fragments in the ground layer compared to in other members of the Taupo Pumice Formation. This indicates that extensive vent erosion has occured at the begining of the ignimbrite eruption. The scarcity of primary basement rocks (greywacke and/or granite?) inclusions in the Taupo Pumice Formation indicates that the magma chamber is located above the basement (< 5 km depth) and conform with the fact that the lithics are derived by vent flaring caused by the down ward movement of the fragmentation level. The lithic content of the Taupo Pumice Formation shows that the lithics are derived from down to a depth of about 3-4 km.

REFERENCES

1. Baumgart, I. L. 1954: Some ash Showers of Central North Island N.Z. Journal of Science and Technology 35B: 456-467

2. Baumgart, I. L. ; Healy J. 1956: Recent Volcanicity of Taupo, New Zealand. Proceedings, 8th Pacific Science Congress 2: 113-125

3. Bence, A. E.; and Albee, A. L. 1968: Emperical correction factor for the electron microanalysis of silicate and oxides. Journal of Geology 76: 382-403

4. Best, M. G. and Mercy, E. L. P. 1967: Composition and crystallization of mafic minerals in the Gedalupe Igneous Complex, California American Mineralogist 52: 436-474

5. Briggs, N. D. 1973: Investigation of New Zealand Pyroclastic flow deposits Unpublished Ph.D. thesis, Victoria University of Wellington

6. Briggs, N. D. 1976: Welding and Crystallization Zonation in Whakamaru Ignimbrite, Central North Island, New Zealand. N.Z. Journal of Geology and Geophsics 19(2): 189-212

7. Browne P. R. L. and Lloyd E. F. 1986: Water dominated geothermal systems and associated mineralization. Taupo Volcanic Zone (Tour Guides A5) New Zealand Geological Survey Record 11: 145-212 Editors Houghton B. F. and Weaver S. D.

8. Bullard F. M. 1976: Volcanoes of the Earth. University of Texas Press Austin & London.

9. Clark, R. H. 1960: Petrology of the volcanic rocks of the Tongariro Subdivision, Appendix 2 in Gregg D. R. "The Geology of Tongariro Subdivision" N.Z. Geological Survey Bulletin n.s. 40: 107-23

10. Cole, J. W. 1973: High Alumina Basalt of Taupo Volcanic Zone, NewZealand. Lithos 6 : 53-64

11 .Cole, J. W. 1978: Andesites of the Tongariro Volcanic Centre North Island, New Zealand. Journal of Volcanology and Geothermal Research 3: 53-64

12. Cole, J. W. 1979: Structure, Petrology, and Genesis of Cenozoic Volcanism, Taupo Volcanic Zone, New Zealand - a review. N.Z.Journal of Geology and Geophysics 22(6): 631-37

13. Cole, J. W. 1985: Taupo-Rotorua Depression: An ensialic marginal basin of North Island, New Zealand. In Marginal Basin Geology: Volcanic and Associated Sedimentary and Tectonic processes in modern and ancient marginal basins. Eds. Kokelar B. P. Howells F., Spec. Publ. Geol. Soc. Lond. 16:109-120

14. Cox, A.:1969 A paleomagnetic study of secular variations in New Zealand. Earth and Planetary Science Letters 6(4):257-67

15. Cox K. G.; Bell, J. D. and Pankhurst, R. J. 1979: The Interpretation of Igneous Rocks. Publishers; George Allen & Unwin Ltd. London

16. Daorerk, V. 1972: Volcanic Geology of the Taupo Basin Unpublished M.Sc. thesis, Victoria University of Wellington

17. Deer W. A.; Howie R. A.; and Zussman J. (1966) An Introduction to Rock Forming Minerals Longmans, England.

18. De Vore, G. W. 1957: The association of strongly polarizing cations as a major influence in element distribution, mineral composition, and crystal growth. Journal of Geology 65: 178-95

19. Ewart, A. 1963: Petrology and Petrogenesis of the Quaternary Pumice Ash in the Taupo area, New Zealand. Journal of Petrology 4: 392-431

20. Ewart, A. 1967: The Petrography of the Central North Island Rhyolite lavas 1. Correlation between the phenocryst assemblages. N.Z. Journal of Geology and Geophysics 10: 182-197

21. Ewart, A.; Stipp, J. J. 1968: Petrogenesis of the volcanic rocks of the Central North Island, New Zealand, as indicated by a study of Sr87/Sr86 ratios, and Sr, Rb, K, U and Th abundunces. Geochemica et Cosmochimica Acta 32: 699-736

22. Ewart, A. 1971: Notes on the chemistry of ferromagnesian phenocrysts from selected volcanic rocks, Central Volcanic Region. N.Z. Journal of Geology and Geophysics 14: 323-340

23. Fisher R. V. and Schminke H. U. 1984: Pyroclastic Rocks Springer-Verlag; New York.

24. Fleet, M. E. 1974: Partitioning of Mg and Fe^{2+} in coexisting pyroxenes. Contributions to Mineralogy and Petrology 44: 251-7

25. Froggatt, P. C. 1979: Lake Taupo-Probable Source of Taupo Pumice Formation (note). N.Z. Journal of Geology and Geophysics 22(6): 763-764

26. Froggatt, P. C.; Wilson, C. J. N.; Walker, G. P. L. 1981: Orientation of Logs in the Taupo Ignimbrite as an indicator of flow direction and Vent Position. Geology 9 : 109-111

27. Froggatt, P. C. 1981: Stratigraphy of Nature of the Taupo Pumice Formation. N.Z. Journal of Geology and Geophysics 24: 231-248

28. Froggatt, P. C. 1981: Did Taupo's Eruption enhance European sunset ? Nature, London 293: 491-492

29. Froggatt P. C. 1982: A study of some aspects of the volcanic history of the lake Taupo area, North Island, New Zealand. Ph.D. thesis lodged in the library, Victoria University of Wellington

30. Froggatt, P. C.; Nelson, C. S.; Carter, L.; Griggs, G. & Black, K. D. 1986: An exceptionally large late Quaternary eruption from New Zealand. Nature 319: 578-582

31. Gill, J. B. 1981: Orogenic Andesites and Plate Tectonics. Springer Verlag

32. Grange, L. I. 1937: The geology of the Rotorua-Taupo subdivision. N.Z. Geological Survey Bulletin n.s. 37

33. Gregg, D. R. 1960: The geology of Tongariro subdivision. N.Z. Geological Survey Bulletin n.s. 40

34. Grindley, G. W. :1959 Sheet N85-Waitapu; Geological Map of New Zealand, 1:63,360 scale Department of Scientific and Industrial Research.

35. Grindley, G. W. 1960: Sheet 8-Taupo, "Geological map of New Zealand 1:250,000. N.Z. Department of Scientific and Industrial Research, Wellington.

36. Grindley, G. W. 1961: Sheet N94, Taupo, Geological map of New Zealand 1:63,360 N.Z. Department of Scientific and Industrial Research, Wellington.

37. Grindley, G. W. 1965: The geology, structure and exploitation of the Wairakei geothermal field, Taupo New Zealand N.Z. Geological Survey Bulletin 75

38. Hatherton, T. 1954: The Magnetic properties of Whakamaru Ignimbrites. N.Z. Journal of Science and Technology 35B:421-32

39. Healy, J.; Schofield, J. C.; Thompson, B. N. 1964: Sheet 5 - Rotorua; Geological map of New Zealand, 1: 250,000 Department of Scientific and Industrial Research, Wellington

40. Healy, J. 1961: Geology and geothermal energy in the Taupo Volcanic Zone, New Zealand Paper G128 U.N. Conference on new sources of energy (Rome)

41. Healy, J. 1962: Structure and Volcanism in The Taupo Volcanic Zone; New Zealand Crust of the Pacific Basin American Geophysical Union, Geophysical Monograph 6: 151-7

42. Healy, J. 1964: Stratigraphy and Chronology of the late Quaternary ash in the Taupo, Rotorua and Gisborne District. N.Z. Geological Survey Bulletin n.s. 73 (Part 1)

43. Heiken G. and Kenneth W. 1985: Volcanic Ash University of Califronia Press, Berkely and Los Angeles, California

44. Heltz, R. T. 1973: Phase relations of basalts in their melting range at P H2O=5Kb as a function of oxygen fugacity. Part 1. Mafic phase. Journal of Petrology 14: 249-302.

45. Howorth, R.; Froggatt, P. C.; Vucetich, C. G.; Collen, J. D. 1981: Proceedings of tephra workshop, June 30-July 1st 1980, Victoria University of Wellington. Publication of Geology Department VUW No20.

46. Irwin, J. 1972: Lake Taupo, Provisional bathymetry, 1:50,000, New Zealand oceonographic Inistitute chart, Lake series.

47. Leake, B. 1971: On aluminious and edenitic amphiboles. Mineralogical Magazine 38: 389-407

48. Marwick, J. and Fyfe, H. E. 1937: Physiography and Structure in Grange, L. I.: The Geology of the Rotorua -Taupo subdivision. N.Z. Geological Survey Bulletin n.s. 37: 15-53

49. Martin, R. C. 1961: Stratigraphy and structural outline of the Taupo Volcanic Zone. N.Z. Journal of Geology and Geophysics 4: 449-78

50. Modriniak, N. and Studt, F. E. 1959: Geological structure and volcanism of the Taupo-Tarawera district. N.Z. Journal of Geology and Geophysics 2(4): 654-84

51. Murphy, R. P. and Seward, D. 1981: Stratigraphy, lithology, paleomagnetism and fission track ages of some ignimbrite formations in Matahana Basin, New Zealand. N.Z. Journal of Geology and Geophysics 24(3): 325-331

52. Nairn, I. A. 1971: Studies of the Earth Quake Flat breccia formation and other unwelded pyroclastic flow deposits of the Central Volcanic Region, New Zealand. Unpublished M.Sc. thesis lodged in the library of Victoria University of Wellington)

53. Nairn, I. A. and Hull, A. G. 1986: Post 1800 years B.P. displacement on the Paeroa Fault Zone (Taupo Volcanic Zone) N.Z. Geological Survey Record 8:135-142

54. Nishimura, M.; Yogi, K.; Yamamato, M. 1968: Nickel content in olivines Proceedings of the Japan Acadamy 44: 686-691

55. Northey, D. J. 1982: Seismic studies of the structure beneath Lake Taupo. Ph.D. thesis, Victoria University of Wellington.

56. Reid F. W. and Cole, J. W. 1983: Origin of Dacites of the Taupo Volcanic Zone, New Zealand. Journal of Volcanology and Geothermal Research 18: 191-214

57. Rogan, A. M. 1982: A geophysical study of Taupo Volcanic Zone, New Zealand. Journal of Geophysical Research 87: 4073-4088

58. Sarver, L.A. 1972: The determination of ferrous iron in silicates. American Chemical Society Journal 49: 1472-1477

59. Self, S. and Sparks, R. S. J. 1978: Characteristics of widespread pyroclastic deposits formed by the interaction of silicic magma and water. Bulltin of Volcanology. 41: 196-212

60. Self, S. 1983:Large Scale Phreatomagmatic Silicic Volcanism: a case study from New Zealand. Journal of Volcanology and Geothermal Research 17, 433-469

61. Seward, T. M. 1971: The distribution of transition elements in the system Ca Mg $Si_2 O_6$ -$Na_2 Si_2 O_5$ - $H_2 O$ at 1000 bars. Chemical Geology 7: 73-95

62. Shapiro, L. and Brannock, W.W. 1962: Rapid analysis of silicates, carbonate and phosphate rocks. U.S. Geological Survey Bulletin., 1144-A: 56 pp

63. Simkin, T.; Smith, J.V 1970: Minor Element distribution in olivines. Journal of Geology 78: 304-325

64. Smith, R. L. 1979: Ash-flow magmatism Geological Society of America: Special Paper 180: 5-27

65. Sparks, R. S. J.; Self, S. and Walker G. P. L. 1973: Products of Ignimbrite eruptions. Geology 3: 115-116

66. Steiner, A. 1953: Hydrothermal rock alteration at Wairakei, New Zealand. Economic Geology 48(1): 354-75

67. Steiner, A. 1977: The Wairakei geothermal area, North Island, New Zealand: Its subsurface geology and hydrothermal rock alteration. N.Z. Geological Survey Bulletin n.s. 90: 1-15

68. Stipp J. J. 1968: The geochemistry and petrogensis of Cenozoic volcanism in the North Island, New Zealand. Ph.D. thesis, Australia National University, Canaberra

69. Stromer, J. C. 1973: Calcium Zoning in olivines and its relationship to silica activity and Pressure. Geochemica et Cosmochemica Acta 37: 389-407

70. Tracy, R. J. and Robinson, P. 1977: Zoned titanian augite in alkali olivine basalts from Tahiti and the nature of titanian substitutions in augite. American Mineralogist 62: 634-45

71. Vucetich, C. G. and Pullar, W. A. 1973: Holocene Tephra Formations erupted in the Taupo area, and interbedded tephras from other volcanic sources. N.Z. Journal of Geology and Geophysics 16: 745-780

71. Vucetich, C. G. and Howorth, R. 1976: Late Pleistocene Tephrostratigraphy in the Taupo District, New Zealand. N.Z. Journal of Geology and Geophysics 19: 51-70

72. Walker, G. P. L. 1980: The Taupo Plinian Pumice: Product of the most powerful known (ultra plinian) eruption. Journal of Volcanology and Geothemal Research 8: 69-94

74. Walker, G. P. L.; Heming R. F.; and Wilson, C. J. N. 1980: Low-aspect Ratio Ignimbrites. Nature 283: 286-287

75. Walker, G. P. L.; Self, S. and Froggatt P. C. 1981a: An Ignimbrite veneer deposit - the trail marker of a pyroclastic flow. Journal of Volcanology and Geothermal Research 9: 409-421

76. Walker, G. P. L.; Self S. and Froggatt P. C. 1981b: The ground layer of the Taupo Ignimbrite - a striking example of sedimentation from a pyroclastic flow. Journal of Volcanology and Geothermal Research 10: 1-11

77.Walker, G. P. L. 1983: Ignimbrite Types and Ignimbrite Problems, Journal of Volcanology and Geothermal Research 17: 65-88

78.Walker, G. P. L. and Wilson, C. J. N. 1983: Lateral Variation in the Taupo Ignimbrite. Journal of Volcanology and Geothermal Research 18: 117-133

79.Watanabe, T. Grapes, R. and Palmer, K. 1981: Quantitative analysis of rock forming minerals by JXA-733 Electron Probe X-ray microanalyzer. Jeol. (news) vol. 19E No 1

80.Wilson, C. J. N., Ambrasey, N. N., Bradley, J. and Walker, G. P. L. 1980: A new date for the Taupo Eruption, New Zealand Nature, London 288: 252-253

81.Wilson, C. J. N. and Walker G. P. L. 1982: Ignimbrite depositional Facies: The anatomy of a pyroclastic flow. Journal of Geologyical Society of London 139: 581-592

82.Wilson, C. J. N.; Rogan, A. M.; Smith, I. E. M.; Northey, D. J.; Nairn, I. A. and Houghton, B. F.: 1984 Caldera volcanoes of the Taupo Volcanic Zone, New Zealand. Journal of Geophysical Research 89: 8463-8484

83. Wilson, C. J. N. and Walker G. P. L. 1985: The Taupo Eruption, New Zealand; Part 1 General Aspects. Philosophical Transaction of the Royal Society of London A314: 199-228

84. Wilson, C. J. N.: 1985 The Taupo Eruption, New Zealand; Part 2. The Taupo Ignimbrite Philosophical Transactions of the Royal Society of London A314: 229-310

85. Wilson, C. J. N., Houghton, B. F. and Lloyd, E. F. 1986: Volcanic History and Evolution of the Maroa-Taupo Area, Cenral North Island. In Late Cainozoic Volcanism in New Zealand (Editor Smith I. E. M.) Royal Society of New Zealand Bulletin 23 : 194-223

86. Williams H. and McBirney A. R. 1979: Volcanology Freeman, Cooper & Co; San Fransisco, CA 94133 USA.

87. Wright J. V. and Walker G. P. L. 1977: The ignimbrite source roblems: significance of a coignimbrite lag-fall deposit. Journal of Volcanology and Geothermal Research 17: 65-88

88. Wright, J. V.; Smith, A. L.; Self, S. 1980: A working terminology of pyroclastic deposits Journal of Volcanology and Geothermal Research 8: 315-336

APPENDIX 1

1.1 DESCRIPTION OF SELECTED SECTIONS OF THE TAUPO PUMICE FORMATION

1.1.1 Station 1 (Waitahanui Road Deviation) N94-553230

(300 m from old road junction)

Thick(m)	Stratig.unit	Description
8	Taupo Ignimbrite	Light grey, massive, unsorted pumice lapilli and blocks supported by a matrix of ash and lithics.
		(sharp erosional contact)
0.5	Ground layer	Lapilli and blocks of lithics with minor glass and crystals and rare pumice lapilli.
		(sharp erosional contact)
10	Taupc Ignimbrite	Light grey and pink, unsorted pumice lappilli and blocks in a matrix of ash and fine crysals and lithics. It contains parallel layers (bands) of well sorted pumice lappilli at the lower part (Taupo Lapilli?)
		(sharp undulating contact)
3	Rotongaio Ash	Dark grey ash, and fine vesicular glass material with rare rounded accereted ash a few mm accross. The layer shows poorly developed, fine, wavy, parallel bedding.

1.1.2 Station 1 (Waitahanui Road Deviation)

(500 m from old road junction)

Thick(m)	Stratig.unit	Description
2	Taupo Ignimbrite	Light grey and pink, massive, unsorted pumice lapilli and blocks supported in a matrix of ash with minor crystals and lithics.
		(sharp erosional contact)
3	Ground layer	Lapilli and blocks of lithics of rhyolite lava (some blocks are intensely altered) lake sediments, ignimbrite and rare andesite, dacite, and rounded greywacke pebbels. Some of the lithic blocks are up to 1.5 m in diameter.
		(sharp erosional contact)
-	Taupo Ignimbrite	Light grey and pink, masssive, unsorted pumice lapilli and blocks supported in a matrix of fine ash with minor crystals and lithics which contain bands of well sorted pumice lapilli (Taupo Lapilli?)

1.1.3 Station 2 Te Hue Hue Road

Thick(m)	Stratig.unit	Description
2	Taupo Ignimbrite	Light grey, massive, unsorted pumice lapilli and blocks supported by a matrix of ash with minor lithics and crystals.
		(sharp erosional contact)
2	Ground layer	Lapilli and blocks of fractured lake sediments (=1.5 m in diameter) rhyolite welded tuff, with rare dacite and andesite and minor crystals and pumice.

(sharp erosional contact)

1.5	Taupo Ignimbrite	Light grey to pink, massive unsorted pumice lapilli and blocks, matrix supported, contains minor ash and fine crysals.
		(sharp undulating contact)
0.6	Rotongaio Ash	Dark grey, bedded, obsidian ash with rare pumice and lithics, undulating bed mantling the previous topography.
		(erosional contact)
0.5	Hatepe Ash	Moderately well sorted light grey pumiceous ash which has a gulleyed upper surface.
0.7	Hatepe lapilli	Light grey well sorted pumice lapilli.

1.1.4 Station 16a

Thick(m)	Stratig.unit	Description
3	Taupo Ignimbrite	White-light grey, unsorted, massive pumice lapilli and blocks supported in a matrix of fine ash. lithic rich lenses occur near the top of the layer.
		(sharp erosional contact)
0.5	Ground layer	Lapilli and blocks of lithics, with minor crystals and pumice.
		(sharp erosional contact)
0.7	Rotongaio Ash	Dark grey, finely bedded, soft ash with rhyolite and obsidian fragments.
		(sharp undulating contact)
		(erosional contact)
0.1	Hatepe Ash	Light grey, pumice lapilli and ash.

0.7	Hatepe Lapilli	Light grey-white, moderately well sorted pumice lapilli with rare lithics.

1.1.5 Station 4a

Thick(m)	Stratig.unit	Description
1	Taupo Ignimbrite	Light grey to pale brown, uniformly massive, unsorted pumice lapilli blocks and ash, with charred charcoal logs near the top of the layer.
		(sharp erosional contact)
0.3	Ground layer	Lapilli and blocks of rhyolite, minor dacite, welded tuff and rare andesite with minor crystals and pumice.
		(sharp erosional contact)
0.2	Rotongaio Ash	Dark grey, finely bedded obsidian ash.
		(sharp undulating contact)
0.1	Hatepe Ash	Light grey-white patchy ash.
0.7	Hatepe Lapilli	Well sorted, white, pumice lapilli which overlies undifferentiated pre-Taupo Pumice Formation Tephra from Taupo and Maroa Volcanic Centres.

1.2 SAMPLING LOCALITIES

St.No	G. Ref.	Sampling remarks
1	N94-553230	Bulk sample was collected from the ground layer the fresh bigger boulders were sampled for whole rock chemistry.
2	N94-495160	Same as above.
3	N94-536324	Bigger blocks eroded out from the ground layer were sampled from the lake shore.
4a	N94-535425	Bulk samples were collected from the ground layer.
4b	N94-514450	Same as above
5	N94-498358	Bulk samples were collected from from the ground layer and lithics collected from the Taupo Plinian Pumice
6	N94-553096	-Lithic inclusions were collected from the Taupo Plinian Pumice and Hatepe Plinian Pumice.
7	N103-510134	-Lithic inclusions were collected from the Hatepe Plinian Pumice.
8	N103-594103	Bulk samples were collected from the ground layer and lithic inclusion samples were collected from the Hatepe and Taupo plinian pumice, and lithic rich lenses in the Taupo Ignimbrite.
9	N103-594103	Inconvenient for sampling
10	N103-563093	Samples were collected from the ground layer, lithic size range from a few cm to 30cm.
11	N103-586080	Lithics were collected from the ground layer
12	N103-627340	Lithic inclusions were collected from Hatepe and Taupo plinian pumice, the ground layer is not exposed.
13	N103-720129	Lithics collected from the ground layer.

14	N103-726133	The ground layer is not well developed, bulk samples collected from the ground layer.
15	N103-654171	Bulk samples were collected from the ground layer, and lithics were collected from the Taupo Plinian Pumice.
16	N103-549156	Bulk samples were collected from all members of the Taupo Pumice Formation including the ground layer.
16a	N103-551154	Bulk sample was collected from the ground layer.
17	N103-579123	Bulk samples were collected from all members of the Taupo Pumice Formation including the ground layer.
18	N94-560350	-Bulk samples collected from the ground layer.
19	N94-542332	Big boulders up to 2 m in diameter exposed alongthe shore by erosion were sampled.
20	N94-695523	Bulk sample collected from the ground layer.
21	N94-647512	Bulk sample collected from the ground layer.
22	N102-163273	Bulk samples were collected from the lithic rich base of the Taupo ignimbrite.
23	N102-178239	Samples collected from the lithic blocks in the ground layer.
24	N103-181219	Bulk sample collected from the ground layer.
25	N103-181195	Lithic blocks were collected from the lithic rich base of the Taupo Ignimbrite.
26	N103-199121	Same as above.
27	N103-727425	Samples collected from the lithic rich base of the Taupo Ignimbrite.
28	N103-713390	Lithic samples were collected from the ground layer.

APPENDIX 2

(A) PETROGRAPHIC DESCRIPTION OF REPRESENTATIVE ROCK SAMPLES FROM THE LITHIC INCLUSIONS FROM THE TAUPO PUMICE FORMATION

2.1 RHYOLITES

2.1.1 VUWN 31127 - Hypersthene Rhyolite

Light grey, banded and porphyritic rock, with rare phenocrysts of zone plagioclase, orthopyroxene and minor resorbed quartz with accessory Fe-Ti oxides, apatite and biotite. The phenocrysts rarely occur in aggregates. Plagioclase phenocrysts contain orthopyroxene and magnetite inclusions. Accessory minerals are Fe-Ti oxide, apatite and biotite. The groundmass is a cryptocrystalline quartzo-feldspathic material.

2.1.2 VUWN 31128 - Hypersthene Rhyolite

Dark grey, banded, porphyritic rock, with rare phenocrysts of zoned plagioclase, orthopyroxene, and minor resorbed quartz with accessory Fe-Ti oxides, apatite and biotite. The phenocrysts rarely occur in aggregates and are set in a cryptocrystalline groundmass. Plagioclase phenocrysts contain orthopyroxene inclusions.

2.1.3 VUWN 31133 - Hypersthene Rhyolite

Dark grey, banded, slightly hydrothermally altered rock with phenocrysts of plagioclase, quartz, orthopyroxene, and accessory Fe-Ti oxide which rarely occur in aggregates. Plagioclase phenocrysts contain orthopyroxene and magnetite inclusions. Plagioclase and quartz phenocrysts often show resorption. The phenocrysts are set in a cryptocrystalline groundmass.

2.1.4 *VUWN 31131 - Hypersthene Rhyolite*

Dark grey, banded, porphyritic rock with phenocrysts of zoned plagioclase, orthopyroxene and minor quartz and accessory Fe-Ti oxides. Inclusions of Fe-Ti oxides, are common in plagioclase and orthopyroxene phenocrysts. The phenocrysts rarely occur in aggregates. The groundmass is cryptocrystalline and contains rare biotite microphenocrysts.

2.1.5 *VUWN 31129 - Hypersthene Rhyolite*

Light grey, banded, porphyritic rock with phenocrysts and glomerophenocrysts of plagioclase, orthopyroxene and minor clinopyroxene set in a cryptocrystalline groundmass of quartzofeldspathic material which contains microcrystals of plagioclase, quartz and accessory Fe-Ti oxides.

2.1.6 *VUWN 31140 - Hypersthene-hornblende Rhyolite*

Dark grey, banded, spherulitic and porphyritic rock, which is slightly altered, and contains phenocrysts of plagioclase, orthopyroxene minor hornblende and clinopyroxene which make up about 12% of the rock, and are set in glassy and cryptocrystalline groundmass which contains accessory Fe-Ti oxides. The phenocrysts rarely form phenocryst aggregates.

2.1.7 *VUWN 31138 - Biotite bearing rhyolite*

Light grey, banded and porphyritic rock with phenocrysts of plagioclase, hypersthene and biotite set in a cryptocrystalline groundmass which contains microcrystals of plagioclase and quartz and accessory Fe-Ti oxides.

2.1.8 *VUWN 31132 - Hypersthene Rhyolite*

Light grey, banded, and porphyritic rock with phenocrysts of plagioclase , quartz and hypersthene set in a fine grained to glassy quartzo-feldspathic groundmass. Accessory minerals include Fe-Ti oxides and apatite.

2.1.9 *VUWN 31137 - Hypersthene Rhyolite*

Yellowish grey, hydrothermally altered rock, porphyritic with phenocrysts of plagioclase orthopyroxene and rare resorbed quartz set in a cryptocrystalline groundmass. Accessory minerals include Fe-Ti oxide, apatite and microphenocrysts of biotite. The phenocrysts rarely form aggregates.

2.1.10 *VUWN 31141 - Hypersthene Rhyolite*

Light grey, porphyritic rock with phenocrysts of plagioclase hypersthene and microphenocrysts of quartz and accessory Fe-Ti oxide set in a cryptocrystalline groundmass of microcrystals of plagioclase and quartz with accessory Fe-Ti oxides. Xenoliths of (andesite? dacite?) about 2 mm in diameter are rarely found. The phenocrysts rarely occur in aggregates and plagioclase phenocrysts rarely contain hypersthene and magnetite inclusions.

2.2 *DACITES*

2.2.1 *VUWN 31150 - Hypersthene-augite dacite*

Dark grey, porphyritic rock with phenocrysts and glomerophenocrysts of plagioclase (which occur in two generations as zoned and sieve textured crystals and smaller euhedral phenocrysts), clinopyroxenes, orthopyroxenes and minor quartz and accessory Fe-Ti oxides. Plagioclase phenocrysts with sieve texture are often altered to sericite. Orthopyroxene phenocrysts often contain inclusions of magnetite. The phenocrysts make about 30% of the rock and are set in a cryptocrystalline groundmass which contains laths of plagioclase which show flow alignment.

2.2.2 *VUWN 31146 - Hypersthene-augite dacite*

Dark grey, porphyritic rock with phenocrysts and glomerophenocrysts of plagioclase (which occurs as zoned and sieve textured and smaller zoned phenocrysts), orthopyroxenes,

clinopyroxenes, minor resorbed quartz and and accessory magnetite. Pyroxene phenocrysts occur as inclusions in the plagioclase, and magnetite inclusions are common in orthopyroxene phenocrysts. The phenocrysts are set in a cryptocrystalline groundmass which contains laths of flow aligned plagioclase.

2.2.3 *VUWN 31163 - Hypersthene-augite dacite*

Dark grey, porphyritic rock with phenocrysts of plagioclase (which occurs as zoned and sieve textured crystals up to 2 mm in size and smaller euhedral phenocrysts), orthopyroxenes, clinopyroxenes, minor resorbed quartz and and accessory magnetite. The phenocrysts rarely form aggregates. Pyroxene phenocrysts occur as inclusions in the plagioclase, and magnetite inclusions are common in orthopyroxene phenocrysts. The phenocrysts are set in a cryptocrystalline groundmass which contains laths of flow aligned plagioclase.

2.3 *ANDESITES*

2.3.1 *VUWN 31153 - Hornblende andesite*

Greyish brown seriate porphyritic rock with mega phenocrysts of resorbed brown hornblende, zoned plagioclase (bigger phenocrysts show seive texture smaller ones are euhedral), clinopyroxenes, and orthopyroxenes with accessory magnetite which form inclusions in the orthopyroxene and also forms the rim of the hornblende phenocrysts. The groundmass consists of microcrystals of plagioclase, pyroxene and accessory Fe-Ti oxides and apatite.

2.3.2 *VUWN 31154 - Plagioclase-pyroxene Andesite*

Dark grey, porphyritic rock with phenocrysts of plagioclase (labradorite-bytownite), orthopyroxene, clinopyroxene. Plagioclase and pyroxene phenocrysts are in almost equal quantity and constitute about 50% of the rock. The phenocrysts rarely occur in

phenocryst aggregates. The groundmass is glassy to cryptocrystalline with rare plagioclase laths, tridymite and microcrysals of pyroxene and accessory titanomagnetites.

2.3.3 *VUWN 31156 - Pyroxene andesite*

Dark grey pophyritic rock with phenocrysts of orthopyroxene, clinopyroxene, plagioclase and rare olivine which make up about 40% of the rock set in a finegrained groundmass of plagioclase laths, pyroxenes and tridymite with accessory titanomagnetite and apatite. The phenocrysts commonly form aggregates and, intergrowths between orthopyroxene and clinpyroxene phenocrysts are common. Orthopyroxene phenocrysts are formed around magnetite core and are frequently jacketed by clinopyroxene (pigeonite). Phenocrysts of plagioclase frequently contain pyroxene inclusions.

2.3.4 *VUWN 31157 - Olivine Andesite*

Dark grey, porphyritic rock with phenocrysts of zoned plagioclase, orthopyroxene, clinopyroxene and fractured and resorbed olivine which constitute about 40% of the rock. Olivine phenocrysts are altered to iddingsite along fractures and and are rarely jacketted by orthopyroxenes and contain chrome-spinel inclusions. The groundmass is fine grained and consists of laths of plagioclase, pyroxene and tridymite with accessory titanomagnetite and apatite. The phenocrysts commonly occur in aggregates and show intergrowths. Plagioclase phenocrysts contain pyroxene inclusions and pyroxene phenocrysts commonly contain granules of opaque Fe-Ti oxide.

2.4 *IGNIMBRITE*

2.4.1 *VUWN 31165 - Lithic crystal rich ignimbrite*

Yellowish brown, moderately welded, pumiceous lithic rich tuff, with corroded crystals of quartz, sodic plagioclase minor hypersthene and hornblende. Quartz crystals are commonly embayed and corroded and makeup about 20% of the rock and are as big as 3

mm. Plagioclase phenocrysts up to 3 mm big are commonly corroded and make up about 5% of the rock. Mafic phenocrysts make up about 5% of the rock. Xenoliths of hydrothermally altered rhyolite, dacite, and andesite (up to 5 mm in size) make up about 10% of the rock. The crystals and lithics are welded in a matrix of pumiceous ash.

2.4.2 *VUWN 31167 - Lithic crystal rich ignimbrite*

Yellowish brown, moderately welded pumiceous lithic rich ignimbrite with corroded phenocrysts of quartz, plagioclase (andesine) and minor partly altered hypersthene and hornblende. Quartz phenocrysts are embayed (=3 mm in size) and makeup about 15% of the rock. Plagioclase phenocrysts are up to 2 mm in size and are commonly have corroded outline and makeup about 5% of the rock. Hypersthene, hornblende and biotite are minor constituents. Xenoliths of andesite, dacite and rhyolite makeup about 10% of the rock and are up to 5 mm.

2.4.3 *VUWN 31169 - Crystal rich ignimbrite*

Light yellow, moderately welded, crystal rich tuff. Consisting of crystals of quartz with embayed and corroded outlines (up to 1 mm), sodic plagioclase (=1mm) with minor amount of hornblende hypersthene and biotite which are commonly < 0.5mm. The crystals makeup about 50% of the rock. Lithics content is very low (< 2%), the crystals and lithics are are supported by a matrix of light yellow pumiceous ash.

(B) LIST OF THIN SECTIONS FROM THE LITHICS IN THE GROUND LAYER.

St.No.	Samp.No.	VUW	Rock type / Remarks
1	1/T/1	31127 *	Hypersthene rhyolite, petrography given.
1	1/T/2	31128 *	Hypersthene rhyolite, petrography given.
1	1/B/3	*31129 *	Hypersthene rhyolite, petrography given.
1	1/B/6	31130	Hypersthene rhyolite, banded, spherulitic, glomeroporphyritic.
1	1/M/7	31131	Hypersthene rhyolite, petrography given, with cavities filled by vapour phase crystals.
1	1/5	31132 *	Hypersthene rhyolite, petrography given.
1	1/6	31133 *	Hypersthene rhyolite, petrography given.
2	2/1	31134	Hypersthene rhyolite, banded with phencrysts of plag, Opx, Mag, Ap.
3	3/1	31135	Hypersthene rhyolite, phenocryst poor, altered.
4	4/5	31136	Hypersthene rhyolite, massive, phenocryst poor.
1	1/B/1	31137	Bt. bearing rhyolite, petrography given
4	4/10R	31138 *	Bt. bearing rhyolite, banded.
4	4/12	*31139	Hypersthene rhyolite, banded.
1	1/M/3	31140	Hyp. hb. rhyolite, petrography given.
1	1/BB/2	31141 *	Hypersthene rhyolite, petrography given.
1	1/BB/4	31142 *	Hypersthene rhyolite, banded, phenocryst poor cavity bands filled with vapour phase crystals.
1	1/BB/5	31143 *	Hypersthene rhyolite, banded, low intensity of hydrothermal alteration.
1	1/BB/6	31144	Rhyolitic breccia.
1	1/M/2	31145	Two pyroxene dacite, glomeroporphyritic, microcystalline groundmass with flow pattern.
1	1/M/4	*31146 *	Two pyroxene dacite, petrography given.
1	1/B/4	31147 *	Two pyroxene dacite, petrography given.

2	2/3	31148	Two pyroxene dacite, banded, glomeroporphyritic
4	4/3	31149	Two pyroxene dacite, glomeroporphyritic with microcrystalline groundmass.
4	4/8	31150	Two pyroxene dacite, petrography given.
4	4/9	31151	Two pyroxene dacite, glomeroporphyritic with microcrystalline groundmass.
5	5/1	31152	Two pyroxene dacite, glomeroporphyritic, moderately altered.
1	4/1	* 31155	Two pyroxene dacite.
2	2/9	* 31153 *	Hornblende andesite, petrography given.
1	1/2	31154 *	Plag-pyx andesite, glassy ground mass.
2	2/8	* 31156 *	Pyroxene andesite, petrography given.
1	1/4	* 31157 *	Olivine andesite, petrography given.
1	1/12	31158 *	Olivine andesite.
3	3/6	31165	Lithic crystal ignimbrite, light brown, pumiceous with rare hb, opx, mafic phenocrysts.
1	1/BB/7	31166	Lithic crystal ignimbrite, light brown, pumiceous lithic and crystal rich.
1	1/B/5	31167	Lithic crystal rich ignimbrite, light brown pumiceous, with lithics, crystals of plag, qtz, opx.
11	11/2	31168	Crystal rich ignimbrite, with crystals of plag qtz, opx, and minor hb in a matrix of ash and minor lithics.
2	2/15	31169	Lithic crystal ignimbrite, with crystals of plag, qtz, opx, and minor hb in a matrix of ash and minor lithics.
2	2/13	31159	Hypersthene dacite, glomeroporphyritic (Opx, plag) in a microcrystalline groundmass.

17	17/1	31160	Two pyroxene dacite, glomeroporphyritic with a microcrystalline groundmass.
25	25/1	31161	Two pyroxene dacite, glomeroporphyritic, with a microcrystalline groundmass.
26	st26	31162	Two pyroxene dacite, glomeroporphyritic, hydrothermally altered.
4	4/10D	31163 *	Two pyroxene dacite, petrgraphy given.
4a	4a/1	31164 *	Two pyroxene dacite, banded, cryptocrystalline quartzofeldspathic groundmass.
2	2/11	31170 *	Obsidian
1	1BB0	31171 *	Obsidian
2	2/12	31172 *	Pumice, Taupo ignimbrite.
1	1/11	31175 *	Hydrothermally altered rhyolite.
1	1/10	31176 *	Hydrothermally altered dacite.
1	1/9	31181	Greywacke pebble.

LIST OF THIN SECTIONS FROM THE LITHICS IN HATEPE AND TAUPO LAPILLI.

6	HT6/3	31179	Hypersthene rhyolite, banded (Hatepe Lapilli).
7	TP7/2	31177	Hypersthene rhyolite, banded (Taupo Lapilli).
8	TP8/2	31178	Two pyroxene dacite, glomeroporphyritic with microcrystalline groundmass (Taupo Lapilli).
7	HT7/1	31180	Two pyroxene dacite, glomeroporphritic with altered, microcrystalline groundmass (Hatepe Lapilli)

OTHERS

-	GPB1	31173 *	Giant floated pumice.

VUWN* - Whole rock analysis given.

*VUWN - Mineral chemistry done on the EPMA.

APPENDIX 3

ANALYTICAL METHODS

3.1 WHOLE ROCK CHEMISTRY

Rock samples were split or crushed into 10-20 mm pieces after all the weathered surface had been removed. The pieces were powdered or crushed for 30-45 seconds in a tungsten carbide tema mill to produce approximately 200 grams of powdered sample. Proper mixing of each batch of powdered material was undertaken to make the powdered sample as representative as possible. Oxidation resulting from a grinding time of less than one minute is considered minimal (Fitton and Gill, 1970)

All major and trace element determinations were done on a Siemens SRS-1 automatic X-ray spectrometer with data reduced on-line using a Hewlett-Packard HP-85 desk-top computer. The spectrometer was calibrated using several international rock standards including those distributed by the U.S. Geological Survey, National Institute of Metallurgy, Geological Surveys of Japan and the International Working Group (A.N.R.T. and C.R.P.G.). The instrumental condition used in all the major and trace element analyses is given on table 1 (p 154b).

For major element analysis, fused glass discs were prepared using David Brown Scientific, Norrish formula "SIGMA" X-ray flux (Norrish and Hutton, 1969). $NH_4\ NO_3$ (Ammonium Nitrate) was used as an oxidizing agent to enable direct Na determinations. Corrections for flux moisture content were applied with a dilution ratio of approximately 5:1. Matrix correction factors were those from Norrish and Chappell (1977).

TABLE 1: Instrument Conditions for XRF Analysis.

MAJOR ELEMENTS

Element	Crystal	Collim.	Aperture	Time(sec)	cps/%
Fe	LiF 200	.4	S	20	1100
Mn	LiF 220	.15	L	40	220
Ti	LiF 200	.15	L	20	6300
Ca	LiF 200	.15	S	20	2600
K	PET	.4	S	20	3700
P	PET	.4	L	40	200
Si	PET	.4	L	40	150
Al	PET	.4	L	40	140
Mg	TAP	.4	L	100	40
Na	TAP	.4	L	200	15

All major elements were analysed under vacuum using the Kα line and a Cr anode X-ray tube operated at 45KV and 50mA. P10 gas (10% methane in argon) was used in the flow counter which was fitted with a 1µm window.

TRACE ELEMENTS

Element	Line	Tube	KV/mA	Crystal	Counter	Vacuum	Pk.Time(sec)	Interf.
As	Kα	Mo	55/44	LiF 200	Scint	No	100	PbLβ
Ba	Lα	Au	45/55	LiF 200	Flow	Yes	40	TiKα
Co	Kα	Au	45/55	LiF 200	Flow	No	40	FeKβ
Cr	Kα	Au	45/55	LiF 220	Flow	Yes	100	VKβ
Cu	Kα	Au	55/44	LiF 200	Scint	No	40	Cu*
Ga	Kα	Mo	55/44	LiF 200	Scint	No	40	-
Mn	Kα	Au	45/55	LiF 200	Flow	Yes	40	-
Mo	Kα	Au	55/44	LiF 200	Scint	No	100	ZrKβ
Nb	Kα	Au	55/44	LiF 220	Scint	No	100	-
Ni	Kα	Au	55/44	LiF 200	Scint	No	40	Ni*
Pb	Lβ	Mo	55/44	LiF 220	Scint	No	40	-
Rb	Kα	Mo	55/44	LiF 220	Scint	No	40	Au*
Sr	Kα	Au	55/44	LiF 220	Scint	No	40	-
Th	Lα	Mo	55/44	LiF 220	Scint	No	200	-
Ti	Kα	Au	45/55	LiF 200	Flow	Yes	20	-
U	Lα	Mo	55/44	LiF 220	Scint	No	200	-
V	Kα	Au	45/55	LiF 220	Flow	Yes	100	TiKβ
Y	Kα	Mo	55/44	LiF 220	Scint	No	40	RbKβ
Zn	Kα	Au	55/44	LiF 200	Scint	No	40	-
Zr	Kα	Au	55/44	LiF 220	Scint	No	40	SrKβ

* Interference originating from the X-ray tube and/or components within the spectrometer.

Trace elements were determined on 4 cm diameter boric acid backed pressed pellets using 3.5 g of rock powder. Background under peaks were calculated by extrapolation from one or more interference free background positions. "Spectrosil" ultra pure SiO_2 glass was used to determine non-linear factors. All analyses were corrected at run-time for mass absorption at an appropriate wave-length using the power curve relationship between mass absorption and the scattered anode radiation (Compton peak). Correction for the absorption edge effect of Fe, Mn, Cr, and Ti were applied to the mass absorption measurements. All significant spectral interferences were corrected.

Sample loss was measured at 1000°c (using porcelain crucibles) corrected for oxidation assuming complete conversion of FeO to $Fe_2 O_3$. FeO was determined by the conventional titrimetric method using standard $K_2 Cr_2 O_7$ (Potassium dichromate) solution, with diphenylamine sulphonic acid as the indicator (Sarver, 1927). The method is described in Shapiro and Brannock (1962).

CIPW Norms were calculated using a computer program in the Research School of Earth Sciences (Victoria University of Wellington) and incorporated all major element data (given below). A ratio of 0.2 was taken for FeO : $Fe_2 O_3$ of the total Fe for the norm calculations. All norms were recalculated on 100% anhydrous basis.

3.2 ELECTRON PROBE MICROANALYZER

Major rock forming minerals in polished thin sections cut from seven selected rock samples from the inclusions in the Taupo Pumice Formation (four andesites, two dacites and two rhyolites) were analysed using the JXA-733 electron probe microanalyzer (EPMA) in the Research School of Earth Sciences (Victoria Univesity of Wellington). The JXA-733 at Victoria University is fully automated with on line reduction of data using Bence and Albee (1968) correction factors, into wt% oxide and structural formulae (atomic proportions). All analyses were performed at 15 kv accelerating voltage, 0.12 uA beam current, and a focussed beam of about 3 um diameter for the olivines, pyroxene, hornblende, biotite and titanomagnetite analyses and a beam diameter of 10 um for the

plagioclase analyses to account for the loss of alkali metals. A peak search routine was used for each analysis, followed by 3 x 10 sec counts on the peak and one 10sec background count either side of the peak (Watanabe et al. 1981). Prior to mineral analysis, the probe calibration was checked against standard minerals of pyroxene or plagioclase of known chemical composition.

3.2.1 NORM CALCULATION

A programme in basic for the calculation of the normative components of the fresh and unaltered rocks is given below. The calculation was done with an HP-85 desk top computer at the RSES.

```
10 ! **** C.I.P.W. NORMS PROGRA
   M
15 T=100
20 DIM Y$[435],O$[55]
30 DIM M1(11),W(29),A(11),B(11)
   ,C(11),M(23),K(29)
40 O$[1,25]="SiO2 TiO2 Al2O3Fe2
   O3FeO  "
50 O$[26,55]="MnO  MgO  CaO  Na
   2O K2O  P2O5 "
60 Y$[1,45]="Quartz          Cor
   undum       Orthoclase     "
70 Y$[46,90]="Albite          An
   orthite      Leucite
   "
80 Y$[91,135]="KaliophiliteK
   metasilicate  Nepheline
   "
90 Y$[136,180]="NAmetasilicate
   Acmite          Diopside
   "
100 Y$[181,225]="--Wollastonite
   --Enstatite     --Ferrosilite
   "
110 Y$[226,270]="Hypersthene
   --Enstatite     --Ferrosilite
   "
120 Y$[271,315]="Olivine
   --Forsterite    --Fayalite
   "
130 Y$[316,360]="CAorthosilicate
   Magnetite       Hematite
   "
140 Y$[361,405]="Ilmenite
   Sphene          Rutile
   "
150 Y$[406,435]="Apatite
   Wollastonite  "
160 FOR I=1 TO 11
170 READ M1(I)
180 NEXT I
190 DATA 60.09,79.9,101.96,159.7
   ,71.85,70.94,40.32,56.08,61.
   98,94.2,141.95
200 FOR I=1 TO 29
210 READ W(I)
220 NEXT I
230 DATA 60.09,101.96,556.7,524.
   482,278.22,436.52,316.34,154
   .39,284.12
240 DATA 122.07,462.04,0,116.17,
   100.41,121.94,0,100.41,131.9
   4,0,140.73
250 DATA 203.79,86.125,231.55,15
   9.7,151.75,196.07,79.7,328.8
   8,116.17
255 CLEAR @ DISP "DO YOU WANT Fe
   2O3/FeO RATIO      NORMALISED
    TO 0.2 (Y/N)"
256 INPUT R$
260 CLEAR @ DISP "ENTER SAMPLE N
   AME";
270 INPUT S$
280 FOR I=1 TO 11
285 IF R$="Y" AND I=5 THEN I=6
290 CLEAR @ DISP "ENTER ";O$[(I-
   1)*5+1,I*5]
300 INPUT A(I)
310 NEXT I
311 IF R$="N" THEN 320
312 A(5)=A(4)/1.2113
313 A(4)=A(4)/6.5565
320 S=0
330 FOR I=1 TO 11
340 S=S+A(I)
350 NEXT I
360 FOR I=1 TO 11
370 B(I)=A(I)*100/S
380 C(I)=B(I)/M1(I)
390 NEXT I
400 FOR I=1 TO 23
410 M(I)=0
420 NEXT I
430 ! **** P2O5 TO APATITE
440 M(23)=C(11)
450 C(8)=C(8)-M(23)*10/3
460 ! **** TiO2 TO ILMENITE, SPH
   ENE, RUTILE
470 C(5)=C(5)+C(6)
480 IF C(5)-C(2)<0 THEN 510
490 M(1)=C(2)
500 C(5)=C(5)-M(1) @ GOTO 620
510 M(1)=C(5)
520 C(2)=C(2)-M(1)
530 C(5)=0
540 IF C(8)-C(2)<0 THEN 570
550 M(2)=C(2)
560 C(8)=C(8)-M(2) @ GOTO 620
570 M(2)=C(8)
580 C(2)=C(2)-M(2)
590 M(3)=C(2)
600 C(8)=0
610 ! **** K2O TO KALIOPHILITE A
   ND K-METASILICATE
620 IF C(3)-C(10)<0 THEN 650
630 M(4)=C(10)
640 C(3)=C(3)-M(4) @ GOTO 700
650 M(4)=C(3)
660 C(10)=C(10)-M(4)
670 M(5)=C(10)
680 C(3)=0
690 ! **** Na2O TO NEPHELINE, AC
   MITE, NA-METASILICATE
700 IF C(3)-C(9)<0 THEN 730
710 M(6)=C(9)
720 C(3)=C(3)-M(6) @ GOTO 840
730 M(6)=C(3)
740 C(9)=C(9)-M(6)
750 C(3)=0
760 IF C(4)-C(9)<0 THEN 790
```

```
770 M(7)=C(9)
780 C(4)=C(4)-M(7) @ GOTO 840
790 M(7)=C(4)
800 C(9)=C(9)-M(7)
810 M(8)=C(9)
820 C(4)=0
830 ! **** A1203 TO ANORTHITE AN
    D CORUNDUM
840 IF C(8)-C(3)<=0 THEN 870
850 M(9)=C(3)
860 C(8)=C(8)-M(9) @ GOTO 920
870 M(9)=C(8)
880 C(3)=C(3)-M(9)
890 M(10)=C(3)
900 C(8)=0
910 ! **** Fe203 TO MAGNETITE, H
    EMATITE
920 IF C(4)-C(5)>0 THEN 950
930 M(11)=C(4)
940 C(5)=C(5)-M(11) @ GOTO 1000
950 M(11)=C(5)
960 C(4)=C(4)-M(11)
970 M(12)=C(4)
980 C(5)=0
990 ! ****CaO,MgO,FeO TO OLIVINE
    , MONTICELLITE, CA-ORTHOSILI
    CATE
1000 C9=C(7)+C(5)
1010 IF C9>0 THEN C8=C(7)/C9 @ G
     OTO 1030
1020 C8=0
1030 IF C9-C(8)>=0 THEN 1070
1040 M(20)=C9
1050 C(8)=C(8)-M(20)
1060 M(13)=C(8)/2 @ GOTO 1110
1070 M(20)=C(8)
1080 C9=C9-M(20)
1090 M(21)=C9/2
1100 ! **** ALLOCATION OF SiO2
1110 C(1)=C(1)-M(2)-2*M(4)-M(5)-
     2*M(6)-4*M(7)-M(8)-2*M(9)-M
     (20)-M(13)-M(21)
1120 IF C(1)<0 THEN 2000
1130 IF C(1)=0 THEN 1610
1140 ! **** KALIOPHILITE TO LEUC
     ITE
1150 X=M(4)*2
1160 IF C(1)-X>0 THEN 1190
1170 M(14)=C(1)/2
1180 M(4)=M(4)-M(14) @ GOTO 1610
1190 M(14)=M(4)
1200 C(1)=C(1)-X
1210 M(4)=0
1220 ! **** CA-ORTHOSILICATE TO
     WOLLASTONITE
1230 IF C(1)-M(13)/0 THEN 1260
1240 M(15)=2*C(1)
1250 M(13)=M(13)-M(15)/2 @ GOTO
     1610
1260 M(15)=M(13)*2
1270 C(1)=C(1)-M(13)
1280 M(13)=0
1290 ! **** MONTICELLITE TO DIOP
     SIDE
1300 IF C(1)-M(20)>0 THEN 1330
1310 M(19)=C(1)
1320 M(20)=M(20)-M(19) @ GOTO 16
     10
1330 M(19)=M(20)
1340 C(1)=C(1)-M(20)
1350 M(20)=0
1360 ! **** LEUCITE TO ORTHOCLAS
     E
1370 X2=M(14)*2
1380 IF C(1)-X2>0 THEN 1410
1390 M(16)=C(1)/2
1400 M(14)=M(14)-M(16) @ GOTO 16
     10
1410 M(16)=M(14)
1420 C(1)=C(1)-X2
1430 M(14)=0
1440 ! **** NEPHELINE TO ALBITE
1450 X3=M(6)*4
1460 IF C(1)-X3>0 THEN 1490
1470 M(17)=C(1)/4
1480 M(6)=M(6)-M(17) @ GOTO 1610
1490 M(17)=M(6)
1500 C(1)=C(1)-X3
1510 M(6)=0
1520 ! **** OLIVINE TO HYPERSTHE
     NE
1530 IF C(1)-M(21)>0 THEN 1560
1540 M(22)=C(1)*2
1550 M(21)=M(21)-M(22)/2 @ GOTO
     1610
1560 M(22)=M(21)*2
1570 C(1)=C(1)-M(21)
1580 M(21)=0
1590 M(18)=C(1)
1600 ! **** DETERMINATION OF MAF
     IC COMPONENTS
1610 R=1-C8
1620 X4=M(21)+M(20)/2
1630 F1=R*X4
1640 F2=C8*X4
1650 M(13)=M(13)+M(20)/2
1660 D1=M(19)
1670 D2=C8*D1
1680 D3=R*D1
1690 H1=C8*M(22)
1700 H2=R*M(22)
1710 K(1)=M(18) @ K(3)=M(10) @ K
     (3)=M(16) @ K(4)=M(17) @ K(
     5)=M(9)
1720 K(6)=M(14) @ K(7)=M(4) @ K(
     8)=M(5) @ K(9)=M(6) @ K(10)
     =M(8)
1730 K(11)=M(7) @ K(12)=M(19) @
     K(13)=D1 @ K(14)=D2 @ K(15)
     =D3
```

```
1740 K(16)=M(22) @ K(17)=H1 @ K(
     18)=H2 @ K(19)=M(21) @ K(20
     )=F2
1750 K(21)=F1 @ K(22)=M(13) @ K(
     23)=M(11) @ K(24)=M(12) @ K
     (25)=M(1)
1760 K(26)=M(2) @ K(27)=M(3) @ K
     (28)=M(23) @ K(29)=M(15)
1770 ! **** CALCULATE WT %
1780 FOR I=1 TO 29
1790 K(I)=K(I)*W(I)
1800 NEXT I
1810 K(12)=K(13)+K(14)+K(15)
1820 K(16)=K(17)+K(18)
1830 K(19)=K(20)+K(21)+K(22)
1835 K1=K(4)+K(5) @ IF K1<=0 THE
     N 1845
1840 A7=100*K(5)/(K(4)+K(5))
1845 K2=K(20)+K(21) @ IF K2<=0 T
     HEN 1860
1850 F7=100*K(20)/(K(20)+K(21))
1860 PRINT @ PRINT "SAMPLE : ";S
     $ @ PRINT
1870 PRINT "OXIDE     WT%     R WT
     %"
1880 FOR I=1 TO 11
1890 PRINT USING "5A,2X,3D.2D,2X
     ,3D 2D" ; O$[(I-1)*5+1,I*5]
     ;A(I);B(I)
1900 NEXT I
1901 PRINT "          ------  -----
     -"
1902 PRINT USING "5A,2(2X,3D.2D)
     " ; "TOTAL";S;T
1910 PRINT @ PRINT
1920 PRINT "MINERAL              WT
      %"
1930 PRINT
1940 FOR I=1 TO 29
1950 PRINT USING "15A,X,3D.2D" ;
      Y$[(I-1)*15+1,I*15];K(I)
1960 NEXT I
1965 IF K1<=0 THEN 1975
1970 PRINT @ PRINT USING "19A,3D
     .2D" ; "Plagioclase is An.-
     ";A7
1975 IF K2<=0 THEN 1990
1980 PRINT @ PRINT USING "15A,3D
     .2D" ; "Olivine is Fo.-";F7
1990 GOTO 3000
3000 BEEP @ WAIT 100 @ BEEP @ WA
     IT 100 @ BEEP @ WAIT 100 @
     BEEP
2010 CLEAR @ DISP @ DISP @ DISP
2020 DISP "NOT ENOUGH SiO2 TO FO
     RM          UNDERSATURATED M
     INERALS"
2030 DISP @ DISP "COMPUTATION ST
     OPPED!" @ GOTO 9999
3000 PRINT @ PRINT USING "23A,3D
     .2D" ; "Thornton Tuttle Ind
     ex =";K(1)+K(4)+K(3)+K(9)+K
     (8)+K(6)
3001 PRINT USING "12A,3D.2D" ; "
     Kuno Index =";A(7)*100/(A(7
     )+A(4)+A(5)+A(9)+A(10))
3002 PRINT USING "15A,3D.2D" ; "
     Magnesium No. =",100*A(7)/4
     0.32/(A(7)/40.32+A(5)/71.85
     )
3009 IMAGE 6A,3D.2D," wt%"
3010 PRINT @ PRINT USING 3009 ,
     "'F' =";A(4)+A(5)
3020 PRINT USING 3009 ; "'M' =";
     A(7)
3030 PRINT USING 3009 ; "'A' =";
     A(9)+A(10)
3040 PRINT @ PRINT @ PRINT @ PRI
     NT @ GOTO 260
9999 END
 21268
```